THE IMPACT OF PROGESTIN-BASED CONTRACEPTIVE INITIATION ON THE CERVICOVAGINAL PROTEOME AND ITS RELATIONSHIP WITH HIV ACQUISITION IN THE ECHO TRIAL

BY

HOSSAENA AYELE

A THESIS SUBMITTED TO THE FACULTY OF GRADUATE STUDIES OF THE UNIVERSITY OF MANITOBA IN PARTIAL FULFILLMENT OF THE REQUIREMENTS OF THE DEGREE OF

MASTER OF SCIENCE

DEPARTMENT OF MEDICAL MICROBIOLOGY AND INFECTIOUS DISEASES

UNIVERSITY OF MANITOBA

WINNIPEG

TABLE OF CONTENTS

A. ABSTRACT

In sub-Saharan Africa, one of the most popular contraceptives of choice is depo-medroxyprogesterone acetate (DMPA). In many observational studies, DMPA has been associated with an increased acquisition risk of HIV in comparison to other hormonal contraceptives (HC). The recent ECHO (Evidence for Contraceptive options and HIV Outcomes) trial was a clinical trial designed to directly answer the question by randomizing women to three contraceptive types: DMPA-IM (Intramuscular), Copper IUD, and the LNG (Levonorgestrel) Implant. However, this trial found no difference in HIV incidence rates between contraceptive types. Nevertheless, there is an intense debate over concerns regarding the effect of HC's and DMPA on the mucosal biology of the female genital tract. This thesis is an examination of vaginal mucosal biospecimens from a subset of women who were enrolled in the ECHO trial. Here, we performed mass spectrometry-based proteomic analysis of cervicovaginal soft-cup samples from a subset of women from clinical sites in South Africa and Kenya, for baseline and 1-month post contraception initiation time points, to examine changes to the mucosal proteome and microbiome. Proteome changes associated with DMPA-IM revealed a decrease in proteins involved with innate immune response, with no changes to the vaginal microbiome. Minor changes to the proteome with LNG implant use were observed which precluded pathway analysis. Additionally, no significant changes to the vaginal microbiome were observed. The largest proteome changes were observed with Copper IUD use and included increased immune cell chemotaxis and complement activation, with a decrease in factors relating to cell-cell adhesion and keratinocyte differentiation. The bacterial component of the vaginal microbiome was significantly impacted with Copper IUD use, showing a significant increase in alpha-diversity with a decrease in *Lactobacillus* and *L. iners* and an increase in *Prevotella* and *Sneathia* species. Additionally, we performed a case-control sub-analysis of women who seroconverted in each contraceptive arm. Proteomic analysis revealed no significant difference to the vaginal microbiome. However, host proteomic signatures associated with cell-cell adhesion were observed to increase amongst HIV seroconverters, which was observed to overlap with signatures identified with Copper IUD use. This research contributes to the discussion on vaginal health and the impact of contraceptives with insight into potential mechanisms associated with HIV incidence.

B. ACKNOWLEDGEMENTS

I would like to express my deepest gratitude to a number of people for the support and guidance that they've provided, for without them this journey would not have been possible. I would first and foremost like to thank my supervisor Dr. Adam Burgener for giving me this amazing opportunity to work on a project that inspired me to further pursue a career in public health. I feel immensely blessed to have worked in a lab with diverse scientific backgrounds providing sky's the limit possibilities for analysis. This has pushed me to broaden my understanding far beyond microbiology and into other realms like statistics and coding.

Thank you to the many people apart of the Burgener lab that I had the opportunity to work with. Laura Noël-Romas you have been an amazing help these past few years! Thank you for answering my endless questions guiding me through a field of analysis I knew nothing about. Samantha Horne, thank you for always being available to talk through statistical theories and providing codding support when R programming was less than kind. Kenzie Birse, thank you for everything you do as lab manager and the additional support you've provided through manuscript editing, talking through ideas, and so much more. In addition, thank you to Max Abou for running all my samples on the Liquid Chromatographer. Finally, thank you to the other members of the Burgener lab; Michelle Perner, Kat Kratzer, Marlon De Leon, Christina Farr, Alicia Berard, Peter McQueen, Alana Lamont, and Ilda Medeiros it has been an honour sharing this experience with you all.

Thank you to the mass spectrometry core at the Public Health Agency of Canada, more specifically Dr. Garrett Westmacott, Stuart McCorrister and Chris Grant, for running my samples through the mass spectrometer. I would also like to thank my committee members. Thank you, Drs. Kevin Coombs, Denice Bay, and Vanessa Poliquin for agreeing to be on my committee. The diversity of your fields garnered questions and comments that have challenged me and for that I am immensely grateful.

I would also like to send my deepest thanks to the administrative staff at the department of Medical Microbiology and Infectious Diseases. One in particular that has gone above and beyond for not only me but for each graduate student part of the department, is Angela Nelson. Angela, I hope

you know how appreciated and loved you are by the MMID students. You are a beacon of light in the department!

Thank you to the team apart of the Evidence of Contraceptive Options and HIV Outcomes (ECHO) for allowing access to a subset of samples from the cohort to study biological mechanisms. Thank you to our collaborators apart of this ancillary study: Heather B. Jaspan, Renee Heffron, Steve Bosinger, JoAnn S. Passmore, Caitlin Scoville, Kate Heller, Jared M. Baeten, Kelly B. Arnold, Bryan Brown, Maricianah Onono, Gonasagrie Nair, Thesla Palanee-Phillips, Ramla Tanko, and Rubina Bunjun. Most importantly I would like to thank the women that took the time to participate in this trial, for without them this project nor any scientific insight that comes from this project would not have been possible.

Thank you to Research Manitoba for awarding me a master's studentship. I am honoured and greatly appreciated the support to pursue my graduate studies.

Lastly, but certainly not least, thank you to my amazing mother for being my rock during the last few years. Thank you for your prayers and reminding me of God's amazing grace which kept me positive and motivated to push through any challenges that I faced.

C. DEDICATION

I dedicate this thesis to my wonderful mother who has been an amazing support system throughout this process. Thank you for teaching me the value of hard work. It never ceases to amaze me how much you had to sacrifice to give me this opportunity in life and for that I will forever by grateful.

D. PUBLICATIONS THAT AROSE FROM THIS PROJECT (In progress)

An Updated Review on the Effects of Depo-Medroxyprogesterone Acetate on the Mucosal Biology of the Female Genital Tract. **Ayele H,** Perner M, Birse KD, Zuend Farr C, and Burgener A. 2021. *American Journal of Reproductive Immunology.*

- The references cited in this review paper informed the background of this project, discussed in chapter 1 of this thesis.

Initiating intramuscular depot medroxyprogesterone acetate (DMPA-IM) increases frequencies of Th117-like HIV target cells in the genital tract of women in South Africa: a randomized trial. Rubina Bunjun, Tanko F Ramla, Laura Noël-Romas, **Hossaena Ayele**, Shameem Z Jaumdally, Hoyam Gamieldien, Rushil Harryparsad, Smritee Dabee, Gonasagrie Nair, Maricianah Onono, Thesla Palanee-Philips, Caitlin Scoville, Kate B Heller, Jared M Baeten, Steven E Bosinger, Adam Burgener, Jo-Ann S Passmore, Heather Jaspan, Renee Heffron. In Preparation.

- This paper utilizes host proteomic data from those randomized to DMPA-IM use, discussed in section 3.5.1 of this thesis.

The Impact of Progestin-based Contraceptive Initiation on the Cervicovaginal Proteome in participants from the ECHO trial. **Ayele H**, Noël-Romas L, Birse KD, Horne S, Onono M, Nair G, Palanee-Phillips T, Tanko R, Bunjun R, Arnold KB, McCorrister S, Grant C, Westmacott G, Scoville C, Heller K, Baeten JM, Bosinger S, Passmore JS, Jaspan HB, Heffron R, and Burgener A. In Preparation.

- This paper utilizes host and bacterial proteomic data from those randomized to DMPA-IM use, discussed in sections 3.5.1 and 3.6.1 of this thesis, respectively.

The Impact of Copper IUD use on the Cervicovaginal Proteome in participants from the ECHO trial. **Ayele H**, Noël-Romas L, Birse KD, Horne S, Onono M, Nair G, Palanee-Phillips T, Tanko R, Bunjun R, Arnold KB, McCorrister S, Grant C, Westmacott G, Scoville C, Heller K, Baeten JM, Bosinger S, Passmore JS, Jaspan HB, Heffron R, and Burgener A. In Preparation.

- This paper utilizes host and bacterial proteomic data from those randomized to Copper IUD use, discussed in sections 3.5.2 and 3.6.2 of this thesis, respectively.

E. LIST OF TABLES

F. LIST OF FIGURES

G. LIST OF ABBREVIATIONS

LARC: Long-acting reversible contraceptives

IUD: Intrauterine device

CIUD: Copper Intrauterine device

STI: Sexually transmitted infection

BV: Bacterial vaginosis

DMPA: depot-medroxyprogesterone acetate

HSV-2: Herpes Simplex Virus-2

HIV: Human Immunodeficiency Virus

SIV: Simian Immunodeficiency Virus

PBMC: Peripheral blood mononuclear cells

FGT: Female genital tract

PRR: Pathogen recognition receptors

PAMP: Pathogen-associated molecular patterns

DC: Dendritic cells

NK: Natural killer cells

CCR5: C-C chemokine receptor type 5

IL: Interleukin

TLR: Toll-like receptor

MPA: Medroxyprogesterone acetate

CVL: Cervico-vaginal lavage

RNA: ribonucleic acid

RANTES: Regulated upon Activation, Normal T Cell Expressed and Secreted

MIP: Macrophage inflammatory protein

MCP: Monocyte chemoattractant protein

IP: Inducible protein

PCR: Polymerase chain reaction

BVAB: Bacterial vaginosis associated bacterium

DSG: Desmoglein

LNG: Levonorgestrel

ECHO: Evidence for Contraceptive Options and HIV Outcomes

UCT: University of Cape Town

WRHI: Wits Reproductive Health and HIV Institute

BCA: Bicinchoninic acid

BSA: Bovine serum albumin

UEB: Urea Exchange Buffer

MS: Mass spectrometer

dH2O: distilled water

ddH2O: double distilled water

HEPES: 4-(2-hydroxyethyl)-1-piperazineethanesulfonic acid

LC: Liquid chromatography

QE: Q Exactive

MGF: Mascot generic file

VMP: Vaginal metaproteome

KEGG: Kyoto Encyclopedia of Genes and Genomes

PVCA: Principal Variance Component Analysis

PCA: Principal Component Analysis

VCA: Variance Component Analysis

BH: Benjamini-Hochberg

DAVID: Database for Annotation, Visualization and Integrated Discovery

IPA: Ingenuity Pathway Analysis

LASSO: Least Absolute Shrinkage and Selection Operator

PLSDA: Partial least squares discriminant analysis

ARV: Anti-retrovirals

SD: Standard deviation

BMI: Body mass index

LD: Lactobacillus dominant

nLD: non-Lactobacillus dominant

MD: mean difference

CT: community types

CHAPTER 1: INTRODUCTION

1.1 THE IMPORTANCE OF FAMILY PLANNING FOR WOMEN'S HEALTH

The use of family planning methods is relied on for the prevention of unintended pregnancies. In the United States alone approximately 49% of pregnancies were unintended totaling 52 unintended pregnancies for every 1000 women between the ages of 15-44 in 2006 (*1*). In 2015, Canada's unintended pregnancy rates were approximately 40% with the majority of unintended pregnancies occurring for women between 20 and 29 years of age (*2*). Rates of unintended pregnancies have also shown considerable associations with income, with low-income women having higher rates of unintended pregnancies compared to their higher-income counterparts (*1*). In addition, rates of abortion for women between the ages of 15 and 17 were also observed to increase as a noticeable consequence of the increase in unintended pregnancies (*1*). An observational study examining the outcomes of unintended pregnancies between 2001-2008 observed that 40% of unintended pregnancies resulted in abortion (*3*). As a result, significant financial implications are expected. In the United States unintended pregnancies have amounted to a total expenditure of $12.5 billion in 2008 in health care costs (*4*). In Canada estimated costs totalled $320 million for an annual frequency of 180 700 unintended pregnancies (*2*). There have also been discussions that rapid population growth may have negative implications on climate change (*5, 6*). This has prompted governing bodies to support initiatives limiting population growth by increasing access to methods of contraception.

Control over one's fertility is a fundamental human right with several health implications including; 1) reduction of pregnancy-related complications (i.e. hypertension and ectopic pregnancies); 2) reduction of high-risk behaviours (i.e. cigarette smoking or exposure, drug use, caffeine intake); 3) the avoidance of high-risk pregnancies, for example, that result due to injury caused by a previous pregnancy or shorter birth intervals; and 4) for those seeking an abortion, the prevention of unsafe/illegal abortions by unlicensed personnel under potentially unsanitary conditions (*7, 8*). Thus, contraception should be a resource that is readily available worldwide. The right to contraception also demonstrates beneficial economic and social implications (*7*). Governmental bodies in developing regions have supported the introduction and use of multiple contraceptive methods for furthering economic and social developments for decelerating

population growth. Other potential benefits are financial. In circumstances where financial resources are limited, the prevention of unintended pregnancies eliminates the potential hindering of resources that could otherwise provide basic needs for other family members, from food to medical care (*7*). Fewer children allow families to utilize their existing resources to ensure the health and safety of their loved ones, which may be otherwise limiting with larger family sizes (*7*). Due to the benefits both economically and personally for the health of the woman and their families, international goals were set to increase access to reproductive health education and services. Family Planning 2020 set out to achieve access to effective contraceptives for 120 million women by the year 2020 (*9*). The Sustainable Development Goal target 3.7 was also set to ensure resources relating to sex and reproductive health, are universally accessible by the year 2030 (*10*).

Despite access to contraception being identified as a fundamental human right by the Sustainable Development Goal 3.7, in developing countries nearly 214 million women have an unmet need for modern methods of contraception (*11*). A systematic review focusing on contraceptive effectiveness and their advantages and disadvantages identified potential factors attributing to this unmet need in developing regions, factors of which include; socioeconomic status, concerns regarding side effects, and lack of proper contraceptive counselling to support informed decisions regarding method selection (*11*). It has been predicted that if the unmet need for contraception in developing regions is met this may thwart 67 million unintended pregnancies, 36 million induced abortions, and 76000 maternal deaths per year (*11*).

1.1.1 NEED FOR MODERN METHODS OF EFFECTIVE CONTRACEPTION.

Worldwide there are approximately 922 million contraceptive users, with 842 million using modern methods of contraception (*12*). With the desire to circumvent the unmet need for contraception in developing regions has come a priority of parallel importance; contraception effectiveness (*13*). Within the realm of modern contraception includes methods that are either reversible or irreversible and long-acting or short-acting. Irreversible, long-acting methods include male sterilization (i.e. vasectomy) and female sterilization (i.e. abdominal, laparoscopic, hysteroscopic) and worldwide include 219 and 16 million users, respectively (*12*). Long-acting reversible methods are categorized as Long-Acting Reversible contraceptives or LARCs and include the intrauterine device (IUD) and implant, which constitutes 159 and 23 million users,

respectively (*12*). LARCs are highly effective methods of contraception due to their lack of dependence on the user. Unlike oral contraceptives which require the user to ensure one pill is taken daily, LARCs are applied by a trained clinician without further action by the user (*14*). According to the Centers for Disease Control and Prevention, the implant and IUDs have a failure rate between 0.05 and 0.8% (*15*). Amongst the short-lived methods of contraception include injectables (74 million users), oral pill (151 million users), and condoms-only (189 million users) (*12*). The injectable contraceptives, much like LARCs, have a failure rate ranging between 0.2% and 6%, with perfect and typical use, respectively (*16-19*), in comparison to the more common short-lived contraceptive, condoms, which has a failure rate of 9% (*15*).

1.2 LONG-ACTING AND SHORT-TERM, REVERSIBLE CONTRACEPTIVES

1.2.1 INJECTABLE DEPOT MEDROXYPROGESTERONE ACETATE

Clinically referred to as Depo-Provera (Pfizer, Puurs, Belgium), the progestin-based contraceptive DMPA is an injection of 150mg (1mL) of medroxyprogesterone acetate (MPA), administered every 3-months. Two methods of DMPA administration exist: subcutaneous (SC) involving injection just under the skin and intramuscular (IM) injection in deep muscle tissue. DMPA-SC contains a lower dose of progestin at 104mg/0.65mL. IM method of administration of MPA achieves highest serum concentrations approximately 1-month following injection and subsequent concentration decline to 1.0-1.5ng/mL until the next injection (*20, 21*). MPA is a progestin that is chemically related to the menstrual cycle hormone progesterone and acts by preventing ovulation (observed in 65% of women taking DMPA (*22*)), inhibiting luteinizing hormone release resulting in a decrease in serum estrogen levels (*21*). MPA also causes thickening the cervical mucus and hinders sperm movement to the uterus and the fallopian tubes (*7, 23*). Reported benefits of DMPA use include being safe for post-partum use, prevention against anemia and potentially endometrial cancer, potential protective effects against pelvic inflammatory disease (via thickening of the cervical mucus protecting against genital infections (*24*)) and return of fertility within 6-9 months (*7, 23*). Side effects include potential for irregular bleeding or lack of bleeding, weight gain, headaches, dizziness, abdominal bloating and discomfort, mood changes, and reduced libido (*7, 23*). In addition, reduced bone mineral density has been shown with DMPA use through its

inhibition of estrogen production, directly impacting bone resorption (*7, 25, 26*). Fortunately, DMPA discontinuation has resulted in the recovery of lost bone density (*7*).

1.2.2 COPPER INTRAUTERINE DEVICE

Copper intrauterine device (copper IUD or CIUD; Optima TCu380A; Injeflex, Sao Paolo, Brazil) is a non-hormonal contraceptive alternative lasting approximately 5-10 years (*27*). The copper IUD is a t-shaped device made of plastic coiled with copper and inserted in the uterus. Its mechanism of pregnancy prevention is by preventing egg fertilization by incoming sperm. The release of copper ions into the cervical mucus triggers a host inflammatory response altering the hospitality of the endometrium to incoming sperm by hindering sperm viability and migration (*27, 28*). Copper IUD use shares similar benefits to DMPA-IM, including reducing the occurrence of ectopic pregnancies (*7*). Common side effects include irregular menstrual cycle bleeding and discomfort (*7*).

1.2.3 LEVONORGESTREL IMPLANT (JADELLE)

The Levonorgestrel implant (Jadelle; Bayer, Turku, Finland) is another progestin-based contraceptive containing a total of 150 mg (two rods containing 75mg) of levonorgestrel, a synthetic progestin (chemically similar to MPA), with a low daily dose released for approximately 5-years (Jadelle FDA Information sheet). Following placement of the LNG Implant peak serum concentration of LNG has been shown within 2 days (*20*). Serum concentrations were then reported to decline to 100ug/day by the 1-month, 40ug/day by 12-months, and 30ug/day from 24 months until the implant is replaced (*20*). Much like DMPA, LNG prevents ovulation, thickens the cervical mucus preventing incoming sperm from accessing the uterus and fallopian tubes, and reduced ciliary action in the fallopian tube (*7, 29*). Benefits to its use are very similar to that of DMPA in addition to return to fertility mimicking that of non-hormonal contraceptive methods (*7, 23*). Side effects also mimic that of DMPA use (*7, 23*).

1.3 CONCERNS RAISED WITH USE OF HORMONAL LARCs

Despite the positive health outcomes that are associated with the use of contraceptives, uptake remains considerably low. Reservations for their use have been attributed to misconceptions over recommended use (i.e., use of IUDs for nulliparous women) and safety concerns. The prevalence

of specific modern contraceptives does appear to differ based on region. Women in Europe and North America appear to prefer the use of the oral contraceptive pill and the male condom. In contrast, women in sub-Saharan Africa are more commonly using injectables (*12*).

Several studies have gauged potential barriers associated with minimal uptake of the more effective methods of contraceptives, specifically LARCs, to include cost, lack of comprehensive information on the available contraceptive methods, and clinician bias (*30-38*). A study that utilized online surveys to gauge awareness, experiences, and interest in LARCs found concerns regarding the use of IUDs and implants to include potential side effects and their overall safety (*39*). In terms of the injectable, several concerns have been raised regarding the potential relationship between sexually transmitted infections (STIs) and bacterial vaginosis (BV). These concerns have been more specifically raised with the use of the injectable, depot-medroxyprogesterone acetate (DMPA).

In a recently published review, Deese *et al* 2018 outlined several studies that explored the association of STIs, specifically *Chlamydia trachomatis, Neisseria gonorrhoea,* Herpes Simplex Virus-2 (HSV-2), and Human Immunodeficiency Virus (HIV), among others, with the use of DMPA (*40*). Masese *et al* 2013, in their cohort of women from Kenya participating in transactional sex, saw the incidence of *C. trachomatis* to be higher amongst women 25 years and younger (27.6 per 100 person-years) compared to women between 25 and 34 (8.4 per 100 person-years) and older than 35 (2.6 per 100 person-years) (*41*). Besides age, other factors that were seen to relate to *C. trachomatis* infection included the use of DMPA, time since enrollment (with more recent enrollees having a higher incidence), having one or more sex partners or encounters in the last 7-days, HIV status, and concurrent *N. gonorrhoea* infection (*41*). Following multivariate analysis age, DMPA use, and *N. gonorrhoea* infection were factors that remained significantly associated with *C. trachomatis* in this cohort (*41*). The overall incidence of *C. trachomatis* was 5.0 per 100 person-years (*41*). After multivariate analysis, other studies have confirmed the prevalence of Chlamydia infection to associate with injectable contraceptive use (adjusted odds ratio (OR) ranging from 1.8-2.24) (*42, 43*). While slight or no associations have also been observed, Pettifor *et al* 2009 observed a slight (IRR 1.24) increased risk in their South African cohort (*44*). Russel *et al* 2016*,* observed a higher incidence of *C. trachomatis* of 28 per 100 person-years in their cohort

of American women, which was significantly associated with DMPA use alongside the withdrawal technique (involving removal of the penis from the vagina before ejaculation) and lack of condom use, however, significance did not pass multivariate analysis (*45*). In contrast, Romer *et al* 2013 observed DMPA use to have no association with *C. trachomatis* infection (*46*). Data before 2009 also showed significant trends of an association between *C. trachomatis* and DMPA use with hazard ratios (HR) ranging from 1.2-4.3 (*47-50*). *N. gonorrhoea* infections have been observed to increase the risk of coinfections with other STIs such as *C. trachomatis (41)*. However, *N. gonorrhoea* infection risk with DMPA use has not demonstrated to have a significant association (*42-44, 46*). Data before 2009 has also shown an absence of risk (*47, 49, 50*).

In the absence of HIV coinfection, Herpes Simplex Virus (HSV)-2 has also been speculated to increase HIV acquisition risk. A cohort of Canadian and Rwandan sex workers observed incidence of HSV-2 to be higher amongst sex workers using DMPA with adjusted HR of 4.43 and OR of 6.34 observed, respectively (*43, 51*). Grabowski *et al* 2015 observed women who were consistently using DMPA in Uganda to have an incident HSV-2 incidence adjusted HR of 2.26 (*52*). While in the same cohort, women who again were consistently using DMPA and whose partner was HSV-2 positive had an incidence adjusted HR of 6.23, demonstrating a positive association in their two groups (*52*). Before 2009 this positive association was not observed amongst prospective studies (*53*).

1.4 PREVALENCE OF HIV INCIDENCE AND SUSCEPTIBILITY WITH HORMONAL CONTRACEPTIVES

In sub-Saharan Africa, DMPA is the preferred method of contraception for nearly half (47%) of contraceptive users (*54*), this region also exhibits a disproportionally high cluster of HIV infection. As such, many have pondered the potential correlation between the high uptake of DMPA and HIV infection rates in sub-Saharan Africa (*55*). Additional concerns have been raised with the use of such an effective contraceptive like DMPA to include potential changes in safe-sex practices [i.e., decrease in condom use per coital act] which could confound data suggesting a correlation with HIV risk.

The transmission of HIV has been speculated to associate with the use of DMPA since the late 1960s. A systematic review focusing on published relationships between STI/HIV and injectable

contraception published between 1966 and 2008, observed an increased risk in cohorts that were considered high-risk due to practicing sex work (*53, 56, 57*). Women that are considered low risk for HIV infection were also seen to exhibit a significant increase in risk with DMPA use (*58-60*). While other cohorts of low-risk women exhibited either no significant risk (*61, 62*) or protective effects (*63, 64*) for HIV infection. More recently Heffron *et al* 2012, in their cohort of HIV-1 serodiscordant couples, saw the use of hormonal injectables to associate with a 2-fold increase in risk, reaching statistical significance (*65*).

Animal models using non-human primates have often been used to study the incidence of HIV infection with DMPA use. Much like what has been observed in humans, an increased risk has been demonstrated with either DMPA or progesterone treatment for the macaque equivalent of HIV, simian immunodeficiency virus (SIV). Progestin treatment is often used to increase macaque susceptibility to SIV infection when studying viral pathogenesis (*66*). Marx *et al* 1996*,* in their macaque model, compared the susceptibility of placebo and progesterone-treated group to SIV, isolated at several timepoints from peripheral blood mononuclear cell (PBMC) samples (*67*). In their progesterone treatment group, they observed SIV infection to have a higher incidence compared to the placebo group, with progression to acquired immunodeficiency syndrome to be higher in the former (*67*). Similarly, Smith *et al* 2015 observed their DMPA treated macaques to be more likely to achieve simian-human immunodeficiency virus infection following challenge compared to normally menstruating macaques (*68*).

Further exploration of the mechanisms behind the observed risk of HIV infection with DMPA use would require a focus on the most prevalent routes of infection. In terms of the disproportionate degree of HIV infections in sub-Saharan Africa, particularly in women, the main route of infection is observed to be through heterosexual sexual contact (*69*). In addition to the use of hormonal contraceptives, other factors that have been postulated to contribute to an increased risk of HIV infection include the viral load of their infected partner, coinfections with other STI's, cervical ectopy, and vaginal cleansing practices (*70-72*). Therefore, understanding how DMPA is mechanistically altering the female genital tract (FGT) may provide a better picture as to how the risk of HIV infection is increasing with use.

1.5 MUCOSAL BIOLOGY OF THE FEMALE GENITAL TRACT

Components of the FGT that are involved in contributing to mucosal homeostasis and defense against invading pathogens can be categorized into three groups based on their purpose for maintaining vaginal health: 1) physical barrier referring to the vaginal epithelium, 2) mucosal fluid, and 3) the commensal microbiome. Our understanding of these components of the FGT has progressed tremendously due to advancements in technologies allowing the study of molecular and cellular compositions.

1.5.1 VAGINAL EPITHELIUM

The FGT is compartmentalized into the upper and lower FGT. The upper FGT includes the endocervix, uterus, fallopian tubes, and ovaries (*73*). The epithelium in this region includes columnar cells which are held together by tight junctions preventing the movement of incoming pathogens to the sup-epithelia and lamina propria (*73*). The lower FGT includes the ectocervix and the vaginal tract. The epithelium in this region includes a multi-layer of different cell types. The basal layer, much like the upper FGT, includes columnar cells that are held together by tight junctions and are actively undergoing mitosis, replenishing itself (*73*). The apical layer consists of squamous cells, which are terminally differentiated and lack tight junctions classifying it as a semi-permeable barrier (*73*). The layer of squamous cells in the lower FGT allows passive movement of small molecules and proteins, however preventing movement of viruses and vaginal organisms. As such the epithelium in the lower and upper compartments of the FGT provide a physical barrier for the prevention of invading pathogens. FGT epithelial cells also partake in the recognition and activation of immune defense against invading pathogens by their expression of pathogen recognition receptors (PRRs). PRRs recognize pathogen-associated molecular patterns (PAMPs) which upon detection provoke the secretion of cytokines, chemokines, and other soluble factors (*73-75*). The epithelium also consists of several immune cells such as Langerhans cells, dendritic cells (DC), macrophages, neutrophils, and lymphocytes (CD4+ and CD8+ T cells, natural killer (NK) cells, and B cells) that aid in mounting a response against invading organisms (*73, 76*). Although the frequency of these cells has been shown to differ depending on their location in the FGT (*77*).

1.5.2 MUCOSAL FLUID

The cervical vaginal fluid lines the epithelium in the FGT and consists of factors that contribute to a protective effect against pathogens. Such factors include mucins and several host defense molecules like antibodies, β-defensins, secretory leukocyte protease inhibitor, neutrophil gelatinase-associated lipocalin. (*73, 76, 78*). Vaginal epithelial cells in the lower FGT secret mucins into the vaginal lumen contributing to the composition of the vaginal mucosa (*73*). At the upper FGT cell-surface and gel-forming mucins have also been imaged (*78*). Cell-surface mucins include MUC4, MUC16, and MUC1, while gel-forming mucins, which are the main contributors to the gel-like layer and secreted by goblet cells, include MUC5AC, MUC5AB, and MUC6 (*73, 78*). Mucins are heavily glycosylated proteins with glycosylation accounting for approximately 50-90% of their molecular mass (*79*). Mucins contribute to the rather viscous nature of mucosal fluid providing an additional physical barrier of protection hindering the movement of pathogens to the underlying epithelium.

1.5.3 COMMENSAL MICROBIOME

The lower genital tract is colonized by a community of microbial species referred to as its commensal microbiome. Bacterial tenants in this community exist in a homeostatic relationship with the mutually beneficial host. Bacterial species that have been repeatedly identified as optimal belong to the bacterial genus *Lactobacillus,* in particular *L. crispatus* and *L. jensenii.* These optimal bacterial species are observed to produce lactic acid and H_2O_2 which contribute to maintaining a low vaginal pH and several anti-microbial factors (i.e., bacteriocins) (*80*). The importance of the low vaginal pH is due to the establishment of an environment that is not conducive to the colonization of detrimental pathogens (*81*). The dominance of anaerobic non-*Lactobacillus* organisms including *Gardnerella vaginalis*, *Prevotella*, *Mobiluncus*, *Ureaplasma,* and *Mycoplasma* are considered less optimal due to their association with cases of BV (*82*). Dominance by BV-associated organisms such as these have shown to have an association with vaginal inflammation and risk of STI acquisition (*80, 83*). BV refers to a dysbiotic shift of the microbiome, clinically diagnosed using Amsel's criteria which includes the presence of the following; high vaginal pH, vaginal discharge, presence of clue cells following microscopic examination of vaginal discharge, and fish-like odor following the addition of 10% potassium hydroxide (*84*). Another common method is through Nugent scoring of vaginal smears by identifying bacterial morphotypes (*85*). Molecular classifications, focusing on the presence of specific bacterial species

mentioned as non-optimal have been done using 'omics techniques. These methods have been shown to identify cases of asymptomatic BV that are not readily captured by clinical methods (*86*).

1.6 HIV TRANSMISSION AND THE FEMALE GENITAL TRACT

Factors that have been identified in the literature to contribute to HIV transmission in the female genital tract include the surface area of the FGT, seminal exposure, endogenous female sex hormones, and the vaginal microbiome. Female to male transmissibility of HIV disproportionally affects women during heterosexual sex, but also differs depending on male circumcision. Per sex act estimated risk of HIV transmission is generally <0.0001%, however for uncircumcised men this increases 110-fold to 1% risk per sex act (*87, 88*). In terms of female infectivity, heterosexual women have accounted for 16% and 29.3% for new HIV infections in the United States (www.hiv.gov) and Canada, respectively (*89*). While in sub-Saharan Africa, women account for 63% of new HIV infections (2021 UNAIDS fact sheet, www.unaids.org). One proposed explanation for the disproportionate rates of HIV infections in women is the rather large surface of the cervicovaginal mucosa compared to the site of susceptibility in men, which is the foreskin (*90*). Looking more specifically at the different compartments of the cervicovaginal mucosa, as mentioned in *Section 1.3.1 Vaginal Epithelium,* the endocervix consists of a single layer of columnar cells, while the ectocervix and vaginal epithelium consist of a multi-layer of squamous and columnar cells. The lack of dimensionality and certain immune characteristics of the endocervix has raised concerns relating to HIV susceptibility, suggesting greater risk at this region of the FGT. In animal models, increased virus entry (*91*) and greater expression of C-C chemokine receptor type 5 (CCR5) (*92, 93*) at the endocervix compared to the foreskin was observed (*90*). In addition, cervical ectopy, which is when the columnar cells of the endocervix are exposed and project where squamous epithelial cells naturally preside in the ectocervix, has consequently demonstrated frailty of the cervical epithelial barrier and reports have observed increased risk of HIV acquisition (*94*). Rather contradictory are studies that have observed HIV infection to occur despite the absence of a cervix or with the use of a physical barrier method of contraception (i.e., diaphragm) (*90, 95, 96*). The vaginal compartment has also shown great susceptibility to HIV infection suspectedly due to its relatively large surface area, 15-times the area of the endocervix (*90, 97, 98*), showing greater penetration of HIV-1 virions. (*99*). Micro abrasions to the FGT epithelium from sexual intercourse have also been attributed to increased susceptibility by increasing access to susceptible immune cells in the submucosa (*90, 100*). In addition, HIV-

infected seminal exposure in the FGT has shown an increased likelihood of infection due to the influx of pro-inflammatory cytokines, a biological event known as a "leukocyte reaction", which consequently increases the frequency of susceptible immune cells following coitus (*101-103*).

Endogenous female sex hormones have also been associated with HIV acquisition risk. The menstrual cycle consists of changes in endogenous sex hormones, estradiol, and progesterone, over the course of 28 days. The menstrual cycle can be compartmentalized into two phases: the follicular and luteal phases. In terms of hormone levels, the follicular phase is when estradiol concentrations dominate whereas during the luteal phase, progesterone dominates. These endogenous hormones are essential in regulating ovulation, implantation, fertilization, and when fertilization of an egg by sperm does not occur, menstruation (*67, 73*). The follicular phase of the menstrual cycle consists of menses and the proliferative stages, during which estradiol levels steadily increase while sloughing of the endometrial lining occurs (menses), once the proliferative stage is reached the epithelium of the endometrium begins thickening until ovulation is reached at day 14. After ovulation occurs the luteal phase at which point estradiol levels drop while progesterone concentrations rise. During the luteal phase, secretory stage, the endometrial lining thickens. It is apparent, even with the simplification of the stages of the menstrual cycle that changes in the concentrations of endogenous hormones estradiol and progesterone have a significant effect on the physical barriers of the FGT as seen by changes in the thickness of the endometrial lining. In terms of the vaginal epithelium, *in vitro* models have observed progesterone treatment to cause epithelial thinning, increased permeability, and decreased cell proliferation (*104, 105*). The luteal phase has also shown to associate with immune suppression and an increased presence and expression of susceptible cellular factors and receptors, thus classifying it as the "window of vulnerability" in these studies (*106, 107*). Macaque models examining Simian-Immunodeficiency Virus (SHIV) infection during the course of the macaque menstrual cycle have observed more productive infection to occur during the luteal phase (late secretory) compared to the follicular phase (*108-110*). Human cervical explants obtained from the follicular and luteal phase were also examined *ex vivo* as per their ability to support a productive viral life cycle for HIV. Saba *et al* observed their explants obtained from the luteal phase to be more productive at supporting HIV infection than their follicular counterparts (*111*). These findings have not been unique to animal and *ex vivo* models, Birse *et al* observed proteins associated with remodelling of

the epithelial barrier and activation of the immune system and recruitment of immune cells to be more abundant in women in the luteal phase of their menstrual cycle compared to the follicular phase, suggesting a compromised epithelial barrier and inflammation during progesterone high state (*112, 113*). In addition, gene expression analysis of endocervical and endometrial tissues has also observed increased inflammatory factors during the luteal phase (*113, 114*). Nevertheless, contradictions in the literature are present (*115*).

The commensal microbial communities in the lower genital tract have also been observed to influence susceptibility in the FGT to HIV, which has been demonstrated in the literature with BV. For clinically defined cases of BV, the majority have observed a reduction or "protection" amongst DMPA users (*116-120*). Achilles *et al* 2018 observed the prevalence of BV to increase from enrollment (29.3%) to 6-months (30.8%) with DMPA use, although not significant (*121*). A lack of a significant association has also been observed in other cohorts (*43, 44*). The presence of the BV-associated bacteria has been observed to induce several pro-inflammatory cytokines (interleukin (IL)-1B, IL-8, IL-1a) compared to BV negative women (*122*). Genital secretions from BV-positive women, consisting of bacterial peptidoglycan, have also been observed to activate toll-like receptor (i.e. TLR2) responses, conducive to the activation of pro-inflammatory cytokines (*123*). Thus, the composition of the vaginal microbiome may also contribute to the recruitment of susceptible immune factors, increasing the likelihood of infection in the presence of HIV virions.

1.7 OBSERVATIONAL EFFECTS OF DMPA USE ON THE FEMALE GENITAL TRACT

It is apparent from *Section 1.4 HIV and the Female Genital Tract* that there are several components of the FGT that may facilitate HIV susceptibility. However, whether these components change with DMPA use has been a particular area of interest. According to a recent review published by Hapgood *et al* 2018 DMPA is likely to: compromise the mucosal epithelial barrier, facilitate immune suppression of pDCs and T cells while increasing the presence of HIV-1 target cells and CCR5 coreceptor expression, have no significant effect on the microbiome, with inconsistent but significant changes to certain cytokines, chemokines and other soluble factors (*124*). Data on other progestin-based contraceptives, such as LNG Implants, are sparse and quite variable, so would require further experimentation to further elucidate its effects on the vaginal mucosa. Due to concerns raised specifically with DMPA use in sub-Saharan Africa an in-depth discussion of past

and recent literature discussing the effects of DMPA use on the FGT follows below with only significant observations discussed unless otherwise noted.

1.7.1 EFFECT OF DMPA USE ON MUCOSAL IMMUNOLOGY AND INFLAMMATION

Immune cells. The majority of studies that assessed how DMPA use may alter immune cell phenotypes or functions have focused on HIV acquisition. This resulted in a focus on HIV-relevant cell surface markers present on CD4+ T cells such as CCR5 or CXCR4, which are essential targets of HIV-1 aiding in a productive infection (*124, 125*). The overall abundance of immune cells has been explored with DMPA use with several reports showing an increase (CD45+ and CD3+) in the lamina propria and vaginal epithelium (*125, 126*). In support, proteomic analysis observed an overabundance of inflammatory proteins (IL36G, HMGB1, PPBP) in DMPA users compared to no-HC controls (*127*). These observations imply an overall inflamed environment with DMPA use. When focusing on specific components of said inflamed environment several reports have narrowed in on the frequency of CD4+ and CD8+ lymphocytes, although observations on their changes with DMPA use have been variable.

Achilles *et al* 2020 observed decreased frequency of CD3+CD4+ cells in the cervix (*128*) while Michel *et al* 2015 observed no significant change (*126*) in vaginal biopsies. Thurman *et al* 2019 and Edfeldt *et al* 2020 observed an increase in the frequency of CD3+CD4+ cells in vaginal (*125*) and ectocervical biopsies (*129*), respectively. Both the Achilles *et al* 2020 and Thurman *et al* 2019 studies were longitudinal cohorts recruiting women that were seeking contraceptive counselling that had no active STI's upon enrollment, however, sampling protocols did vary. The Achilles *et al* 2020 study conducted sample collection days 30 and 180 post-DMPA injections (*128*) while for Thurman *et al* 2019 sample collection was 42 days (6 weeks) post-injection (*125*). These cohorts also differed geographically, with the Achilles *et al* 2020 cohort in Zimbabwe and the Thurman *et al* 2019 cohort in the United States and the Dominican Republic. The Edfeldt *et al* 2020 the cohort consisted of women from the Pumwani sex worker cohort, which alludes to potential behavioural differences that may or may not contribute to variability in comparison to other cohorts of non-sex workers. In terms of CD8+ T cells, Achilles *et al* 2020 and Thurman *et al* 2019 observed an increase in proportion and frequency (*125, 128*), respectively; however, Michel *et al* 2015 and

Smith McCune *et al* 2017 observed no significant changes in their cohorts (*126, 130*). These studies differed in their study design, where Achilles *et al* 2020 and Thurman *et al* 2019 assessed longitudinal DMPA use comparing to pre-contraception initiation, while both Michel *et al* 2015 and Smith McCune *et al* 2017 were cross-sectional comparing to no-HC use.

Several studies have identified variation in the proportion of cells that express CCR5 and CXCR4, HIV co-receptors, with several reports observing increases with DMPA use, mainly with CCR5+CD4+ T cells (*129, 131-133*). Smith McCune *et al* 2017 found increased proportions of CD4+ and CD8+ T cells expressing CCR5+CXCR4+ and CXCR4+CCR5-, while proportions of CXCR4-CCR5+ on CD4+ and CD8+ T cells were seen to decrease (*130*). In contrast, several reports observed no significant association with CCR5+ cell frequency (*125, 128, 134*). From the studies that saw an increase in CCR5+CD4+ T cells; two were based on self-reported use of DMPA (*131, 133*), one saw significance 3-months post-DMPA injection (*132*), and two were sex worker cohorts (*129, 133*) within which it is difficult to discern effects of behavioural differences (i.e. sex frequency). These cohorts also differed geographically.

T cell activation (GRB2, LCP1) was observed by proteomic analysis to increase with DMPA use (*127*). In terms of specific markers of activation, CD25+ (*131*), CD38+HLA-DR+CD4/8+ (*130*), CD38-HLA-DR+CD8+ (*130*), and CD69+ (*133*) cells have been observed to increase with DMPA use. However, several reports have shown no significant change (*125, 128, 131, 132, 134*). The reports that saw an increase in the proportion of lymphocytes expressing these activation markers were cross-sectional in study design and based on self-reported use of DMPA, while the majority of reports that saw no significant change were designed to compare pre-and-post-DMPA injection from samples.

Animal and *in vitro* models have also been utilized to understand the impact of DMPA use on the frequency of immune cell populations. Carias *et al* 2016 observed increased frequencies of CD4+ T cells and CD68+ macrophages with the treatment of a high dose of DMPA in the FGT of rhesus macaques (*110*). The effects of DMPA use have also been explored *in vitro* on DCs isolated from whole blood, where treatment of DCs with physiological concentrations of MPA showed a significant reduction in CD40 expression, which interacts with CD40L (CD154) on activated T

cells (*135, 136*). In their *in vitro* model, Quispe Calla *et al* 2015 showed that the reduced expression of CD40 on DCs treated with MPA limited the ability of DCs to stimulate T cell proliferation (*135*). In line with some *in vivo* studies, treatment of ectocervical explants with MPA showed increased total CD4+ as well as CD69+CD4+ T cell frequency (after MPA incubation for 7-days), with surface expression of CCR5 showing no change (*137*).

Cytokines, chemokines, and other soluble factors. In the review by Hapgood *et al* 2018, they observed inconsistencies regarding specific cytokines, chemokines, and other soluble factors and their observed changes with DMPA use (*124*). As such, they hypothesized that increased inflammation, although inconsistent for certain inflammatory factors, may be a result of the adaptive immunosuppression caused by MPA (*124*).

Recent studies have shown that inflammatory cytokines IL-1α and IL-1β decrease (*125, 128, 132*) in CVL, and an increase (*134, 138*). The two studies observing an increase included healthy women who were sexually active and seeking contraceptive counselling with one measuring RNA expression in ectocervical biopsies (*138*) as opposed to direct concentrations or abundances of cytokines, while the other examined soft-cup (*134*) samples. Besides that, these cohorts differed in geographic location, study design, and sample time points relative to DMPA injection. For IL-10, two studies saw a decrease (*128, 132*) and one observed an increase (*125*) after DMPA initiation. The study that saw an increase included women enrolled in the CONRAD (*125*) randomized clinical trial. A study of pig-tailed macaques supports the observations of Thurman *et al* 2019 (CONRAD study) showing an increase in IL-10 two weeks following DMPA injection (*139, 140*). Expression of either IL-12p40 and IL-12p70 has also been variable, Jespers *et al* 2017 and Dabee *et al* 2019 observed a significant increase (*134, 141*), while Tasker *et al* 2020 observed a decrease (*132*) in DMPA users. For IL-17 which is produced by T helper 17 cells, Tasker *et al* 2020 observed differences in abundance dependent on sample type (*132*). In CVL a significant decrease was observed between baseline and 1-month post-DMPA injection, while in endocervical swabs an increase was observed (*132*). For the adaptive cytokine IFN-γ, recent reports have observed no significant change (*128, 142*), an increase (*134*), or a decrease (*132*). Among chemokines commonly measured factors include RANTES, IL-8, MIP-1α, MIP-3α, MIP-1β, MCP-1, MCP-3, and IP-10. Again, variability in expression of these factors with DMPA use has

been observed. For RANTES a decrease (*128, 132*) or no significant changes (*125, 143*) have been observed. For neutrophil chemokine IL-8 an increase was observed by Jespers *et al* 2017 and Dabee *et al* 2019 (*134, 141*), while Tasker *et al* 2020 observed a decrease (*132*) with DMPA use. For recruitment factors MIP-1α and MIP-1β, both were found to decrease by Tasker *et al* 2020 (*132*), while Jespers *et al* 2017 observed increased (*141*) MIP-1β. No significant change in MIP-1α has also been reported with DMPA use (*125*). Lajoie *et al* 2019*,* after controlling for how long sex work was practiced and douching, observed an increase in MIP-3α (*133*). Tasker *et al* 2020 observed frequency of MCP-1 to decrease 1-month and 3-months following DMPA injection (*132*). Collectively, these studies display a complex, convoluted relationship between cytokines, chemokines, and other soluble factors involved in the recruitment of macrophages, T cells, and neutrophils *in vivo* with DMPA use.

1.7.2 EFFECT OF DMPA USE ON THE COMPOSITION OF THE VAGINAL MICROBIOME

A meta-analysis by Vodstrcil *et al* 2013 focused on studies published before January 2013 and showed decreased incidence of BV, defined by Nugent or Amsel scores, with use of both progestin-based contraceptives and combined hormonal contraceptives (*116*). More recently, Haddad *et al* 2019 showed rates of Amsel-defined BV to decrease with DMPA use (*144*). However, according to the "iceberg" concept, cases of BV by clinical methods of diagnosis do not capture a significant portion of asymptomatic cases with which molecular-BV delineates and has been shown to influence subclinical genital inflammation and risk of STI acquisition (*86*).

Contrary to clinical observations (*144*), in cervical swabs, Byrne *et al* 2016 and Gosmann *et al* 2017 observed no significant change in the microbiome with DMPA use (*131, 145*). This was similarly seen in several much smaller cohorts with DMPA use (*43, 125, 127, 134, 142, 146, 147*). Although compositional changes to the commensal microbiome with DMPA use have also been observed.

Brooks *et al* 2017 observed colonization by BV-associated bacteria including *Atopobium*, *Mobiluncus, Megasphaera, Prevotella, Ureaplasma, Mycoplasma, Fusobacterium, Leptotrichia, Gardnerella, Sneathia,* and BVAB1-3 to be significantly less common with DMPA users compared to non-HC, condom only users (*82*), and observed increased abundance of *L. iners* (*82*).

Similarly, a small longitudinal cohort observed *G. vaginalis* concentrations to decline by 2 orders of magnitude upon DMPA initiation, however, they observed no significant changes in *L. iners*, *L. crispatus*, and *L. jensenii* (*148*). Rather the contrary, Achilles *et al* 2018 observed no significant change in BV-associated bacteria, although their observations are limited to abundances of *G. vaginalis* and *Megasphaera*, additionally they observed decreased concentrations of *L. iners* (*121*). From studies that observed no significant change in microbiome composition; cohort dynamics, sampling, and methods of taxa identification may be potential factors contributing to variability in results. Brooks *et al* 2017 reported on a retrospective study based on self-reported contraceptive use, thus sampling relative to last DMPA injection is likely to be variable between participants with varying serum MPA concentrations (*82*). Achilles *et al* 2018 only measured the abundance of seven bacterial species, four of which were *Lactobacilli* (*L. crispatus*, *L. gasseri*, *L. jensenii*, *L. iners*) and three were BV-associated species *(G. vaginalis, A. vaginae, Megasphaera)* (*121*). Roxby *et al* 2016 also focused on select species as well, specifically *Lactobacilli* (*L. iners*, *L. crispatus*, and *L. jensenii*) and *Gardnerella vaginalis*. Both Achilles *et al* 2018 and Roxby *et al* 2016 used quantitative polymerase chain reaction (PCR) to measure species abundance (*121, 148*). Only two other studies used similar methods and saw no significant change (*125, 146*), however, they did not measure down to the species level, only to genera. Therefore, Achilles *et al* 2018 and Roxby *et al* 2016 may be capturing change not readily detectable in the other studies (Whitney *et al* 2020 and Thurman *et al* 2019). Overall, *in vivo*, the common observation is that DMPA use does not influence the composition of the microbiome. For the exploration of compositional changes to the vaginal microbiome, other model systems are less common. This is due to difficulties emulating the complexity and diversity of bacterial species present in the human vaginal microbiome *in vitro*. Additionally, there are differences in resident bacterial species that are found in different animal models, as such very few reports have examined DMPA use with these model systems.

1.7.3 EFFECTS OF DMPA USE ON THE VAGINAL EPITHELIAL BARRIER

Recent studies employing advanced molecular tools have made observations of a compromised FGT epithelium with DMPA use with a focus on signatures related to the integrity of the epithelial barrier. Such studies included a proteomic analysis of vaginal swabs which showed signatures for vaginal epithelial barrier integrity disruption, pathways associated with injury, cell death, and

decreased tissue adhesion to be overabundant in women using DMPA (*127*). Similarly, another study using whole-genome transcriptomics of cervical tissue showed DMPA users had increased expression of genes involved with tissue necrosis and decreased cellular proliferation (*149*). A study by Zalenskaya *et al* 2018 observed genes associated with the development of the stratum corneum (layer of squamous epithelial cells present at the surface of the epithelium (*150*)) cell junction proteins, and those involved in the epidermal differentiation complex to also be downregulated (*151*). These findings agree with observations in endometrial and ectocervical biopsies (*138, 152*). Simbar *et al* 2007 observed the vascular density of their endometrial biopsies to decrease (*152*). Quispe Calla *et al* 2016 observed permeability of ectocervical tissues to increase with DMPA use and expression of cell junction protein DSG-1 to be decreased (*138*). In contrast, Edfeldt *et al* 2020 and Thurman *et al* 2019 observed no significant change in the thickness of ectocervical and vaginal biopsies at 2 and 6 weeks post-DMPA injection, respectively (*125, 129*). Contrary to the studies that saw a significant decrease in the physical thickness of the FGT epithelium with DMPA, Edfeldt *et al* 2020 and Thurman *et al* 2019 examined cell-cell adhesion protein E-cadherin and physically measured epithelial thickness (*125, 129*), whereas Simbar *et al* 2007 measured vascular density by counting CD34-positive vessels and Quispe Calla *et al* 2016 measured cell junction protein DSG and permeability of the epithelium using a fluorescently labeled dye (*138, 152*). The different methodologies may be a contributor to variability between these studies.

Non-human primate models have also shown thinning of the vaginal epithelium with DMPA treatment (*110, 139, 140, 153*). Carias *et al* 2016, in rhesus and pig-tailed macaques, showed DMPA treatment to associate with the absence of a stratum corneum at the ectocervix and thinning of the vaginal stratum corneum (*110*). Quispe Calla *et al* 2020 also observed thinning of the stratum corneum, decreased expression of cell junctional proteins DSG-1 and DSC1, and increased permeability of vaginal biopsies to low-molecular-weight molecules in rhesus macaques (*153*). Bosinger *et al* 2018 and Butler *et al* 2015 observed thinning of the vaginal epithelium in their pig-tailed macaque models (*139, 140*). These observations were similarly seen in C57BL/6J and humanized (Nod-scid-IL-2Rgc^{Null} with intravenous human peripheral blood mononuclear cells) mouse models with DMPA treatment (*138, 154*). Overall, both *in vivo* and *in vitro* model systems

thus suggest a compromised epithelium whether that be physical thinning or increased permeability of the barrier to small molecules representative of a virion.

1.8 EVIDENCE FOR CONTRACEPTIVE OPTIONS AND HIV OUTCOMES

To answer the long-standing question, whether a causative relationship exists between hormonal contraceptives and HIV acquisition the Evidence for Contraceptive Options and HIV Outcomes (ECHO) trial was designed. ECHO consortium included partners within FHI360, University of Washington, University of Witwatersrand, and the World Health Organization. Funding for this trial was obtained from the Bill & Melinda Gates Foundation, U.S. Agency for International Development, Swedish Sida, and the Wellcome Trust and amalgamated. ECHO took an intent-to-treat approach, randomizing women to one of the three contraceptive options of interest in this study (DMPA-IM, Copper IUD, and LNG Implant) with HIV infection as its primary endpoint. ECHO was poised to longitudinally follow contraceptive initiation from enrollment (pre-contraception) for 18-months, utilizing 12 research sites across the continent of Africa: in eSwatini (1 research site), Kenya (1 research site), South Africa (9 research sites), and Zambia (1 research site). At the time of enrollment, according to UNAIDS data 2020 (www.unaids.org) HIV prevalence in these countries were 28.9, 5.1, 19.3, and 12.2 percent, respectively. Enrollment for the ECHO trial began in December of 2015, with outreach to several clinics (i.e., family planning and reproductive health clinics, post-partum and post-abortion serving clinics) and the general community.

Between 2015 and 2017, the ECHO trial enrolled approximately 7800 sexually active women between the ages of 16-35, whom were HIV-negative and seeking contraceptive counselling. Conditions of enrollment included agreement to use of a randomized method of contraception, although switching their method of contraception once in the trial was supported if necessary. Use of any hormonal, intrauterine or implantable methods of contraceptives at least 6-months before enrollment in the study was an additional exclusion criterion. As mentioned, the women enrolled in the ECHO trial were randomized to DMPA-IM (N=2556), Copper IUD (N=2571), and LNG Implant (N=2588) use - section 2.3 discusses details on each method of contraception. The ECHO consortium took an open-label blinding approach blinding all personnel to contraceptive methods except for the clinician administrating the contraceptive and the women receiving the

contraceptive. Each woman provided samples for post-contraception initiation time points; one month and every three months until the end of the trial (18 months). Basic demographics, contraceptive and reproductive history were recorded before enrollment and at screening. Subsequent visits gathered feedback on the randomized contraceptive method (i.e., side effects) and testing for HIV and STIs (method differed by clinical site). This project had access to a sub-set of samples from the ECHO trial in order to understand mucosal biological mechanisms that may be changing within each contraceptive arm.

1.9 STUDY RATIONAL

Reported observations discussed in the sections above would suggest a trending association between DMPA use and changes in the immunologic/inflammatory, microbiological, and physiological properties of the genital mucosa. In human cohorts these observations include an increase in cervicovaginal CCR5+CD4+ T cells (*129, 131-133*), decrease in vaginal epithelial barrier integrity (*127, 138, 149, 151, 152*), and no significant alteration to the composition of the microbiome (*43, 125, 127, 131, 134, 142, 145-147*). Although, specifically in terms of reported changes of pro-inflammatory cytokines data has been variable between studies. While these studies indicate that the interactions between DMPA and the vaginal mucosa are complex, it generally supports an environment that is less favourable immunologically with significant disruption to the integrity of the vaginal epithelial barrier. These observed alterations to the FGT with DMPA use suggest an environment that is conducive to the acquisition of sexually transmitted infections, such as HIV. Unfortunately, the majority of studies focusing on the risk of HIV infection with DMPA use, for example, were not designed with infection as a primary endpoint. As such, these studies have suffered from many confounding variables. Examples of these biases: include age bias, younger women have tended to favour DMPA use; condom use practices, due to the effectiveness of DMPA, condom usage often becomes less consistent; and lastly, differences in time between sampling and last DMPA injection, which alludes to varying serum MPA concentrations which declines between the first and subsequent injections with peak concentrations observed between 20-30 days (*21, 128*). Understanding the effects of DMPA use, as well as other HCs, at the molecular level within the vaginal compartment is imperative for deciphering how DMPA may be mechanistically compromising the vaginal compartment, and whether this correlation with adverse reproductive health outcomes (i.e., STI/HIV infection).

1.10 HYPOTHESES

(1) Progestin-based contraceptives (DMPA and/or LNG Implant) will increase proteomic signatures relating to genital inflammation and decrease signatures relating to epithelial maintenance and repair in comparison to the non-hormonal Copper IUD arm, signatures that we suspect to associate with HIV acquisition in ECHO trial participants in this cohort.

(2) Progestin-based contraceptive (DMPA and/or LNG Implant) initiation will have no effect on the diversity and composition of the vaginal microbiome which is similarly expected with use of the non-hormonal Copper IUD.

1.11 OBJECTIVES

(1) To determine the longitudinal effect of DMPA-IM and LNG Implant initiation on the host proteome, with comparisons to Copper IUD use.

(2) To determine the longitudinal effect of DMPA-IM and LNG Implant on the vaginal microbiome composition, in addition to exploring bacterial metabolic pathway changes that are observed upon initiation with each contraceptive arm. All of which in comparison to use of the Copper IUD.

(3) To determine whether proteomic signatures and microbiome composition changes observed with contraceptive use are associated with HIV seroconversion in the Case/Control component of the ECHO ancillary cohort.

CHAPTER 2: MATERIALS AND METHODS

2.1 STUDY POPULATION

2.1.1 MUCOSAL BIOMECHANISMS SUB-STUDY OF THE ECHO TRIAL

This project, conducted in the lab of Dr. Adam Burgener at the J.C. Wilt Infectious Disease Centre, involved a subset of samples from the ECHO parent trial to determine mucosal biological mechanisms associated with contraceptive use and their relationship with HIV acquisition risk. Eligibility criteria mirrored that of the parent ECHO trial, although to participate in this sub-study additional consent was required. We received mucosal samples from 202 women from sites in South Africa (University of Cape Town (UCT) Emavundleni Research Centre and Wits Reproductive Health and HIV Institute (WRHI)) and Kenya (Kenya Medical Research Institute). The UCT Emavundleni Research Centre and WRHI sites in South Africa enrolled 82 and 60 women, respectively, and in Kenya, 60 women participated. Women were randomized to use of DMPA-IM (N=69), Copper IUD (N=67), and LNG-Implant (N=66). Mucosal samples were received at enrollment (baseline) and post-contraception (month 1 and 3) initiation. Within each contraceptive arm, this study was powered (>80%) to detect a moderate effect size between pre- and post-contraceptive initiation with DMPA (FC=0.48), Copper IUD (FC=0.50) and LNG Implant (FC=0.49) use. This project also had access to another subset of samples from the ECHO trial to identify proteomic changes relating to HIV seroconversion, determined following PCR positive identification. For this study 2 age and timepoint matched controls were chosen for each randomly selected HIV seroconversion sample. We received 127 randomly selected mucosal samples from seroconverted women (N=22 cases) and their age-matched controls (N=105 controls). For the women that seroconverted, we received mucosal samples immediately preceding seroconversion. We were 80% powered to detect an effect size of 0.66 between cases and controls.

2.2 SAMPLE COLLECTION

Mucosal samples using disposable menstrual cups, referred to as soft-cup samples, were collected by licensed professionals at the defined clinical sites mentioned above. Collection of soft-cup samples involved the use of commercially available menstrual cups which are generally made up of either medical-grade silicone, rubber, latex or elastomer and inserted in the vagina for fluid collection. Upon collection, samples were immediately stored at -80°C. The Burgener lab received

403 mucosal samples. Once received, before commencing our proteomic sample processing pipeline, each sample was lab spun down at 14,000xg for 20 minutes, pelleting any cellular debris. The supernatant was then aliquoted and stored at -80°C for use in our proteomic sample processing pipeline.

2.3 BCA (BICINCHONINIC ACID) PROTEIN ASSAY

Total protein content of all 403 mucosal samples was determined using a BCA assay (EMD Millipore) following the standard protocol provided by the manufacturer. In summary, standards were prepared using bovine serum albumin (BSA; 2mg/mL) supplied by the EMD Millipore BCA assay kit and was serially diluted with distilled water (dH2O) for concentrations between 0-1000µg/mL. The resulting standard curve determined the unknown protein content in our mucosal samples. The predominant dilution for our standards and mucosal samples was a 1:5 dilution, in duplicate, in a 96-well plate. For each sample whose protein concentration surpassed the maximum of the standard curve, the assay was repeated at a 1:25 dilution. BCA working reagent was prepared as a master mix consisting of 1ml of BCA solution and 20µL of 4% Cupric Sulfate (w/v), 200µl of this master mix was then added to each well using a multi-channel pipette. The plate was then allowed to incubate at 37°C for 30 minutes with absorbance subsequently read at 562nm using a microplate reader (Biotek Synergy H1 Hybrid Reader, Gen5 v2.05, VT, USA).

2.4 PROTEIN DIGESTION AND MASS SPECTROMETRY RUNS/ANALYSIS

2.4.1 OVERNIGHT TRYPSIN DIGESTION

A standard digestion protocol for biological samples (i.e., mucosal samples) as previously described (*155*), was used, with modifications described below. Following protein quantification by BCA assay (See Section 2.4), µg of protein necessary for trypsin digestion was determined. For the majority of samples 50µg of protein were digested and for clinical samples for which we were provided lower volumes (<200ul) 25µg of protein were digested.

Mucosal samples underwent protein denaturation using 600µL of 8M Urea (CH_4N_2O) Exchange Buffer (UEB). Samples were incubated for 10 minutes at room temperature in UEB before the digestion protocol commenced. Preparation of the Nanosep® with 10K Omega cartridges (Pall Corporation) involved adding 200uL of mass spectrometer (MS)-grade or double-distilled H2O

(ddH2O) and allowing the water to pass through the cartridge and into the collection tube underneath using a microcentrifuge for 1 minute at 10,000xg. Subsequently, 200µL of UEB was added and allowed to pass through for 2 minutes. Following preparation of the cartridges, sample was added and spun down for 5 minutes at 10,000xg. Once the entire sample had been loaded and passed through the cartridges, cartridges were then washed 3-times with UEB for 5 minutes at 10,000xg. Throughout the digestion protocol, in order to avoid compromising peptide yield, caution was practiced avoiding drying out the filter.

After centrifugation, the remaining protein samples within the cartridges was treated with 100µl of DL-Diotheritol (DTT; Sigma; MO, USA) for 20 minutes at room temperature to reduce protein disulfide bonds. Following DTT, each sample was treated with an alkylating agent, iodoacetic acid (IAA; Sigma; MO, USA), for 20 minutes to prevent reforming of disulfide bonds giving access to digestive enzymes in coming steps. Each denatured sample was subsequently washed with UEB and HEPES (4-(2-hydroxyethyl)-1-piperazineethanesulfonic acid). Finally, 50µL HEPES solution containing 2µg of trypsin (Promega; WI, USA), a serine protease, was added to the cartridges and incubated at 37℃ overnight, cleaving the polypeptides at their lysine and arginine residues. The resulting cleaved peptide solution was then eluted by adding HEPES and centrifuged at 10-14,000xg until the entire elute was retrieved. Using the vacuum centrifugation, the peptide solution was dried (2-3 hours) into a gel-like pellet and stored at -80℃ for later use.

2.4.2 REVERSE PHASE LIQUID CHROMATOGRAPHY

Cleaning of peptide pellets was conducted using reverse-phase liquid chromatography (LC; high pH RP, Agilent 1200 series micro-flow pump, CA, USA; Water XBridge column C18 3.5µm, 2.1x100mm, ON, Canada) of sample resuspended in 40µL of buffer A solution (20mM ammonium formate, pH 10) to remove any salts or detergents lingering from the digestion protocol. The LC operates by a step-function gradient which elutes peptide from each sample in a single-fraction manner using a buffer solution of 97% buffer A and 70% buffer B (90% acetonitrile; 20mM ammonium formate, pH 10) at a flow rate of 150 ul/min for approximately 27 minutes per sample. The cleaned peptide solution was then dried by vacuum centrifugation and stored at -80℃ for later use.

2.4.3 PEPTIDE QUANTIFICATION

LC cleaned peptide pellets were resuspended in 100uL MS-grade H2O and quantified for peptide using the Pierce Quantitative Fluorometric Peptide Assay (Thermo Fischer Scientific; IL, USA). Standard peptide concentrations (0-1000µg/mL) were prepared using the supplied peptide standard (1 mg/mL; tryptic digestion of protein standard in 50mM ammonium bicarbonate and 0.05% sodium azide) and serially diluted with MS-grade H2O in sterile Eppendorf tubes. Standards (10µL) and resuspended sample (10µL of a 1:4 dilution of the sample) were added to a flat bottom black-96 welled microplate in duplicate (when calculating final peptide concentration fluorescence readings were averaged). Using a multichannel pipette, 70µl of Fluorometric peptide assay buffer was added followed by 20µL of Fluorometric peptide assay reagent. The test plate was then shielded from light using an aluminum foil cover and allowed to incubate for 15 minutes at room temperature. Fluorescence was determined using a microplate reader (Biotek Synergy H1 Hybrid Reader, Gen5 v2.05, VT, USA) at Excitation/Emission wavelengths of 390nm/475nm, respectively.

2.4.4 MASS SPECTROMETRY

Sample preparations for the mass spectrometer (MS) involved prepping each sample for a concentration of 0.125µg/ul, translating to 0.25µg of peptide per 2µl injection in buffer A (2% acetonitrile and 0.1% formic acid). For this project, LC/MS/MS analysis involved the Q Exactive (QE) Quadrupole Orbitrap mass spectrometer. The method used by the QE involves an injection of 2µl of each sample into the nano-flow LC system that is connected inline to the QE mass spectrometer. Within the QE system peptide separation occurs using a 50cm long, 2.0µm particle-size Easy Spray C-18 column with an elution gradient at a constant flow rate of 200 nl/min using 98% buffer A and 30% buffer B for 200 minutes. From the orbitrap analyzer, MS-spectra with a resolution of 70 000, 200m/z was obtained. The most prominent precursor ions (n=15) were then chosen for fragmentation by higher-energy collisional dissociation with a 28% normalized collision energy colliding with neutral molecules. Generated fragments then underwent mass analysis by injection back into the orbitrap at 17,500 resolution, 200m/z. Files received from the mass spectrometer include MS/MS spectra for each sample (.raw).

2.4.5 PROTEOMIC DATA ANALYSIS

MS/MS spectra from the mass spectrometer was processed through several types of proteomic software to identify host and bacterial peptides within the vaginal mucosa.

Host proteome: MS spectra was imported into the Progenesis LC-MS software (Nonlinear Dynamics, New Castle, UK) to align sample ion intensity maps to a chosen reference sample, to account for variation been MS runs. This allows for between-sample comparisons. Reference samples were made by pooling approximately 37% of the pre/post sample cohort and were run on the MS every 10 samples. Following alignment, to filter out contaminate peptide ions (which include peptides where cleavage was incomplete or peptides that are too small to make confident identifications), charge states between +2 and +7 were retained. Additional filtering involved retaining peptides with retention times between 10 and 125 minutes, discarding peptides with retention times before 10 minutes and in the last 15 minutes of the MS run.

Based on retention time and mass (m/z), peptide ions were grouped and identified by Mascot Daemon (Matrix Science, London, UK), mapping peptide amino acid sequences against a curated Human-only UniprotKB/SwissProt search parameter. Validation of peptide identifications was then carried out by uploading Mascot DAT files into Scaffold (Proteome Software, OR, USA) with the following criteria: 80% peptide identification confidence, 95% protein identification confidence, with a minimum of 2 peptides identified for each protein at a false discovery rate of <1%. The spectrum report was then exported from Scaffold and uploaded back into Progenesis to match the compound (peptide) list made in Progenesis with the identifications made by Mascot and validated in Scaffold. Peptide and Protein measurements were then exported from Progenesis.

Microbial proteome: Mascot generic files **(**Mgf) files from the mass spectrometer were imported into Mascot to map peptide amino acid sequences to the vaginal metaproteome (VMP) database, curated from the CAPRISA-004 cohort (*156*). The resulting Mascot files (.DAT) were then uploaded into Scaffold with the same validation criteria as seen with the host proteome. The following scaffold files were then exported: accession, protein, peptide, and sample reports for analysis of the microbial proteome. Functional annotation of the bacterial proteome was conducted using Kyoto Encyclopedia of Genes and Genomes (KEGG) which is publicly available tool for

matching gene and genome information with available functional profiles. KEGG provides pathway level information which is referenced in this thesis as b-level and ko-level pathways. B-level pathways refer to the overarching pathway (i.e., carbohydrate metabolism), while the ko-level provides a more specific description of the pathway (i.e., glycolysis).

2.5 STATISTICAL ANALYSIS OF PROTEOMIC DATA

2.5.1 DATA CLEANING PIPELINES FOR PREPARATION OF DATASET FOR STATISTICAL ANALYSIS

Determination of technical variability and sample outliers: Potential sample outliers were determined by comparing median protein abundance within each MS batch. Sample outliers in each run were determined by looking at median protein abundance with those outside the 1.5X interquartile range being flagged and noted as a potential outlier (Figure 1A). To further validate, hierarchical clustering further distinguished 'true outliers', based on whether flagged outliers clustered together, and subsequently removed them from downstream analysis. (Figure 1B). Variability between samples was determined using mixes. The mixes are a pool of samples from the cohort, its purpose being to represent the majority of host proteins identified in the cohort. Covariance was determined using these replicates. A covariance greater than 25% was our threshold for exclusion of proteins for downstream analysis.

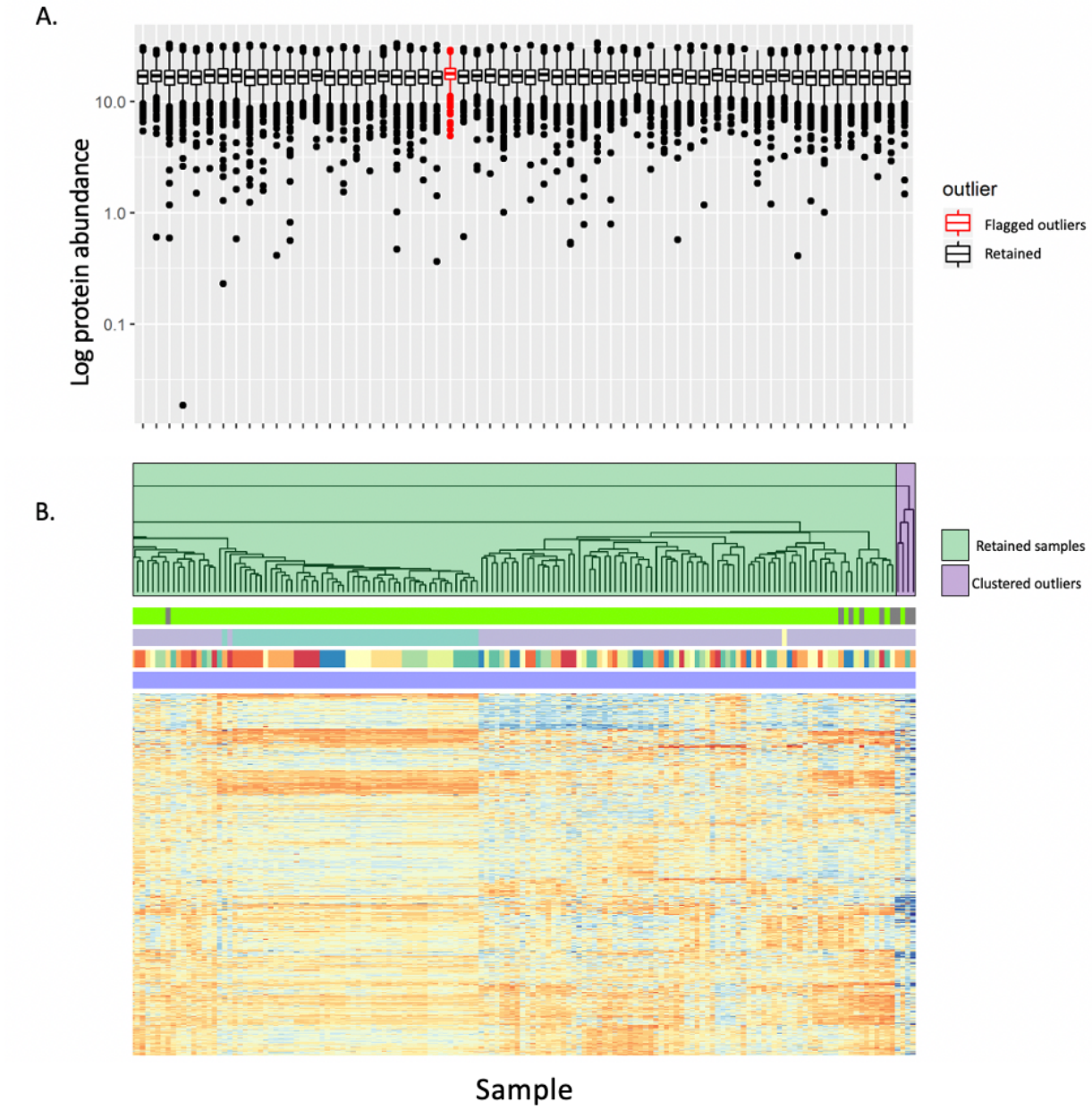

Figure 1. Example of quality control figures obtained during data cleaning pipelines for determination of sample outliers. (A) Example outlier determination plot which was obtained for each batch of samples run on the MS. Figure represents protein abundance for each sample in the batch. Median abundances were compared between each sample, with those that fall outside 1.5 times the interquartile range flagged as a potential outlier in red. (B) Hierarchical clustering analysis of all samples, from each MS batch, and their protein abundances shows clustering of flagged outliers to the far right of graph (purple box). Samples that were flagged as an outlier in A and were then observed to cluster in B were deemed true outliers and removed from downstream analysis.

Normalization of proteome datasets: Normalization of the host proteome involved dividing the total abundance of each protein in each sample to their mean followed by log (base 2) transforming the entire dataset. Our microbial data set, containing genus abundance data, was normalized by centered-log ratio transformation using the "clr" function from the "rgr" package in R. The functional bacterial proteome datasets did not undergo normalization, analysis instead involved protein proportion data (relative to total bacterial protein count for each woman) obtained following power curation. To focus on bacterial pathways that are most prevalent in this cohort power curation was conducted, curating the functional dataset to pathways with 80% power which associated with a coefficient of variance cut-off of 3.49. In addition, proteins that were found to be present in less than 5 women were removed from analysis.

2.5.2 METHODS OF STATISTICAL AND PATHWAY ANALYSIS

2.6.2.1 INFLUENCE OF TECHNICAL AND CLINICAL VARIABLES ON PROTEOME VARIABILITY: The influence of technical variables on variability was determined using Principal Variance Component Analysis (PVCA). For this study, technical variables were defined as those relating to sample processing. PVCA incorporates the strengths of principal component analysis (PCA), reducing the dimensionality of the data without compromising variability, and variance component analysis (VCA), using the variables of interest as random effects to estimate their influence on variability. Combining these models to express the effect of each variable as a proportion of weighted average variance. Clinical variables included those gathered during study enrollment and after contraception initiation and curated to those of particular interest for our study purposes. Significance for clinical variables was determined by Chi-square analysis.

*2.6.2.2 UNIVARIATE ANALYSIS***:** Differential protein abundances were determined by a paired student t-test comparing baseline and post time points within each contraceptive arm for the host proteome and Wilcoxon rank-sum test for the bacterial proteome. Multiple comparison corrections involved the Benjamini-Hochberg (BH) False Discovery Rate (FDR) method ($q<0.05$). In this study, significance was defined as having a p-value<0.05 and FDR-BH p-value<0.05. Functional annotation of significant host proteins was conducted using the following software: Database for Annotation, Visualization and Integrated Discovery (DAVID; MD, USA; v6.8) and ConsensusPathDB-human (release 34; Berlin, Germany). ConsensusPathDB-human was used for

host factor lists that were too short to produce valuable pathway information using DAVID. Pathway analysis was conducted using Ingenuity Pathway Analysis (IPA, Qiagen; Valencia, CA, USA; v51963813) with enriched pathways of interest having P-Values<0.05 and z-scores greater than +2.000 or less than -2.000. Pathway analysis of the bacterial proteome (b- and ko-level), did not include cancer relating pathways even if significance was observed.

2.6.2.3 MULTIVARIATE ANALYSIS: The purpose of multivariate analysis is to determine features in a model that predict overall variation by looking at the biological system as a whole. For this study, feature selection was done using Least Absolute Shrinkage and Selection Operator (LASSO) regression with their effectiveness at explaining the variability tested using partial least squares discriminant analysis (PLS-DA) via R programming. LASSO selects a minimum number of features that distinguish a binary variable, in this case, timepoint (baseline vs. month 1). The selected features were then incorporated into the PLS-DA model to determine how effective these host factors were at influencing the variability observed with M-fold (m=5) validation randomly dividing and excluding subsets equal in size to the LASSO features selected, this model was then repeated 1000 times. The error rate was then obtained to provide an experimental p-value, to determine if the LASSO selected features best describe the model.

2.6 CONTRIBUTIONS TO THIS PROJECT

This sub-study looking at biological mechanism (BioMech) changes within each contraception arm from the ECHO trial was led by Renee Heffron and Heather Jaspan, and included Adam Burgener, Jo-Ann Passmore, and Steven Bosinger. Together the BioMech team designed this sub-study and received R01 NIH funding. The Burgener lab received samples for conducting proteomics analysis. I (Hossaena Ayele) carried out BCA assays for all samples (for both the pre/post contraception and case/control cohorts) and the trypsin digestions for 94.3% (380/403) of samples from the pre/post contraception cohort, while the remaining 5.7% (23/403) of digestions were carried out by Kat Kratzer for the pre/post contraception cohort. For the case/control cohort (N=127) I carried out all trypsin digestions. Following digestions, I prepared all the samples for LC cleaning (both cohorts, N=530). Max Abou operated the LC for all the samples. Following LC cleaning, I dried down and peptide quantified all of the samples (both cohorts, N=530). I prepared all samples for the MS for specific injection concentrations (both cohorts, N=530). Stuart

McCorrister and Chris Grant from MS core at the Public Health Agency of Canada ran all samples on the Q-Exactive MS. I processed the host and bacterial MS data for both cohorts (N=403 pre/post contraception cohort and N=127 case/control cohort) using several proteomic software – a pipeline previously determined and is common practice in the Burgener lab for making protein identifications. I ran the resulting data through the Burgener lab quality control and batch correction R scripts for host and microbial data (scripts previously developed by Laura Noël-Romas, Samantha Horne and Sarah Mutch) with additional validation carried out by Laura Noël-Romas (host data) and Samantha Horne (microbial data). I carried out all statistical analysis of the host, and bacterial data that was gathered and clinical data that we received, with consultation from Laura Noël-Romas and Samantha Horne on appropriate statistical methods and R programming functions. For more complicated machine learning techniques Laura Noël-Romas and Samantha Horne helped me produce an appropriate R script. I carried out the interpretation of all the observations for this project with guidance provided my supervisor Adam Burgener. Additional guidance was received from Laura Noël-Romas and Kenzie Birse.

CHAPTER 3: RESULTS

3.1 OPTIMIZATION OF PROTEOMIC DATA COMPARING PRE- AND POST-CONTRACEPTIVE INITIATION

Across 403 samples from 202 women (contraceptive break down being 69 DMPA-IM, 66 LNG Implant, and 66 Copper IUD) this study identified 634 unique host proteins. Following matching of sample identifiers, to ensure each woman had one baseline and post sample (either month 1 or month 3), our final dataset included 394 samples from 197 women. The majority of post-samples timepoints were collected 1-month after contraception initiation. However, 11 women had their post sample collected 3-months post-initiation (6 using Copper IUD, 2 using DMPA-IM, and 3 using LNG Implant). Herein, when referencing post-contraception initiation sample timepoints this thesis will reference them as "1-month sample timepoints", despite the inclusion of 11 total 3-month timepoints.

For the microbial component of this project, our quality control procedures identified one 1-month sample to lack bacterial data. As a result, this sample and its matched baseline sample were removed. The resulting final dataset for microbial analysis thus consisted of 392 samples from 196 women. Across the 392 samples (focusing on KEGG path type 'pathway') this project identified 439 bacterial proteins, 1419 bacterial protein groups, 163 ko-level pathways and 38 b-level pathways. Following power curation, for bacterial functional analysis, this project identified 356 bacterial proteins, 1237 bacterial protein groups from 46 ko-level and 23 b-level pathways from samples with sufficient bacterial functional data (N=390).

3.2 COHORT DETAILS

In this subset of the ECHO trial, demographic information is summarized in Table 1. Women enrolled were on average 24.15 ± 4.49 years of age with the majority (69.5%) from South Africa, while the remainder of women were from Kenya (30.5%). The women enrolled had an average body mass index (BMI) of 26.64 ± 6.78. At the time of enrollment, the women were either married (27.9%) or never married (71.6%) and had at least attended or completed secondary school (72.1%). The majority of women had been pregnant at least once or more (83.2%) with 1 to 2 living children (67%). In the cohort, the incidence of *Neisseria gonorrhoeae*, *Chlamydia trachomatis*, and yeast was 6.1%, 15.7% and 6.6%, respectively. Herpes-Simplex 2 virus

(serologic test) had an incidence of 50.3% and bacterial vaginosis (Nugent 7-10) at an incidence of 32%. The women in this cohort reported having at least 1 (<=1) partner (91.4%) with a majority having no new sexual partners in the last 3-months (92.9%). With their last vaginal sex act, which the majority reported being more than 3 days before their baseline visit (59.4%), the women reported a nearly equal likelihood of using a condom (49.2%) to non-condom use (47.2%) although in the last 3-months the majority of women reported having practiced unprotected sex (69.5%). The primary partner of these women was, for the most part, were circumcised (78.7%) and HIV negative (73.6%).

3.3 DETERMINATION OF POTENTIAL CONTRIBUTIONS OF TECHNICAL VARIABLES TO PROTEOMIC VARIANCE

Principal variance component analysis (PVCA) was used to explore the effect of sample processing variables (collected throughout the digestion protocol and peptide identification protocol) on the overall proteome variability. This is important to determine whether batches created during each step of the proteomics sample processing pipeline would have a potential confounding effect on the observations made in this thesis. Specific variables of interest included: MS batch number, presence of blood seen as visible discoloration, calendar date of the BCA assay, number of times the BCA assay was performed on a sample, protein content (determined by BCA assay), number of times the sample underwent digestion, calendar date of protein digestions, calendar date of LC cleaning, and calendar date of when peptide quantifications were performed. From the variables of interest (listed above), 4 were identified to have a weighted percent variance greater than 1% (Table 2), including protein content, presence of blood, number of times the sample underwent digestion, and calendar date of LC cleaning, meaning some effect is likely (Figure 2). However, for this project variables with a weighted percent variance >5% were considered to be of particular concern, potentially acting as confounding variables. These variables included protein content and presence of blood.

Table 1a. Baseline demographic information collected at enrollment or screening for this subset of the ECHO trial cohort.

	Average (± SD*)	N	%
		N=197	
Kenya		60	30.46
South Africa		137	69.54
Age	24.15 ± 4.49		
Marriage category			
Married		55	27.92
Never married		141	71.57
Education			
Secondary school, some or complete		142	72.08
Number of times previously pregnant	1.49 ± 1.14		
Number of kids	1.37 ± 1.04		
BMI (kg/m2)	26.51 ± 7.03		
Cervical ectopy >1%❖		85	43.15
Infections and vaginal Dysbiosis[a]			
Negative for *Neisseria gonorrhoeae*		184	93.40
Negative for *Chlamydia trachomatis*		165	83.76
Positive for Herpes-simplex 2		99	50.25
Bacterial Vaginosis (Nugent score)	3.84 ± 3.78		
Negative **(0** to **3)**		109	55.33
BV **(7** to **10)**		63	31.98
No observed yeast infection		184	93.40

Additional Information
*SD = standard deviation
❖186 women were not checked for cervical ectopy.
[a]One women did not have a reported *N. gonorrhoeae* and *C. trachomatis* result and two women did not have a documented HSV-2 result.

Table 1b. Behavioural demographics at enrollment and contraceptive effects post-contraception initiation for this subset of the ECHO trial cohort.

	Average (± SD*)	N	%
		N=197	
Number of partners in last 3 months	1.091 ± 0.31		
No new sexual partners in last 3 months⊙		183	92.89
Condom used with last vaginal sex act*		97	49.24
Any practice of unprotected sex in the last 3 months		137	69.54
Primary partner is HIV negative^		145	73.60
Partner is circumcised¶		155	78.68
Practiced vaginal sex >3 days ago †		117	59.39
Contraceptive effects#			
Bleeding pattern			
Regular		88	44.67
Spotting only		15	7.61
Irregular		16	8.12
No bleeding		61	30.96
Duration of vaginal bleeding			
Too short		10	5.08
About right		84	42.64
Too long		25	12.69
Vaginal irritation			
No		176	89.34

Additional Information

⊙ One women did not report whether they had any new sexual partners in the last 3 months

*7 women reported they had a partner but were not sexually active

^46 women did not know whether their partner was HIV positive or not, while one woman did not report anything

¶ Two women did not know whether their partner was circumcised while one woman did not report anything

† 8 women did not report when they last had vaginal sex.

#For data on contraceptive effects 17 women were unchecked for bleeding pattern, 78 were unchecked for the duration of vaginal bleeding, and 17 were unchecked for vaginal irritation with contraceptive use

Table 2. Sample processing variables determined by principal variance component analysis to have a percent weighted variance greater than 1%.

Sample Processing Variables	Weighted Percent Variance (%)
Residual	80.04
Protein Content	6.26
Presence of blood in sample	5.56
Number of times sample underwent a digestion	3.32
Calendar date of LC cleaning	2.35

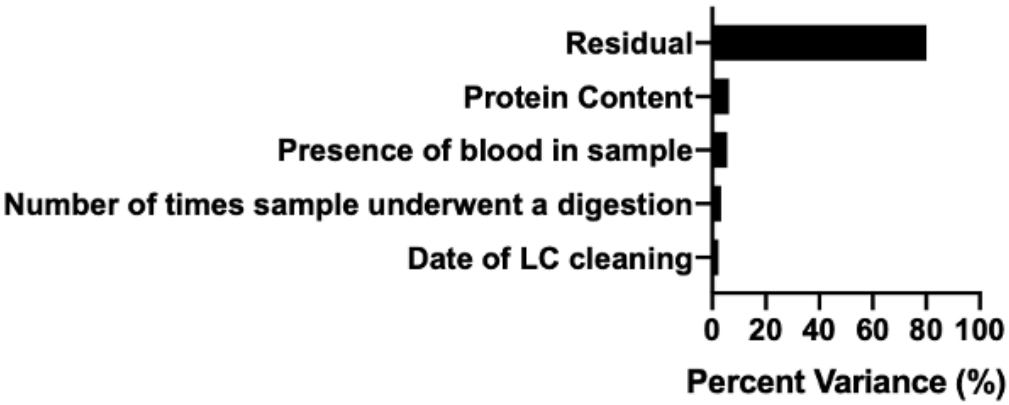

Figure 2. Sample processing variables that contribute to host proteome variability as determined by principal variance component analysis. Sample processing variables are those documented during sample processing. From the total sample processing variables tested (N=9) those that are shown here to have a percent weighted variance greater than 1%.

3.4 DETERMINATION OF POTENTIAL CLINICAL VARIABLES THAT MAY PRESENT AS CONFOUDING VARIABLES

Clinical variables of interest for this cohort were collected at baseline [age, marriage category, education category, BMI category, clinical site, number of times previously pregnant, number of living children] and during the physical exam at enrollment [cervical ectopy, HSV-2 status (positive or negative), *Chlamydia trachomatis* status (positive or negative), *Neisseria gonorrhoea* status (positive or negative), bacterial vaginosis and presence of yeast] before contraceptive initiation (Table 3). Additional clinical variables were related to contraceptive side effects and included bleeding pattern, duration of bleeding, and vaginal itch. Information collected during the ECHO trial on behavioural patterns considered the number of partners in the last 3-months, new sexual partners in the last 3-months, condom use with their last vaginal sex act, practiced any unprotected sex in the last 3-months, HIV status of their primary partner, whether their primary partner is circumcised, and their last vaginal sex act (in days). Comparison of these variables between contraceptive arms by Chi-square test revealed no significant differences (Table 3), except in bleeding pattern following contraceptive initiation (P-value = 4.41E-05).

Table 3a. Comparisons of demographic variables collected at enrollment and screening between contraceptive arms.

	Copper-IUD (N, %)	DMPA-IM (N, %)	LNG Implant (N, %)	P-ValueΦ
	n=64	**n=67**	**n=66**	
Location				0.98
Kenya	20 (31.25)	20 (29.85)	20 (30.30)	
South Africa	44 (68.75)	47 (70.15)	46 (69.70)	
Age at enrollment[a]	24.05±5.01, 16-35	24.40±4.31, 18-35	24.00±4.18, 18-34	0.95
Never married	49 (76.56)	48 (71.64)	44 (66.67)	0.47
Education level (Secondary school)	42 (65.63)	49 (73.13)	51 (77.27)	0.42
Number of times pregnant (>=1)	52 (81.25)	58 (86.57)	54 (81.82)	0.67
Number of children (1 to 2)	42 (65.63)	46 (68.66)	44 (66.67)	0.95
BMI (kg/m2) <=30	46 (71.88)	49 (73.13)	48 (72.73)	0.95
Cervical ectopy >1%	24 (37.50)	35 (52.24)	26 (39.39)	0.24
Infections and vaginal dysbiosis				
Neisseria gonorrhoeae				0.75
Negative	59 (92.19)	63 (94.03)	62 (93.94)	
Chlamydia trachomatis				0.14
Negative	50 (78.13)	56 (83.58)	59 (89.39)	
Herpes-simplex 2				0.63
Positive	31 (48.44)	37 (55.22)	31 (46.97)	
Bacterial Vaginosis (Nugent score)				0.69
Negative (0 to 3)	32 (50.00)	41 (61.19)	36 (54.55)	
Intermediate (4 to 6)	10 (15.63)	8 (11.94)	7 (10.61)	
BV (7 to 10)	22 (34.38)	18 (26.87)	23 (34.85)	
Yeast infection				0.079
Not observed	61 (95.31)	65 (97.01)	58 (87.88)	

Additional Information

Φ P-values were determined using chi-square analysis, for categories consisting of <5 women approximate p-values were determined. Chi-square tests for each variable of interest included additional variables not highlighted in the above table. Age comparisons were made between those that were above 25 and below 25. For marriage category women that reported being previously married and currently married were included. For education category women that reported no schooling, only post-secondary, and primary school education were included. For cervical ectopy women were compared to those with 0% ectopy. For Body mass index (BMI) women that had a BMI >30 was included. For the number of children variable comparison included women that had either no kids and those that had more than or equal to 3 children. For number of times previously pregnant, women that had reported never being pregnant were included. STI comparisons included women that were positive for the respective STI with the exception of HSV-2 which included a comparison of women that were positive to those that were negative or indeterminant for HSV-2 and for the yeast infection variable comparisons were made with respect to observed yeasts.

[a]Age in this table was reported as mean ± standard deviation, range.

Table 3b. Comparison of behavioural demographics collected at enrollment and contraceptive effects following contraceptive initiation between contraceptive arms.

	Copper-IUD (N, %)	DMPA-IM (N, %)	LNG Implant (N, %)	P-ValueΦ
	n=64	**n=67**	**n=66**	
Number of partners in last 3 months				0.27
<=1	56 (87.50)	61 (91.04)	63 (95.45)	
No new sexual partners in last 3 months	59 (92.19)	60 (89.55)	64 (96.97)	0.34
Condom used with last vaginal sex act	28 (43.75)	36 (53.73)	33 (50.00)	0.53
Any practice of unprotected sex in the last 3 months	47 (73.44)	46 (68.66)	44 (66.67)	0.69
Primary partner is HIV negative	47 (73.44)	49 (73.13)	49 (74.24)	0.089
Partner is circumcised	53 (82.81)	54 (80.60)	48 (72.73)	0.41
Practiced vaginal sex >3 days ago	43 (67.19)	47 (70.15)	46 (69.70)	1.00
Contraceptive effects				
Bleeding pattern				**<0.00010**
Regular	41 (64.06)	17 (25.37)	30 (45.45)	
Spotting only	4 (6.25)	6 (8.96)	5 (7.58)	
Irregular	5 (7.81)	4 (5.97)	7 (10.61)	
No bleeding	6 (9.38)	33 (49.25)	22 (33.33)	
Duration of vaginal bleeding				0.65
Too short	3 (4.69)	4 (5.97)	3 (4.55)	
About right	35 (54.69)	19 (28.36)	30 (45.45)	
Too long	12 (18.75)	4 (5.97)	9 (13.64)	
Vaginal irritation				0.77
No	55 (85.94)	58 (86.57)	63 (95.45)	

Additional information

Φ P-values were determined using chi-square analysis, for categories consisting of <5 women approximate p-values were determined. Chi-square tests for each variable of interest included additional variables not highlighted in the above table. For number of partners a woman had in the last 3-months women that reported having more than 1 partner were included. For whether the women reported having a new sexual partner in the last 3-months women that reported "yes" were included. For whether condom was used with their last vaginal sex act, women that reported no or reported having a partner, but no sex, were included. For whether unprotected sex was practiced in the last 3-months women that reported "no" were included. For whether the woman's primary partner was on ARV women that reported "yes" were included. For whether their primary partner is circumcised women that reported "no" were included. For when the last time the women practiced vaginal sex comparisons were between >3 days and <=3days. Finally, for whether vaginal irritation was experienced following contraception initiation variable comparisons included those that reported irritation.

3.5 OBJECTIVE 1: LONGITUDINAL HOST PROTEOMIC CHANGES WITH CONTRACEPTIVE USE

The aim of this objective was to compare host mucosal proteomic changes observed at enrollment to changes observed following 1-month of contraceptive use for each contraceptive group.

3.5.1 HOST PROTEOMIC CHANGES OBSERVED FOLLOWING 1-MONTH OF DEPO-MEDROXYPROGESTERONE ACETATE (DMPA-IM) USE

Within the DMPA-IM arm, the Burgener lab received samples from 67 women. Use of DMPA-IM for 1-month was associated with differential protein abundance of 116 host proteins; only 19 of which passed BH multiple comparison correction of 5% (Supplementary Table 5) while 97 did not (P-value <0.05, FDR-BH >5%) (Figure 3). Of the 19 host proteins that passed multiple comparison correction, 10 host proteins were observed to increase (fold change range between 0.53 to 1.15) in abundance after 1-month of DMPA-IM use and 9 were observed to decrease (fold change range between -0.92 to -0.57) (Figure 3 and 4). Functional annotation of the BH significant host proteins use was conducted using ConsensusPathDB (Table 4). ConsensusPathDB revealed host pathways increasing with DMPA-IM use to include the regulation of programmed cell death (P=0.00057, Q=0.0079), carboxylic acid metabolic processes (P=0.0011, Q=0.0086), and regulation of protein metabolic process (P=0.0088, Q=0.040) (Figure 5; Table 4). An increase in these pathways indicate an increase in necessary cellular processes. Host pathways observed to decrease included positive regulation of immune response (P=0.00039, Q=0.0039) and regulation of innate immune response (P=0.00059, Q=0.0040) (Figure 5; Table 4).

Looking specifically at the 19 differentially abundant proteins we see proteins associated with the physical barrier and immune response, to name a few. These proteins include TGM3, MUC5B and MUC5A. TGM3 or Protein-glutamine gamma-glutamyl transferase E or transglutaminase 3, is involved with the development of the cornified envelope which is formed within the layer of the vaginal epithelium where terminally differentiated squamous epithelial cells are located (*150*). MUC5A and MUC5B are gel-forming mucins secreted by mucosal epithelial cells into the mucosal fluid contributing to the overall physical barrier of protection against invading pathogens (*157*). Mucin glycoproteins are extensively glycosylated, resembling a filamentous protein (*157*). Their glycosylated components comprise 70% of their total mass, with an influence on the viscosity of

the vaginal mucus (*157*). An association between mucins and innate immune response has been observed through the regulation of their expression by inflammatory cytokines (IL-1β, IL-4, IL-6, IL-9, IL-13, interferons and tumour necrosis factor-α) (*157*). Mucins have also shown anti-microbial and anti-viral characteristics. In saliva concentrated for MUC5B and MUC7, anti-HIV activity has been observed (*158*). For some microbial pathogens (i.e., *Vibrio cholerae* and *Helicobacter pylori*), facilitation of their translocation through the mucosal barrier has been observed via the secretion of degrative enzymes targeting mucin carbohydrates ultimately affecting the viscosity of the mucosal fluid (*157*). Illustrating the importance mucins for maintaining a healthy mucosal barrier.

Following multivariate analysis, biomarkers that were selected by LASSO to contribute to overall proteome variability with DMPA-IM use included Serpin B2 (PAI2), Thioredoxin-dependent peroxide reductase (PRDX3), and Enoyl-CoA delta isomerase 2 (ECI2) (Figure 6). Serpin B2 has often been referred to as the “undecided serpin". Serpin B2 is a urokinase plasminogen activator inhibitor. Therefore, Serpin B2 acts as an anti-coagulation factor inhibiting plasminogen conversion to its active state, plasmin. Plasmin is responsible for the degradation of protein factors essential to the process of coagulation (*159, 160*). Thioredoxin-dependent peroxide reductase acts as an oxidizing agent by reducing hydrogen peroxides to water and alcohols, protecting the cell from oxidative stress which is observed to protection against apoptosis, senescence and DNA damage (*161*). The final host factor identified by LASSO was Enoyl-CoA delta isomerase 1, with catalytic activity essential to the beta-oxidation of unsaturated fatty acids.

In summary, univariate analysis showed host signatures for regulation of innate immune response to decrease, which suggests an immunosuppressive effect post-DMPA (Table 4). In addition, although represented by a single protein (TGM3), a compromised epithelial barrier is likely. Our multivariate analysis made similar overall observations concerning immune response with the identification of Serpin B2. Serpin B2 has been reported in the literature to be involved in processes relating to inflammation such as anti-coagulation activity, macrophage recruitment, T-helper 1/2 immunity, and IL-1β production (*159, 160*). LASSO also identified host factors with essential regulatory roles. Overall, this suggests immunosuppression with a potential for certain inflammatory processes to also occur with DMPA use.

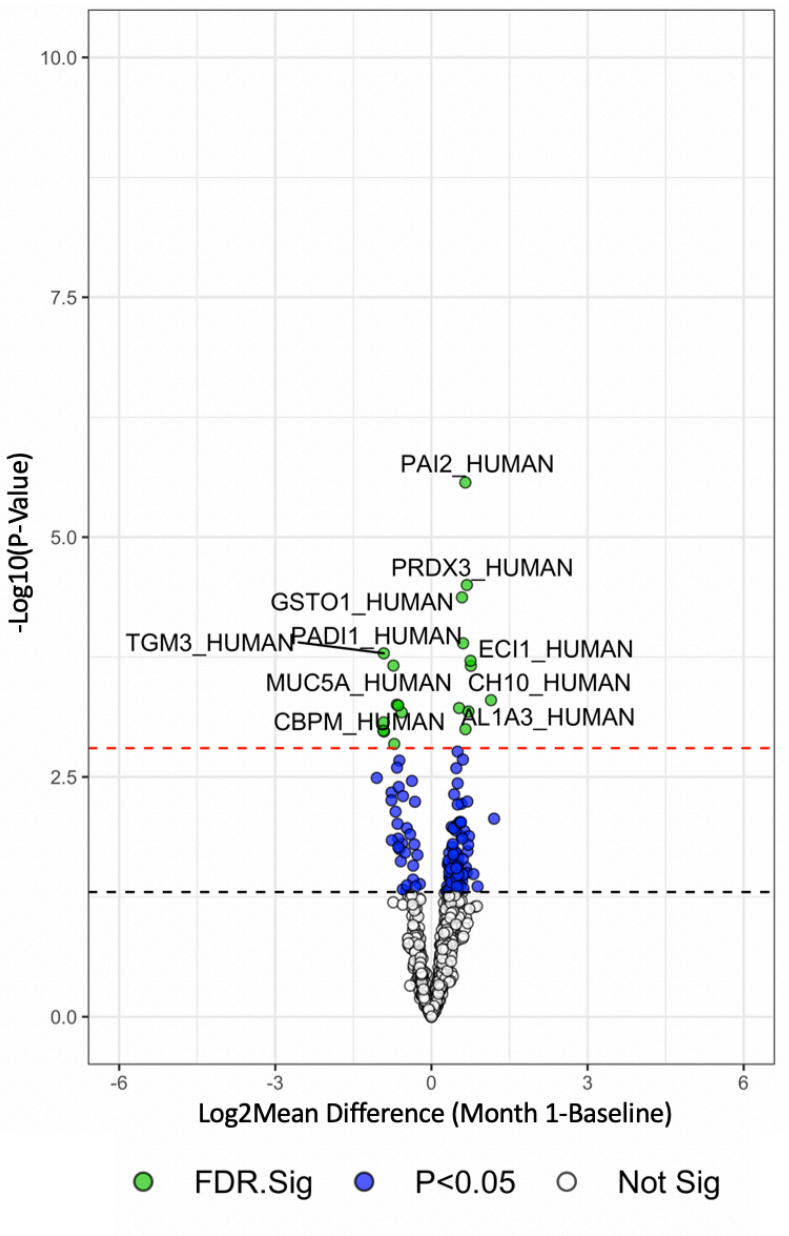

Figure 3. Volcano plot illustrating changes in mean protein abundances between month 1 and baseline timepoints with DMPA-IM use. Protein proportion changes that were significant (p-value<0.05) are indicated in blue and above the dashed black line. Those that passed BH comparison (FDR-BH<0.05) are indicated in green and above the dashed red line. Positive abundance differences suggest changes that are increasing with DMPA-IM use while negative abundance differences suggest a decrease.

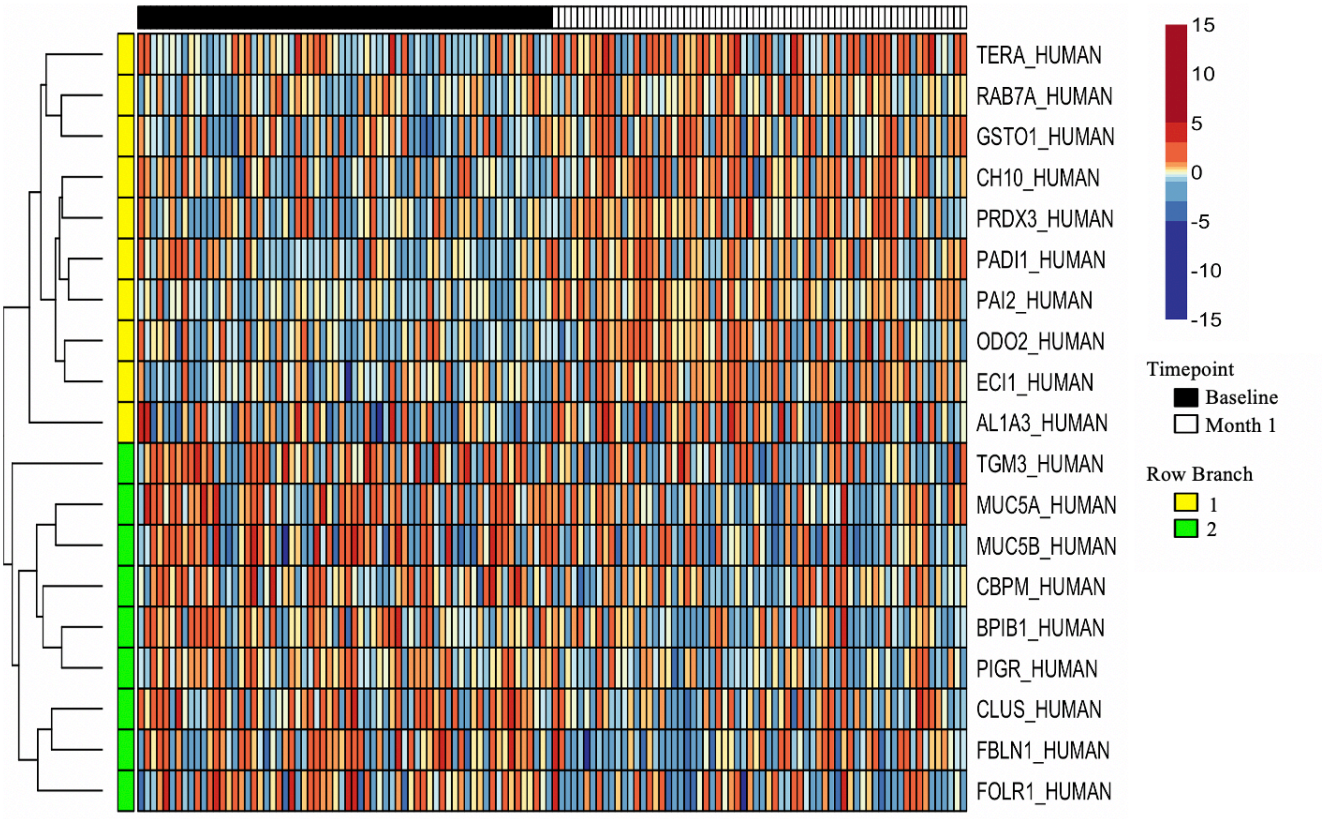

Figure 4. Hierarchical clustering of the 19 differentially abundant host proteins between pre- and post-contraceptive initiation of DMPA-IM. This heatmap illustrates log (base 2) protein abundance differences for host proteins that were significant following BH correction between baseline and month 1 sample timepoints. After 1-month of DMPA-IM use 19 host proteins were observed to be significantly differentially abundant (P-Value<0.05, FDR-BH<0.05) with those that were observed to be more abundant are illustrated in red while the less abundant are in blue. Two branches were identified corresponding to sample timepoint in yellow (branch 1) and green (branch 2). Branch 1 (yellow) represents host proteins that were increasing following 1-month of DMPA-IM use, while branch 2 (green) represents those that decreased.

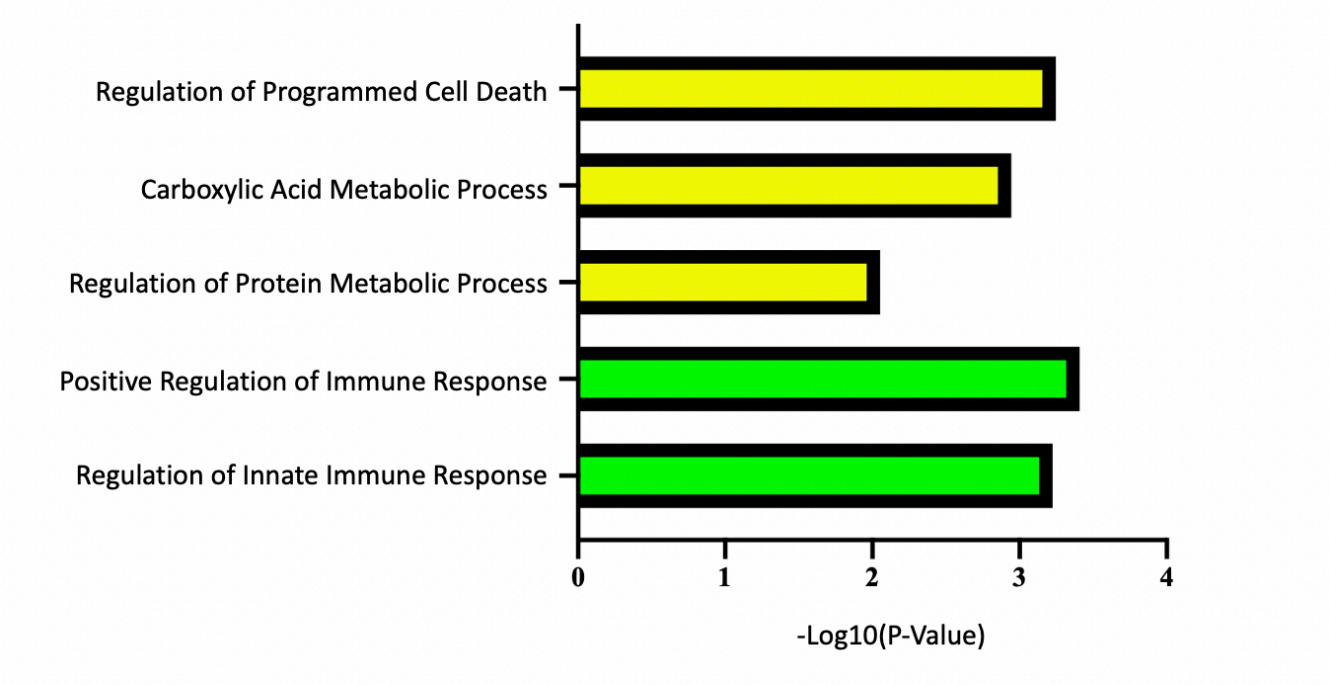

Figure 5. A summary of pathways identified according to the cluster analysis of the 19 differentially abundant host proteins post-DMPA-IM initiation. Pathway analysis was conducted using ConsensusPathDB with those increasing with DMPA use represented in yellow, and those decreasing represented in green. Pathways are specific to those with four or more host factors associated. Host proteins within each identified pathway and their corresponding significance value is provided in Table 4.

Table 4. Biological processes identified by ConsensusPathDB from differentially abundant proteins identified with DMPA-IM use.

Reactome Pathway^	Row Branch*	P-value	Benjamini-Hochberg P-value (*162*)	Molecules
Positive regulation of immune response	2	0.00039	0.0039	CLUS_HUMAN; BPIB1_HUMAN; MUC5A_HUMAN; MUC5B_HUMAN
Regulation of Programmed Cell Death	1	0.00057	0.0079	PAI2_HUMAN; AL1A3_HUMAN; TERA_HUMAN; PRDX3_HUMAN; CH10_HUMAN
Regulation of Innate Immune Response	2	0.00060	0.0040	MUC5B_HUMAN; BPIB1_HUMAN; MUC5A_HUMAN
Carboxylic Acid Metabolic Process	1	0.0011	0.0086	AL1A3_HUMAN; ODO2_HUMAN; ECI1_HUMAN; GSTO1_HUMAN
Regulation of Protein Metabolic Process	1	0.0088	0.041	PAI2_HUMAN; TERA_HUMAN; PRDX3_HUMAN; RAB7A_HUMAN; CH10_HUMAN

*Refers to clusters of host proteins identified by the heatmap in Figure 4 (heatmap annotation row). Host proteins in these branches were run separately through DAVID to identify specific pathways that are changing with DMPA-IM use

^Reactome pathways with 4 or more host proteins identified

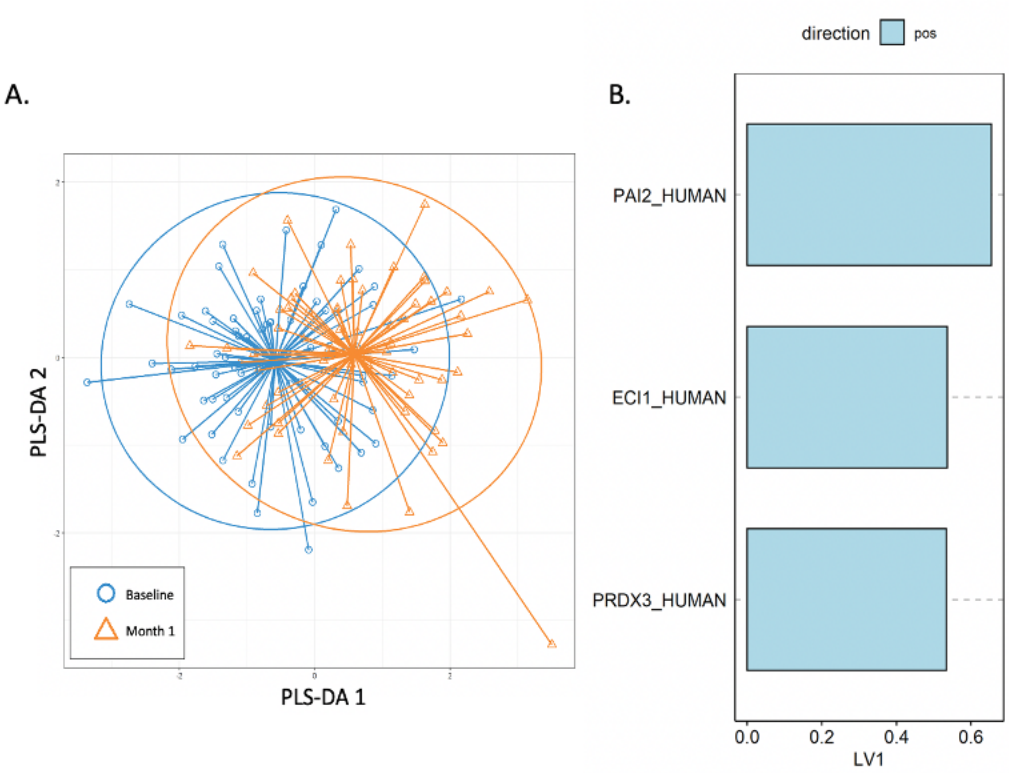

Figure 6. Multivariate analysis using Least Absolute Selection and Shrinkage Operator (LASSO) and Partial Least Squares Discriminant Analysis (PLS-DA) of the entire mucosal host proteome with DMPA-IM use. To add to the univariate analysis LASSO-selection of mucosal host factors was conducted to determine host factors significantly changing between pre- and post-contraception initiation taking into the account the entire biological system that is the host proteome. A. PLS-DA shows slight separation of baseline and month-1 clusters with the 3 host biomarkers identified by LASSO. B. Loading plot for the LASSO-selected host proteins, their direction indicates whether the protein was increasing or decreasing with contraception initiation. A positive loading variable represents an increase in abundance with 1-month of DMPA-IM use.

3.5.2 HOST PROTEOMIC CHANGES OBSERVED FOLLOWING 1-MONTH OF COPPER IUD USE

Samples were collected from 64 women that were randomized to the use of the Copper IUD. Use of Copper IUD for 1-month was associated with differential protein abundance of 345 host proteins; 312 of which passed BH-multiple comparison correction of 5% (Supplementary Table 6) while 33 did not (P-value <0.05, FDR-BH >5%) (Figure 7). Of the 312 host proteins that passed multiple comparison correction, 119 host proteins were observed to increase in abundance after 1-month of Copper IUD use and 193 were observed to decrease (Figure 8).

Functional annotation of host proteins increasing with Copper IUD included (P<0.05, FDR-BH<0.05): regulation of complement activation, fibrinolysis, lipoprotein biosynthetic process, cellular oxidant detoxification, hyaluronan metabolic process, extracellular matrix organization, and endodermal cell differentiation (Table 5; Figure 9). Functional annotation of host protein decreasing included cell-cell adhesion and keratinocyte differentiation (Table 5; Figure 9). Due to the degree of host proteins that were observed as significant with Copper IUD use, additional pathway analysis using Ingenuity Pathway Analysis (IPA; Table 6; Figure 10) was supported.
Pathways that increased (+z-scores) with Copper IUD use included those relating to immune response. Such pathways included: activation of phagocytes (z=3.587), activation of antigen-presenting cells (z=3.299), activation of myeloid cells (z=3.104), activation of leukocytes (z=2.868), activation of blood cells (z=2.841), activation of macrophages (z=2.709), recruitment of myeloid cells (z=2.677), recruitment of leukocytes (z=2.526), cell movement of T lymphocytes (z=2.458), migration of mononuclear leukocytes (z=2.385), adhesion of myeloid cells (z=2.303), cell movement of antigen-presenting cells (z=2.246), adhesion of phagocytes (z=2.217), adhesion of blood cells (z=2.191), and migration of myeloid cells (z=2.081). Top 3 canonical pathways (Table 7) identified with Copper IUD use included acute phase response signalling (P=2.5119E-34), LXR/RXR Activation (P=3.1623E-31) and complement system (P=6.3096E-22). Overall, changes to the host proteome observed with Copper IUD use has shown an inflamed environment.

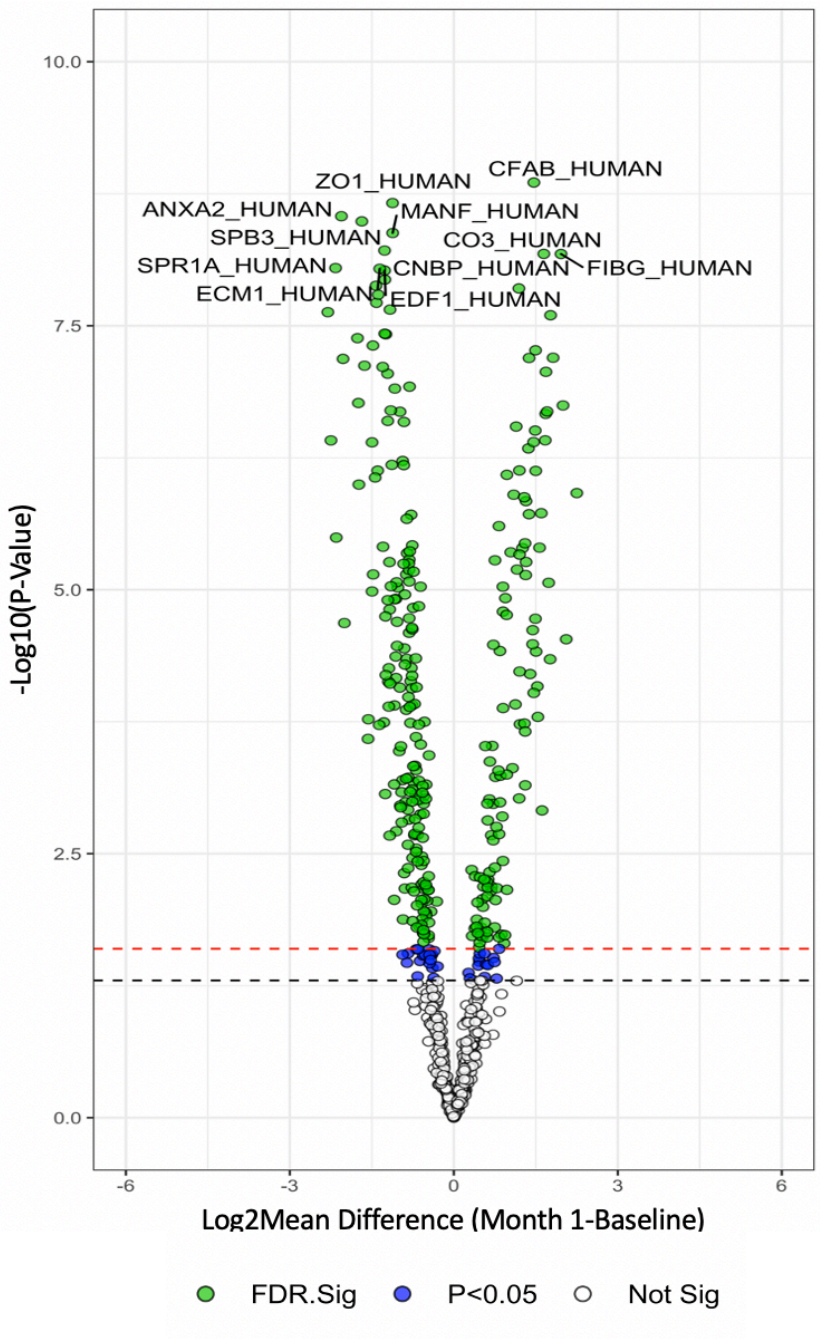

Figure 7. Volcano plot illustrating changes in mean protein abundances between month 1 and baseline timepoints with Copper IUD use. Protein proportions changes that were significant (p-value<0.05) are indicated in blue and above the dashed black line. Those of which that passed BH comparison (FDR-BH<0.05) are indicated in green and above the dashed red line. Positive abundance differences suggest changes that are increasing with Copper IUD use while negative abundance differences suggest a decrease.

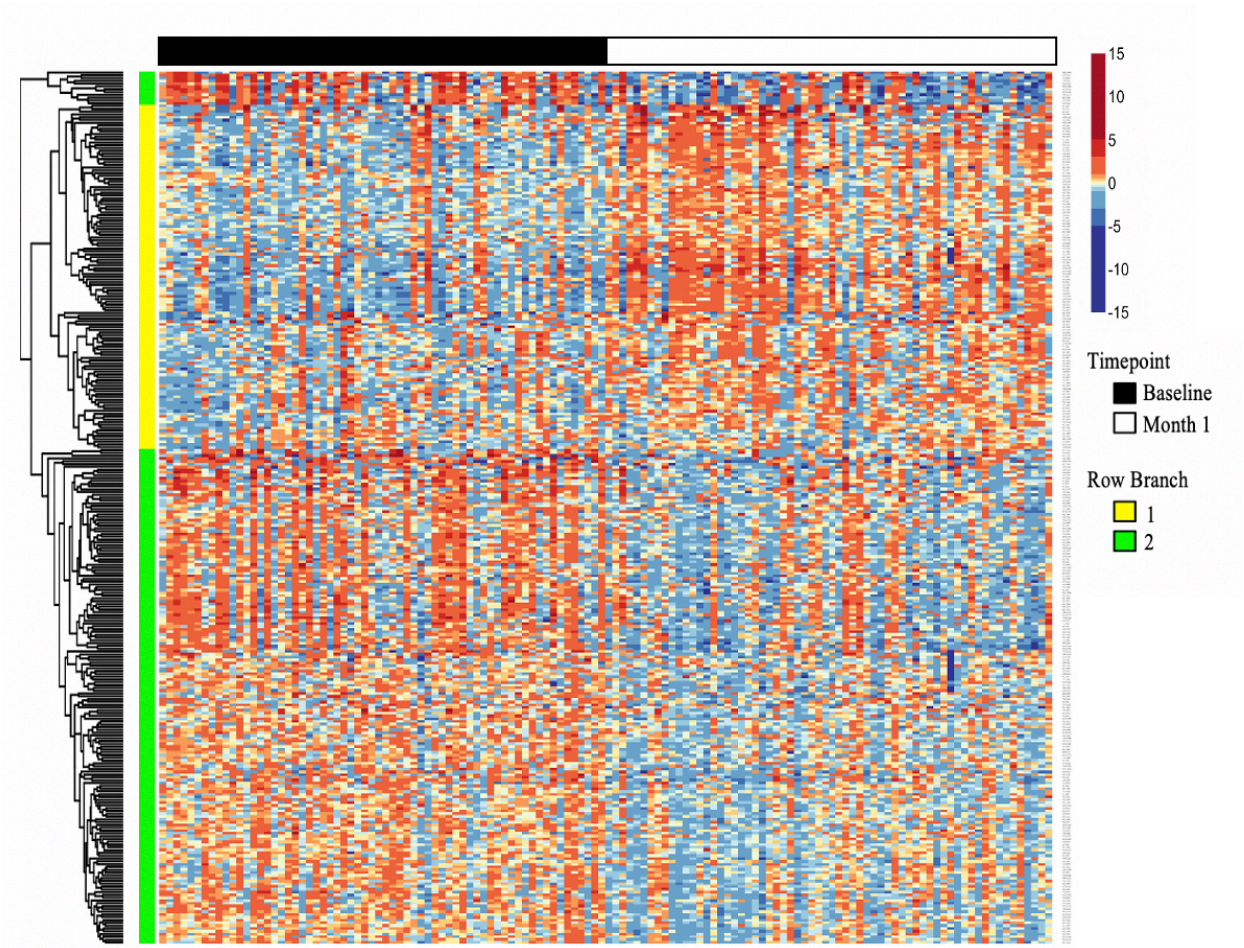

Figure 8. Hierarchical clustering of the 312 differentially abundant host proteins between pre- and post-contraceptive initiation of Copper IUD. This heatmap illustrates log (base 2) protein abundance differences for host proteins (Supplementary Table 6) that were significant following BH correction between baseline and month 1 sample timepoints. After 1-month of Copper IUD use 312 host proteins were observed to be significantly differentially abundant (P-Value<0.05, FDR-BH<0.05) with those that were observed to be more abundant are illustrated in red while the less abundant are in blue. Two branches were identified corresponding to sample timepoint in yellow (branch 1) and green (branch 2). Branch 1 (yellow) represents host proteins that were increasing following 1-month of DMPA-IM use, while branch 2 (green) represents those that decreased.

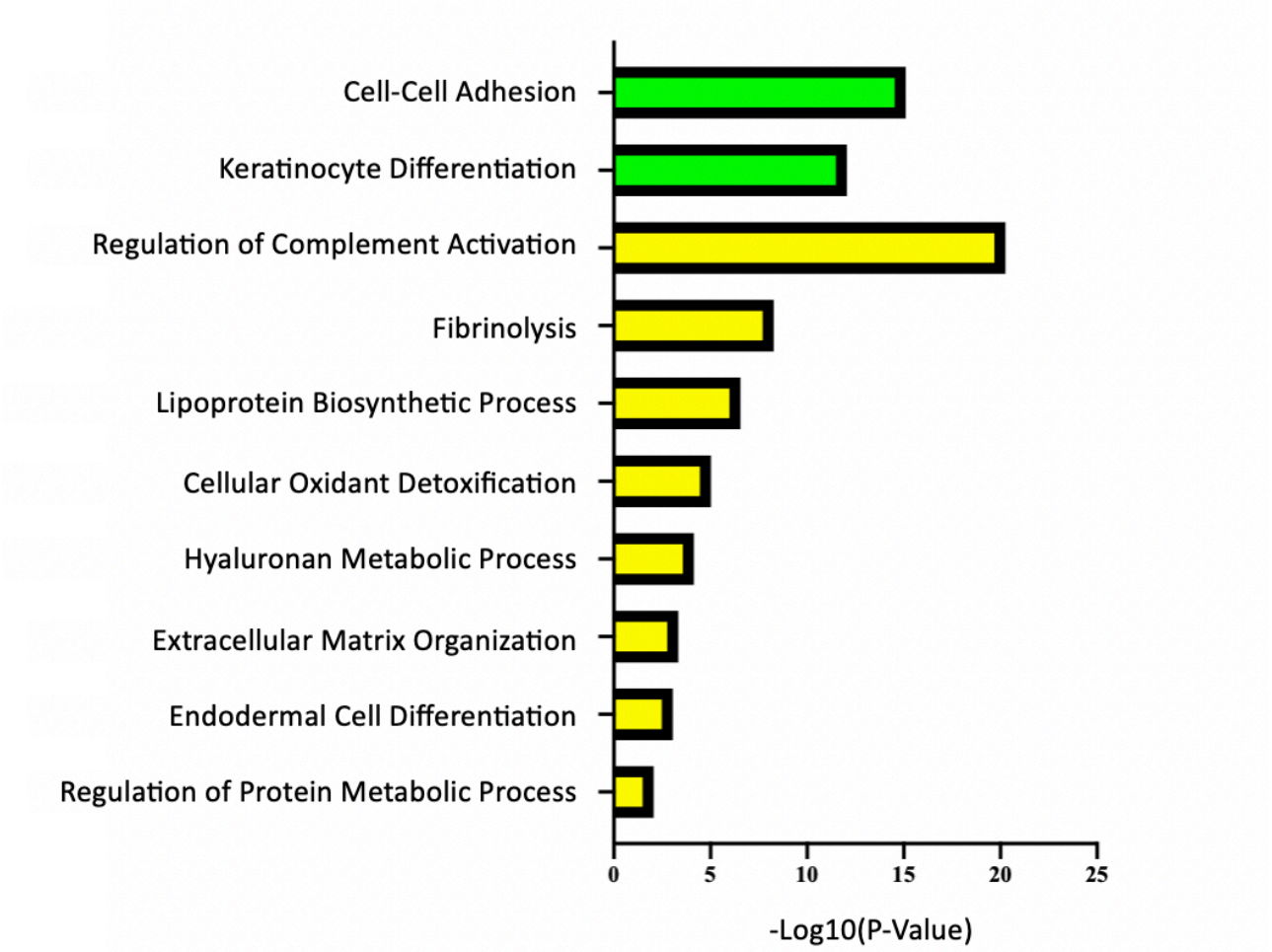

Figure 9. A summary of pathways identified according to cluster analysis of differentially abundant host proteins post-Copper IUD initiation. Pathway analysis was conducted using DAVID with those increasing with Copper IUD use represented in yellow, and those decreasing represented in green. Pathways are specific to those with four or more host factors that were associated. Host proteins within each identified pathway and their corresponding significance value is provided in Table 5.

Table 5. Biological processes identified by DAVID functional annotation from differentially abundant proteins identified with Copper IUD use.

David Functional Annotation	Row Branch	P-Value	Benjamini-Hochberg P-Value	Count
Regulation of Complement Activation	1	5.55E-21	1.66E-18	14
Cell-Cell Adhesion	2	7.83E-16	7.38E-13	25
Keratinocyte Differentiation	2	8.76E-13	4.12E-10	14
Fibrinolysis	1	5.27E-09	5.92E-07	7
Lipoprotein Biosynthetic Process	1	2.84E-07	2.14E-05	5
Cellular Oxidant Detoxification	1	9.63E-06	4.33E-04	7
Hyaluronan Metabolic Process	1	7.11E-05	0.0025	4
Extracellular Matrix Organization	1	4.69E-04	0.012	8
Endodermal Cell Differentiation	1	8.75E-04	0.021	4

*Refers to clusters of host proteins identified by the heatmap in Figure 8 (heatmap annotation row). Host proteins in these branches were run separately through DAVID to identify specific pathways that are changing with Copper IUD use. Only unique pathways identified in each cluster were described.

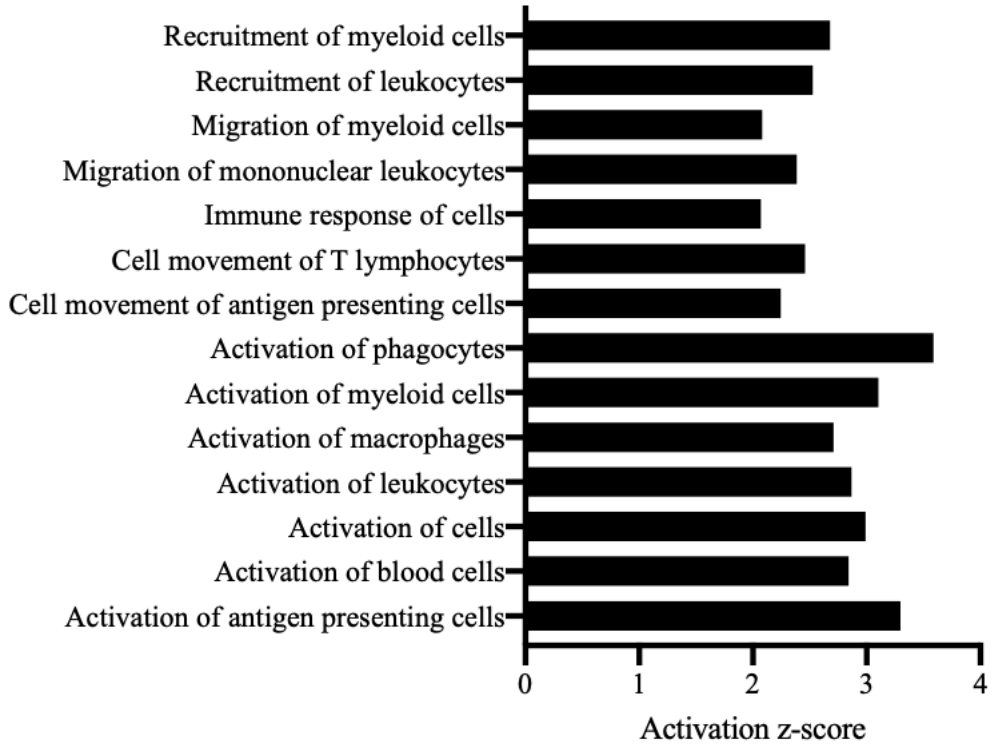

Figure 10. Biological functions identified significantly changing with 1-month of Copper IUD use. Functional analysis was conducted using IPA. Functions with activation z-scores < -2.00 and > +2.00 were identified as significant. Functions of particular interest are illustrated here to display overall trend observed for functions with an *increased* (z-score>2.00) predicted activation state.

Table 6. Disease or Function annotation identified by Ingenuity Pathway Analysis (IPA) from differentially abundant proteins identified with Copper IUD use.

Diseases or Functions Annotation	P-Value	Predicted Activation State	Activation z-score	Count
Activation of antigen presenting cells	5.88E-13	*Increased*	3.299	31
Activation of blood cells	9.27E-14	*Increased*	2.841	53
Activation of cells	6.06E-17	*Increased*	2.992	69
Activation of leukocytes	3.21E-13	*Increased*	2.868	49
Activation of macrophages	7.48E-11	*Increased*	2.709	24
Activation of myeloid cells	6.27E-15	*Increased*	3.104	35
Activation of phagocytes	2.82E-15	*Increased*	3.587	37
Adhesion of blood cells	4.29E-15	*Increased*	2.191	37
Adhesion of myeloid cells	1.8E-11	*Increased*	2.303	20
Adhesion of phagocytes	2.8E-12	*Increased*	2.217	20
Cell movement of antigen presenting cells	1.09E-08	*Increased*	2.246	28
Cell movement of T lymphocytes	6.06E-07	*Increased*	2.458	19
Endocytosis	6.77E-15	*Increased*	2.713	48
Endocytosis by eukaryotic cells	4.44E-10	*Increased*	2.652	30
Engulfment of cells	8.06E-12	*Increased*	2.816	39
Esterification of cholesterol	1.05E-07	*Increased*	2.199	8
Fatty acid metabolism	4.61E-11	*Increased*	2.525	41
Fibrogenesis	5.35E-10	*Increased*	2.261	35
Immune response of cells	5.81E-13	*Increased*	2.071	46
Migration of mononuclear leukocytes	6.16E-08	*Increased*	2.385	27
Migration of myeloid cells	1.43E-10	*Increased*	2.081	21
Morbidity or mortality	7.38E-14	*Increased*	2.404	115
Phagocytosis of cells	1.01E-10	*Increased*	2.071	30
Recruitment of cells	2.43E-09	*Increased*	2.405	28
Recruitment of leukocytes	3.98E-09	*Increased*	2.526	26
Recruitment of myeloid cells	8.46E-07	*Increased*	2.677	20
Release of eicosanoid	2.48E-07	*Increased*	2.057	14
Release of fatty acid	6.99E-07	*Increased*	2.219	15
Release of lipid	2.04E-08	*Increased*	2.932	19
Release of prostaglandin	0.0000013	*Increased*	2.182	9
Synthesis of fatty acid	4.36E-09	*Increased*	2.232	26
Synthesis of nitric oxide	0.0000013	*Increased*	2.265	20
Transport of molecule	4.04E-09	*Increased*	2.911	75
Viral Infection	6.68E-15	*Decreased*	-2.367	86

Table 7. Canonical pathways identified by Ingenuity Pathway Analysis (IPA) from differentially abundant proteins identified with Copper IUD use.

Canonical Pathways	P-Value	z-score
Acute Phase Response Signaling	2.51E-34	1.698
LXR/RXR Activation	3.16E-31	5.303
Complement System	6.31E-22	0.302
Coagulation System	2.00E-12	-0.302
Production of Nitric Oxide and Reactive Oxygen Species in Macrophages	4.68E-06	3.051
Gluconeogenesis I	3.47E-05	0.447
Actin Cytoskeleton Signaling	0.00010	1.265
Glycolysis I	0.00054	0
ILK Signaling	0.0021	2.646
Inhibition of Matrix Metalloproteases	0.0026	-1
Integrin Signaling	0.0046	0
Leukocyte Extravasation Signaling	0.0091	1.633
RhoA Signaling	0.036	2.236
EIF2 Signaling	0.049	-2.646

Following multivariate analysis, biomarkers selected by LASSO to influence overall host proteome variance included MANF (Mesencephalic astrocyte-derived neurotrophic factor), CNBP (Cellular nucleic acid-binding protein), PROS (Vitamin K-dependent protein S precursor), RET4 (Retinol-binding protein 4 precursor), A2MG (Alpha-2-macroglobulin precursor), CFAB (Complement factor B precursor) and FIBG (Fibrinogen gamma chain) (Figure 11). The fibrinogen gamma chain is a host factor essential for blood clot formation and wound repair, specifically in re-epithelialization through guiding cell migration (uniprot.org). Complement factor B precursor is a part of the complement system with specific duties including proliferation and differentiation of B lymphocytes (uniprot.org). Alpha-2-macroglobulin precursor is a proteinase inhibitor with duties essential to anti-blood coagulation through the formation of plasmin (reactome.org) (*163*). Retinol-binding protein 4 precursor is involved in the transport of retinol from the liver to peripheral tissue through the blood (*164*). Cellular nucleic acid-binding protein (CNBP) is a zinc finger protein known for functions essential to cellular processes and differentiation of many tissue types (Uniprot) (*165*). Finally, Mesencephalic astrocyte-derived neurotrophic factor (MANF) is described to support dopaminergic neurons (*166*). However, MANF has also been described to be involved with platelet degranulation (reactome.org). In summary, univariate proteomic analysis (Figure 8; Table 6) revealed pathways relating to immune activation and inflammation increased following Copper IUD initiation. Host proteomic signatures relating to cell-cell adhesion and keratinocyte differentiation were observed (Table 5) to decrease which suggests Copper IUD may potentially disrupt the epithelial barrier with its use. Our multivariate analysis also suggests increased inflammation. LASSO identified host factors that play some role in blood coagulation which may influence inflammation (i.e., FIBG, CFAB, A2MG, PROS) (Figure 11).

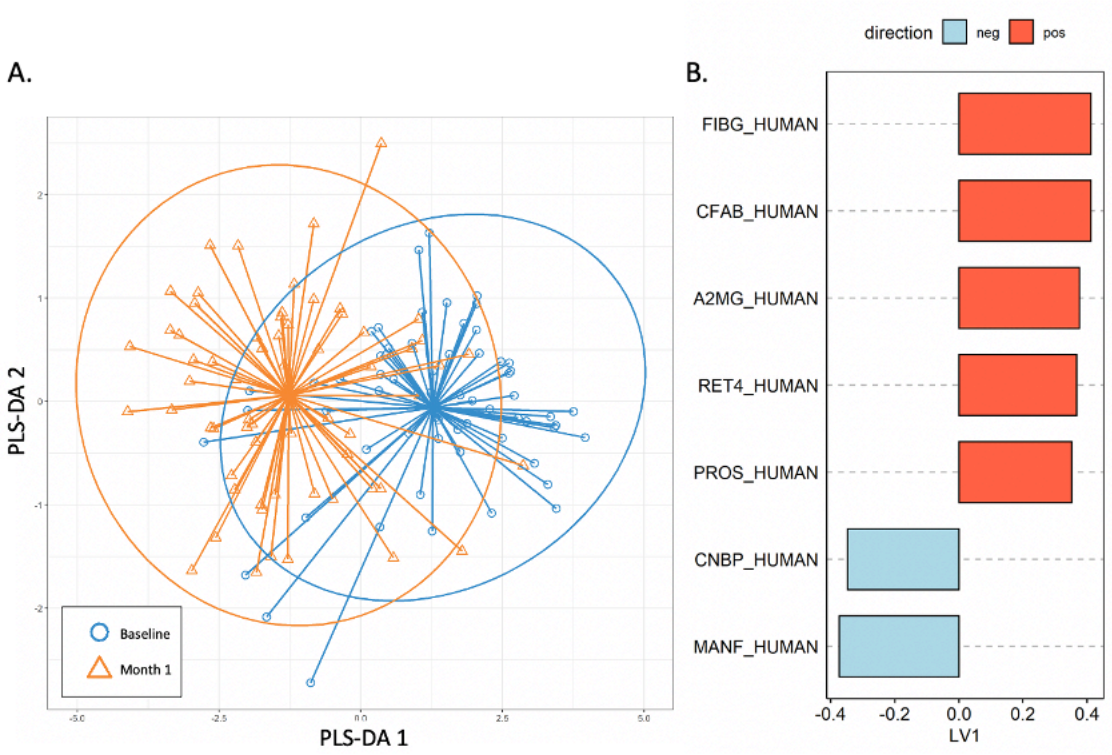

Figure 11. Multivariate analysis using Least Absolute Selection and Shrinkage Operator and Partial Least Squares Discriminant Analysis of the entire mucosal host proteome with Copper IUD use. To add to the univariate analysis LASSO-selection mucosal host factors that were also identified to significantly change following initiation were identified. A. PLS-DA shows slight separation of baseline and month-1 clusters with the 7 host biomarkers identified by LASSO. B. Loading plot for the LASSO-selected host proteins with their direction indicating whether the protein was increasing or decreasing with contraception initiation. A positive loading variable represents an increase in abundance which was seen for FIBG, CFAB, A2MG, RET4, PROS. A negative loading variable represents a decrease in abundance of these biomarkers, which was seen for CNBP and MANF.

3.3.3 HOST PROTEOMIC CHANGES OBSERVED FOLLOWING 1-MONTH OF LEVONORGESTREL IMPLANT (LNG IMPLANT) USE

Samples were collected from 66 women that were randomized to the use of the LNG Implant. Use of the LNG Implant for 1-month was associated with a differential protein abundance of 49 host mucosal proteins; 1 of which passed BH-multiple comparison correction (P-value <0.05, FDR-BH >5%) (Figure 12). The 1 protein that passed multiple comparison correction was CH60 which increased after 1-month of LNG implant use. Multivariate analysis using the LASSO algorithm identified this same protein, CH60. CH60 is a 60 kDa mitochondrial heat shock protein involved in the transport of mitochondrial proteins and their correct folding, and refolding if misfolding in the mitochondrial matrix has occurred. As such, LNG Implant use does not appear to associate with significant changes to the host proteome.

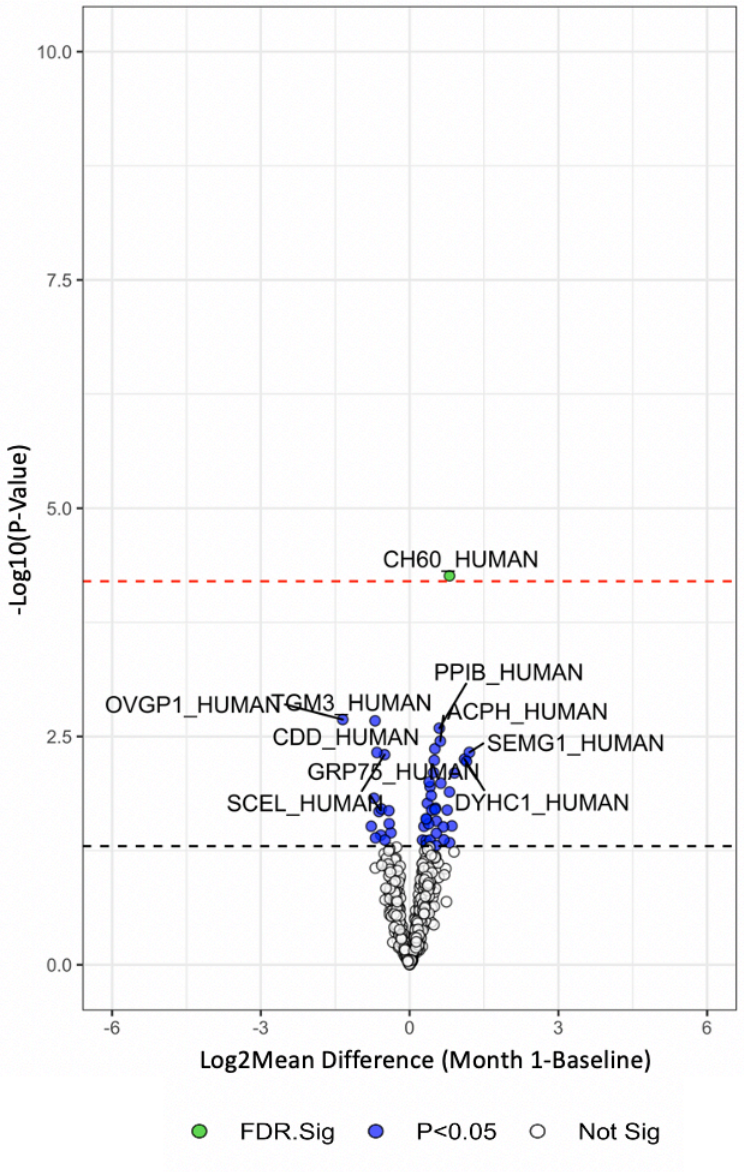

Figure 12. Volcano plot illustrating changes in mean protein abundances between month 1 and baseline timepoints with LNG Implant use. Protein proportions changes that were significant (p-value<0.05) are indicated in blue and above the dashed black line. Those of which that passed BH comparison (FDR-BH<0.05) are indicated in green and above the dashed red line. Positive abundance differences suggest changes that are increasing with LNG Implant use while negative abundance differences suggest a decrease.

3.6 OBJECTIVE 2: LONGITUDINAL BACTERIAL PROTEOMIC CHANGES WITH CONTRACEPTIVE USE

The aim of this objective was to compare vaginal microbiome composition and bacterial proteome changes with contraceptive use. Proteomic analysis of vaginal microbial proteins identified 24 different bacterial taxa and 163 unique bacterial species. Following hierarchical clustering analysis, five community groups were observed: *Lactobacillus iners* dominant (N=134), *Lactobacillus crispatus* dominant (N=31), *Lactobacillus* dominant (N=11), *Gardnerella* dominant (N=69), and polymicrobial microbiome (N=147) (Figure 13). The top ten most abundance bacterial genus/species include (ordered from most to least abundant) were *Lactobacillus iners* (median=0.057), *Gardnerella* (median=0.068), *Lactobacillus sp.* (median=0.042), *Prevotella* (median=0.024), *Lactobacillus crispatus* (median=0.0017), *Megasphaera* (median=0), *Sneathia* (median=0), undistinguishable (median=0.0051), *Mobiluncus* (median=0), and *Pseudomonas* (median=0.0022). In African populations *L. iners* has been the most prevalent *Lactobacillus* species, which this cohort also saw (*145, 167*). The overall bacterial functional diversity is represented in Figure 14. Bacterial functional analysis was conducted using bacterial protein groups with additional sensitivity analysis using three zero-replacement methods: true zero (0), pseudo count (0.0001), and half the minimum value (minimum value unique for each protein). Confidence was given to bacterial protein groups with significant p-values ($P< 0.05$) with at least two of the three zero-replacement methods following comparisons between baseline and month-1 timepoints.

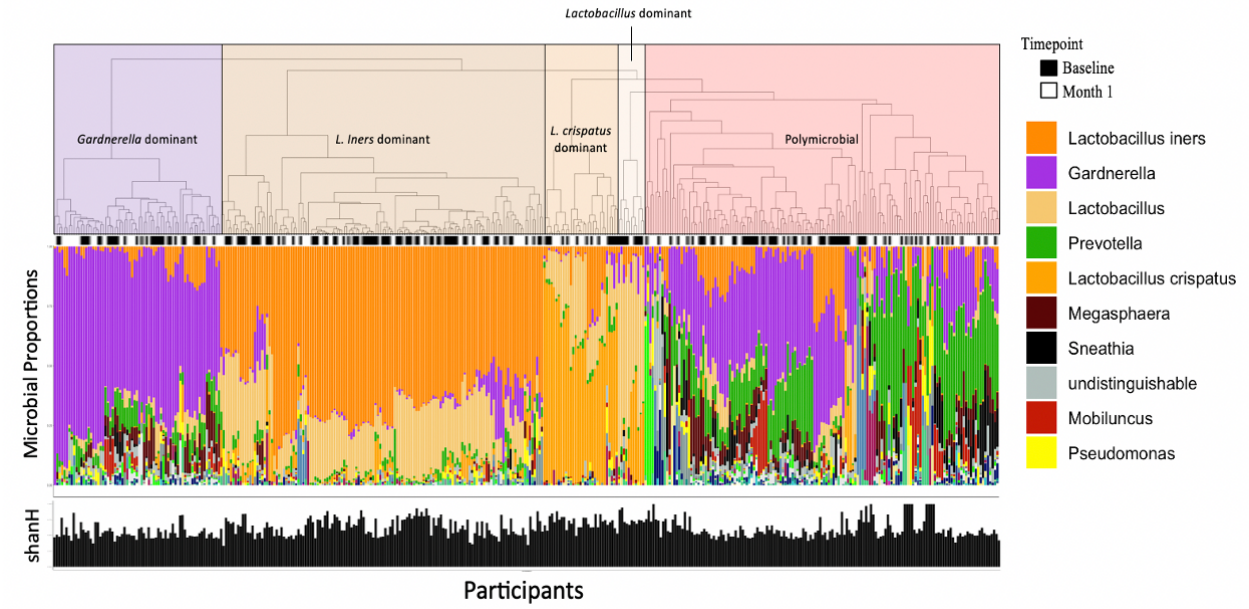

Figure 13. Hierarchical clustering of microbial proportions for each woman at timepoints pre- and post-contraception with clustering distinguishing dominant microbiome community groups. Euclidian clustering identified polymicrobial (N=147), *L. iners* (N=134), *Lactobacillus crispatus* (N=31), *Lactobacillus* (N=11), *Gardnerella* (N=69), and dominant community groups with no significant clustering by sample timepoint. The figure legend highlights the top 10 most abundant bacterial genera ordered from most to least abundant.

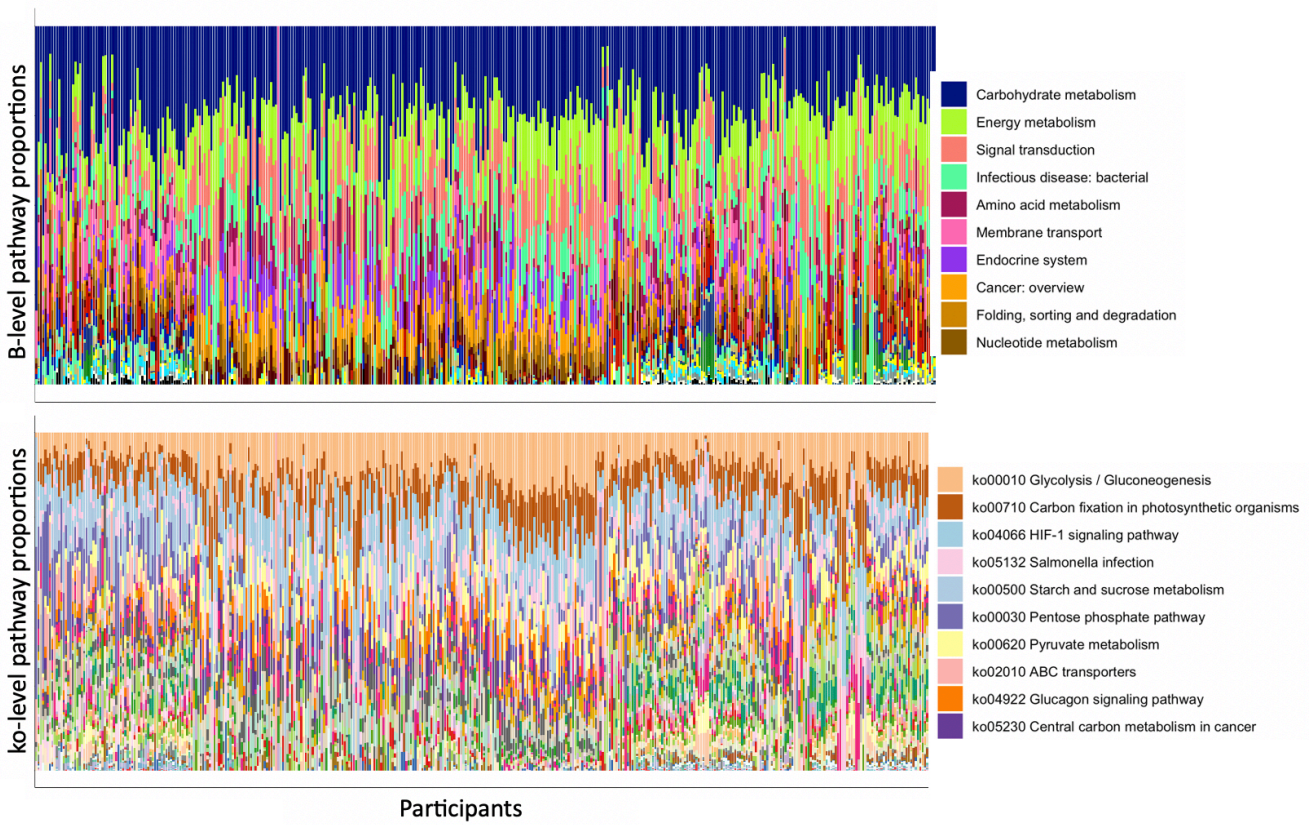

Figure 14. Stacked bar plot of vaginal bacterial functional diversity (b- and ko-levels) for each woman pre- and post-contraceptive initiation. Functions are ordered by most abundant (top) to least abundant (bottom), with the top 10 functions and their corresponding colours in the legend.

3.6.1 MICROBIOME AND BACTERIAL FUNCTIONAL CHANGES WITH DEPO-MEDROXYPROGESTERONE ACETATE (DMPA-IM) USE

Analysis of changes to the overall bacterial diversity at the genus level for 1-month of DMPA-IM use revealed no significant differences (Figure 15B; Wilcoxon rank-sum P=0.23) when comparing baseline Shannon-H diversity to the month 1 sample timepoint. In addition, examining shifts in the microbiome using *Lactobacillus*-dominant (LD) and non-*Lactobacillus* dominant (nLD) classifications showed no significant shifts from baseline to month-1 (McNemar's Chi-square P=1). Species-level changes, following centered-log ratio transformation, revealed no significant change in abundance of any bacterial genera following a BH multiple comparison correction (Table 8; Figure 15A). This project's hypothesis additionally included a comparison of bacterial activity changes with contraception initiation. To determine this, univariate analysis of pathway changes for KEGG annotated b- and ko-levels, as well as changes to specific bacterial protein groups, was conducted. Pathways and protein groups noted as significant have a p-value<0.05 but were not significant following a BH-multiple comparison correction. For b-level pathway changes (Table 9) a significant increase in amino acid metabolism was observed. At the ko-level, galactose metabolism, ribosome, cysteine and methionine metabolism, and pyruvate metabolism significantly increased post-initiation compared to baseline (Table 10). For the analysis of bacterial protein group changes, univariate analysis identified 10 that were differentially abundant (P<0.05; Table 11; Figure 16). The 10 differentially abundant protein groups were Phosphoenolpyruvate carboxykinase ATP from Prevotella (A0A096AAA5_9BACT), elongation factor Tu from Sneathia (A0A0E3ZB99_9FUSO), 14-alpha-glucan branching enzyme from Gardnerella (I4M7G0_GARVA), Glucosamine-6-phosphate deaminase from Prevotella (A0A095ZH76_9BACT), 5-methyltetrahydropteroyltriglutamate from Megasphaera (D3LVK3_9FIRM), ABC transporter solute-binding protein from Gardnerella (I4MDA7_GARVA), Glutamine--fructose-6-phosphate aminotransferase isomerizing from Lactobacillus (I7LEL5_9LACO), Glyceraldehyde-3-phosphate dehydrogenase from Sneathia (A0A0E3UU77_9FUSO), 30S ribosomal protein S1 from Gardnerella (D2RAK2_GARV4), and Phosphoglucomutase from Sneathia (A0A0E3ZA51_9FUSO). Yet none passed multiple comparison correction. In summary, the use of DMPA-IM for 1-month in this cohort did not significantly alter the vaginal microbiome composition nor did it alter the functional processes of the bacterial species.

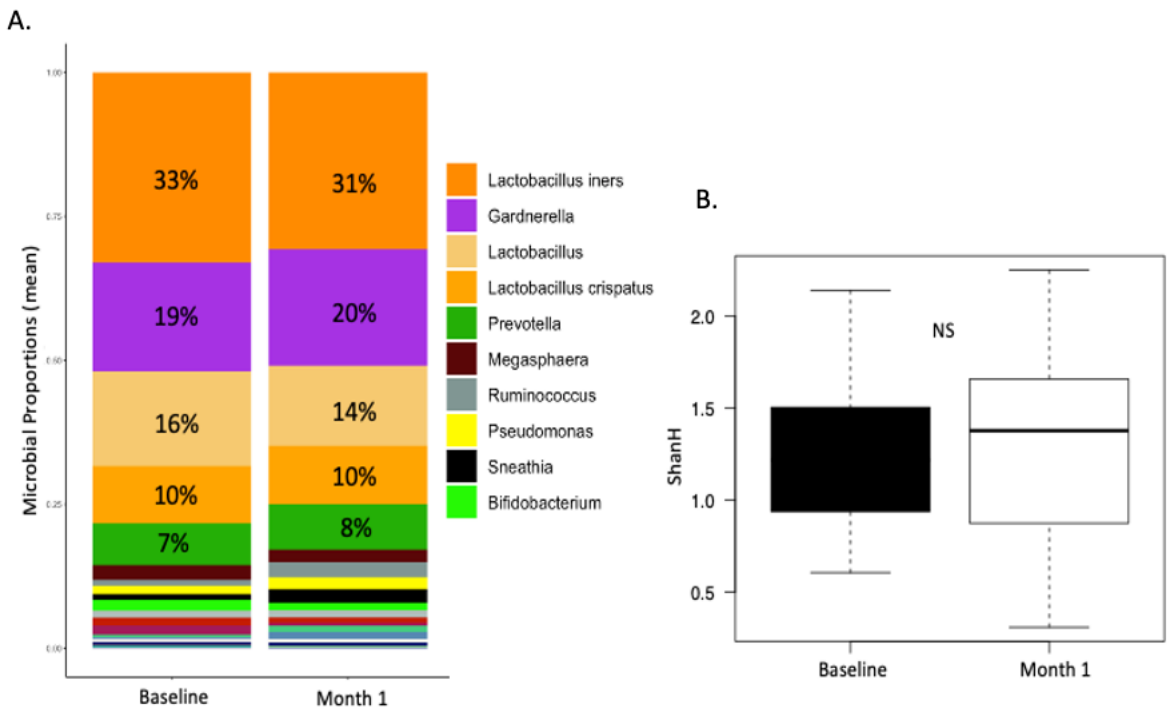

Figure 15. Comparison of microbial proteome changes following 1-month of DMPA-IM use. **(**A) Analysis of average bacterial genus proportion changes between baseline and month 1 with DMPA-IM use show no significant differences. (B) Diversity the microbiome at baseline and month 1 were determined using total bacterial genera identified. No significant difference was observed in Shannon's H diversity between baseline and month 1 (NS = p-value>0.05).

Table 8. Relative abundance of major vaginal bacterial taxa following DMPA-IM initiation compared to baseline as identified by mass spectrometry.

Bacterial genus*	P-Value	Mean Difference (M1-Baseline)	Benjamini-Hochberg P-Value
Sneathia	0.092	0.15	1
Prevotella	0.13	0.31	1
Mobiluncus	0.21	-0.18	1
Other	0.21	-0.082	1
Peptoniphilus	0.37	0.073	1
Lactobacillus iners	0.38	-0.057	1
Escherichia	0.39	0.075	1
Bifidobacterium	0.39	-0.092	1
Porphyromonas	0.40	-0.041	1
Lactobacillus crispatus	0.51	-0.17	1

*Species level identification was used for *L. crispatus* and *L. iners*

Table 9. Bacterial pathway changes at the KEGG annotated b-level associated with initiation of DMPA-IM.

KEGG B-level pathway*	Wilcox rank sum p-value	Benjamini-Hochberg p-value
Amino acid metabolism	0.0080	0.19
Cancer: overview	0.049	0.56
Translation	0.078	0.57
Membrane transport	0.10	0.57
Endocrine system	0.16	0.67
Folding, sorting and degradation	0.19	0.67
Nucleotide metabolism	0.23	0.67
Cell motility	0.26	0.67
Immune system	0.26	0.67
Endocrine and metabolic disease	0.33	0.70

*Top 10 pathways starting with the most significant.

Table 10. Bacterial pathway changes at the KEGG annotated ko-level associated with initiation of DMPA-IM.

KEGG Ko-level pathway*	Wilcox rank sum p-value	Benjamini-Hochberg p-value
ko00052 Galactose metabolism	0.026	0.41
ko03010 Ribosome	0.029	0.41
ko00270 Cysteine and methionine metabolism	0.040	0.41
ko00620 Pyruvate metabolism	0.041	0.41
ko05230 Central carbon metabolism in cancer	0.049	0.41
ko00720 Carbon fixation pathways in prokaryotes	0.054	0.41
ko02020 Two-component system	0.080	0.47
ko00630 Glyoxylate and dicarboxylate metabolism	0.086	0.47
ko02010 ABC transporters	0.099	0.47
ko00640 Propanoate metabolism	0.10	0.47

*Top 10 pathways starting with the most significant.

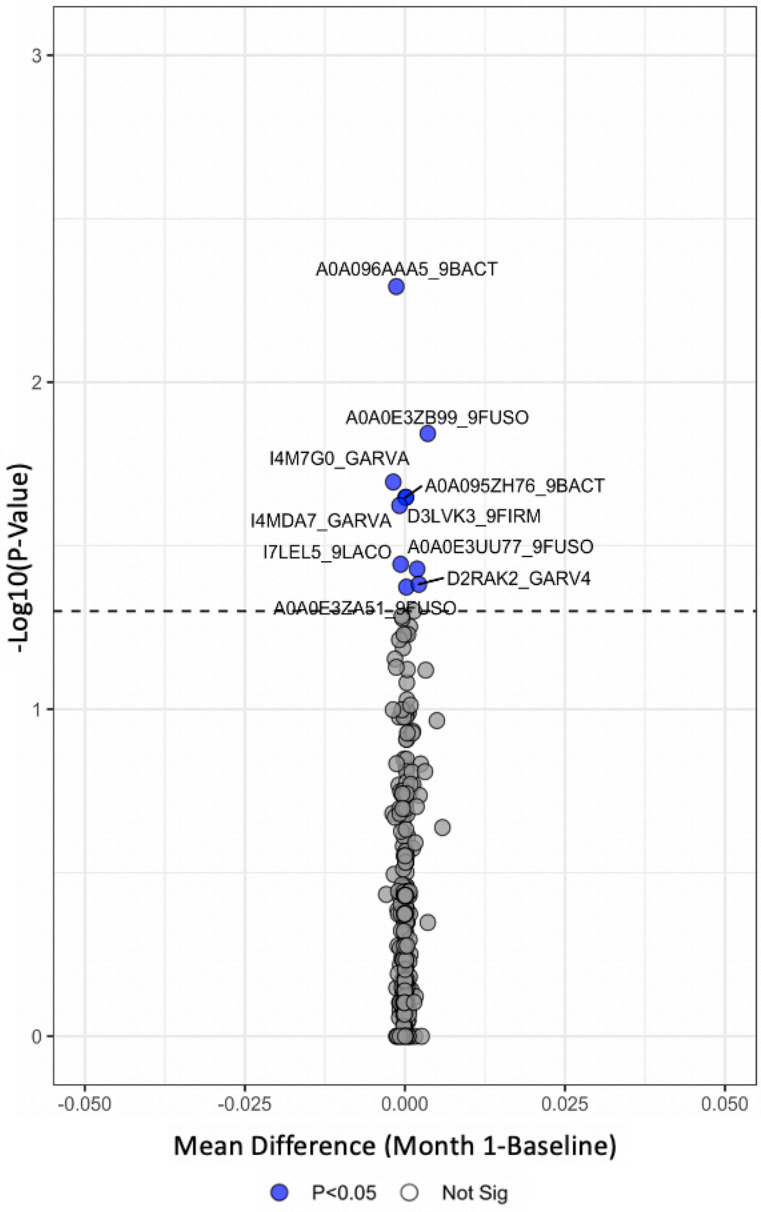

Figure 16. Volcano plot illustrating changes in mean bacterial protein abundances between month 1 and baseline timepoints with DMPA-IM use. Protein proportions that were significant (p-value<0.05) are indicated in blue and above the black dashed line. Positive abundance differences suggest changes that are increasing with DMPA-IM use while negative abundance differences suggest a decrease.

Table 11. Bacterial protein groups that were observed to be differentially abundant at timepoints month 1 and baseline with DMPA-IM use.

Group	Protein[a]	Genus	P-Value*
A0A096AAA5_9BACT	Phosphoenolpyruvate carboxykinase ATP	*Prevotella*	0.0051
A0A0E3ZB99_9FUSO	Elongation factor Tu	*Sneathia*	0.014
I4M7G0_GARVA	14-alpha-glucan branching enzyme	*Gardnerella*	0.020
A0A095ZH76_9BACT	Glucosamine-6-phosphate deaminase	*Prevotella*	0.022
D3LVK3_9FIRM	5-methyltetrahydropteroyltriglutamate--homocysteine methyltransferase	*Megasphaera*	0.022
I4MDA7_GARVA	ABC transporter solute-binding protein	*Gardnerella*	0.024
I7LEL5_9LACO	Glutamine--fructose-6-phosphate aminotransferase isomerizing	*Lactobacillus*	0.036
A0A0E3UU77_9FUSO	Glyceraldehyde-3-phosphate dehydrogenase	*Sneathia*	0.037
D2RAK2_GARV4	30S ribosomal protein S1	*Gardnerella*	0.041
A0A0E3ZA51_9FUSO	Phosphoglucomutase	*Sneathia*	0.042

[a]Proteins identified were significant with at least 2 of the 3 zero replacement methods.
*P-value in table representing that of the "true zero" zero replacement method.

3.6.2 MICROBIOME AND BACTERIAL FUNCTIONAL CHANGES WITH 1-MONTH OF COPPER INTRAUTERINE DEVICE (COPPER IUD) USE

Analysis of bacterial diversity changes after 1-month of copper-IUD use was determined at the genus level and revealed a significant difference in bacterial diversity (Figure 17C; Wilcoxon rank-sum P= 0.014) when comparing baseline Shannon-H diversity to month 1 sample timepoints. Diversity increased following 1-month of CIUD use. Based on LD and nLD microbiome classifications a significant shift between baseline to month-1 (McNemar's Chi-square P=0.0012) was observed. At the genus level (Table 12; Figure 17A) Copper-IUD use associated with a decrease in *Lactobacillus* (mean difference (MD)= -0.86, P=0.000016) and *L. iners* (MD= -0.68, P=0.0041) and a decrease in *Prevotella* (MD=+0.60, P=0.0031) and *Sneathia* (MD=+0.41, P=0.0064) species, all of which passed multiple comparison correction (FDR-BH<0.05).

Bacterial functional changes at the b- and ko-levels identified several pathways that passed BH-multiple comparison correction. These included environmental adaptation; energy metabolism; folding, sorting and degradation; lipid metabolism; cellular community-prokaryotes; and carbohydrate metabolism (Table 13). At the ko-level, several pathways were observed to pass BH-multiple comparison correction and were increasing post-Copper IUD initiation including plant-pathogen interaction, citrate cycle, amino sugar and nucleotide sugar metabolism, pentose phosphate pathway, carbon fixation in photosynthetic organisms, and glyoxylate and dicarboxylate metabolism (Table 14). Univariate analysis identified 60 bacterial protein groups that were significantly (P<0.05) different between baseline and post time points (Table 15; Figure 18). The top five of which (P<0.05, FDR-BH>0.05) included elongation factor Tu from Gardnerella (I4MDV2_GARVA), glyceraldehyde-3-phosphate dehydrogenase from Sneathia (A0A0E3UU77_9FUSO), phosphoenolpyruvate carboxykinase ATP from Prevotella (A0A098YU56_9BACT), 50S ribosomal protein L7/L12 from Sneathia (A0A0E3ZB09_9FUSO), and fructose-bisphosphate aldolase from Prevotella (A0A098YRA3_9BACT). None passed multiple comparison correction. Overall, with CIUD use a decrease in optimal *Lactobacillus* and *L. iners* species and an increase in less-favourable species, *Prevotella* and *Sneathia*, with significant bacterial metabolism changes observed.

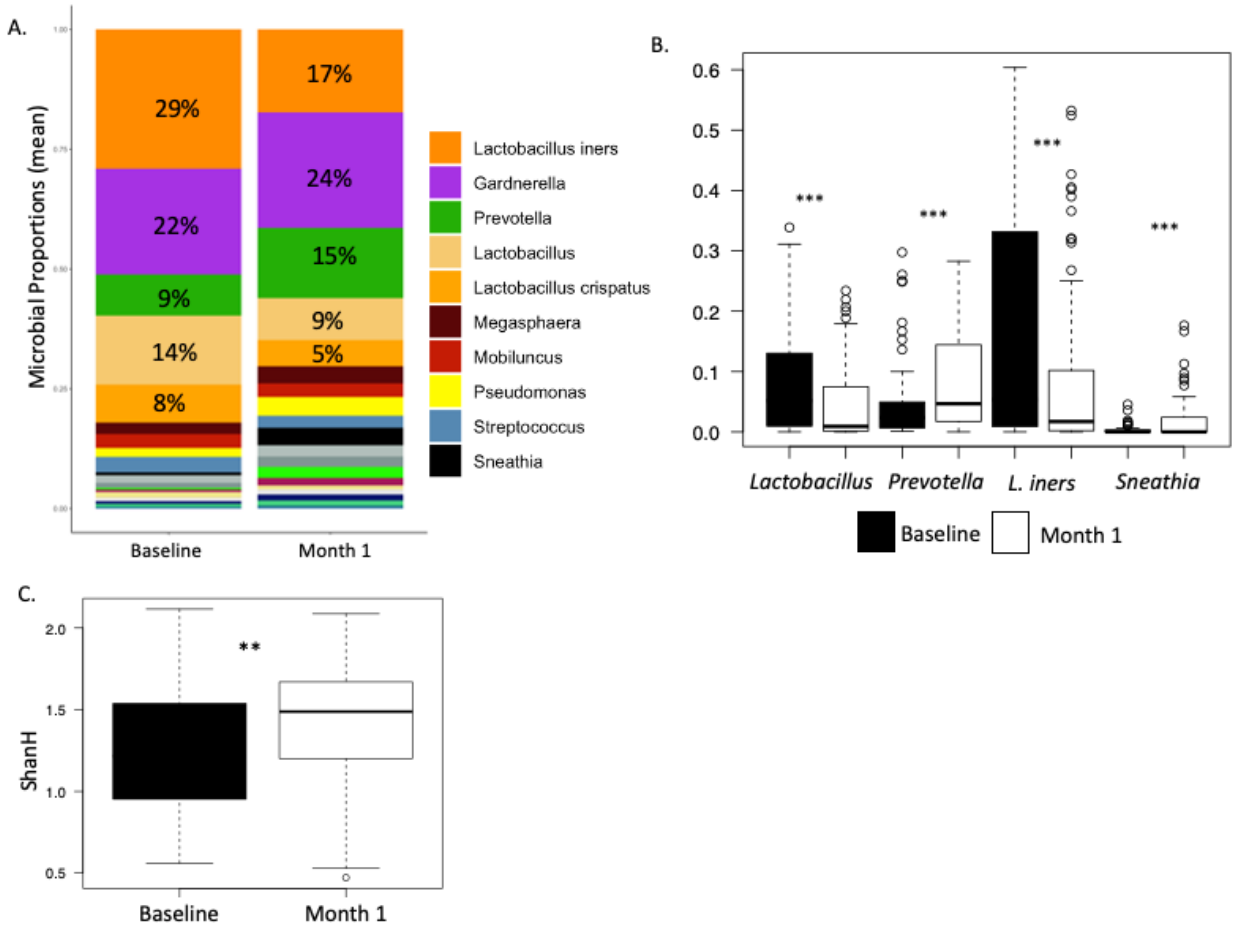

Figure 17. Comparison of microbial proteome changes following 1-month of Copper IUD use. (A) and (B) Analysis of average bacterial genus proportion changes showed significant decreases (P<0.05, FDR-BH<0.05) in mean abundances of *Lactobacillus iners* and *Lactobacillus* species and increased mean abundance of *Prevotella* (P<0.05, FDR<0.05) and *Sneathia* (P<0.05, FDR<0.05) species. (C) Overall diversity of bacterial genera in this cohort observed a significant increase in genus diversity with 1-month of Copper IUD use (** P-value<0.05, *** FDR-BH<0.05).

Table 12. Relative abundance of major vaginal bacterial taxa following Copper IUD initiation compared to baseline as identified by mass spectrometry.

Bacterial genus*	P-Value	Mean Difference (M1-Baseline)	Benjamini-Hochberg P-Value
Lactobacillus	1.58E-05	-0.86	0.00036
Prevotella	0.0031	0.60	0.031
Lactobacillus iners	0.0041	-0.68	0.031
Sneathia	0.0064	0.41	0.037
Peptoniphilus	0.12	-0.14	0.42
Megasphaera	0.11	0.23	0.42
Pedobacter	0.18	0.068	0.58
Pseudomonas	0.24	0.13	0.68
Gardnerella	0.28	0.27	0.71
Bifidobacterium	0.31	0.11	0.72

*Species level identification was used for *L. crispatus* and *L. iners*

Table 13. Bacterial pathway changes at the KEGG annotated b-level associated with initiation of Copper IUD.

KEGG B-level pathway*	Wilcox rank sum p-value	Benjamini-Hochberg p-value
Environmental adaptation	0.00010	0.0024
Energy metabolism	0.0087	0.072
Folding, sorting and degradation	0.012	0.072
Lipid metabolism	0.013	0.072
Cellular community - prokaryotes	0.018	0.081
Carbohydrate metabolism	0.030	0.11
Infectious disease: bacterial	0.064	0.19
Biosynthesis of other secondary metabolites	0.065	0.19
Amino acid metabolism	0.081	0.19
Drug resistance: antimicrobial	0.089	0.19

*Top 10 pathways starting with the most significant.

Table 14. Bacterial pathway changes at the KEGG annotated ko-level associated with initiation of Copper IUD.

KEGG Ko-level pathway*	Wilcox rank sum p-value	Benjamini-Hochberg p-value
ko04626 Plant-pathogen interaction	0.00010	0.0048
ko00020 Citrate cycle	0.00031	0.0072
ko00520 Amino sugar and nucleotide sugar metabolism	0.0014	0.022
ko00030 Pentose phosphate pathway	0.0023	0.026
ko00710 Carbon fixation in photosynthetic organisms	0.0044	0.041
ko00630 Glyoxylate and dicarboxylate metabolism	0.0057	0.044
ko03018 RNA degradation	0.012	0.078
ko00680 Methane metabolism	0.014	0.081
ko02024 Quorum sensing	0.018	0.090
ko00260 Glycine, serine and threonine metabolism	0.021	0.097

*Top 10 pathways starting with the most significant.

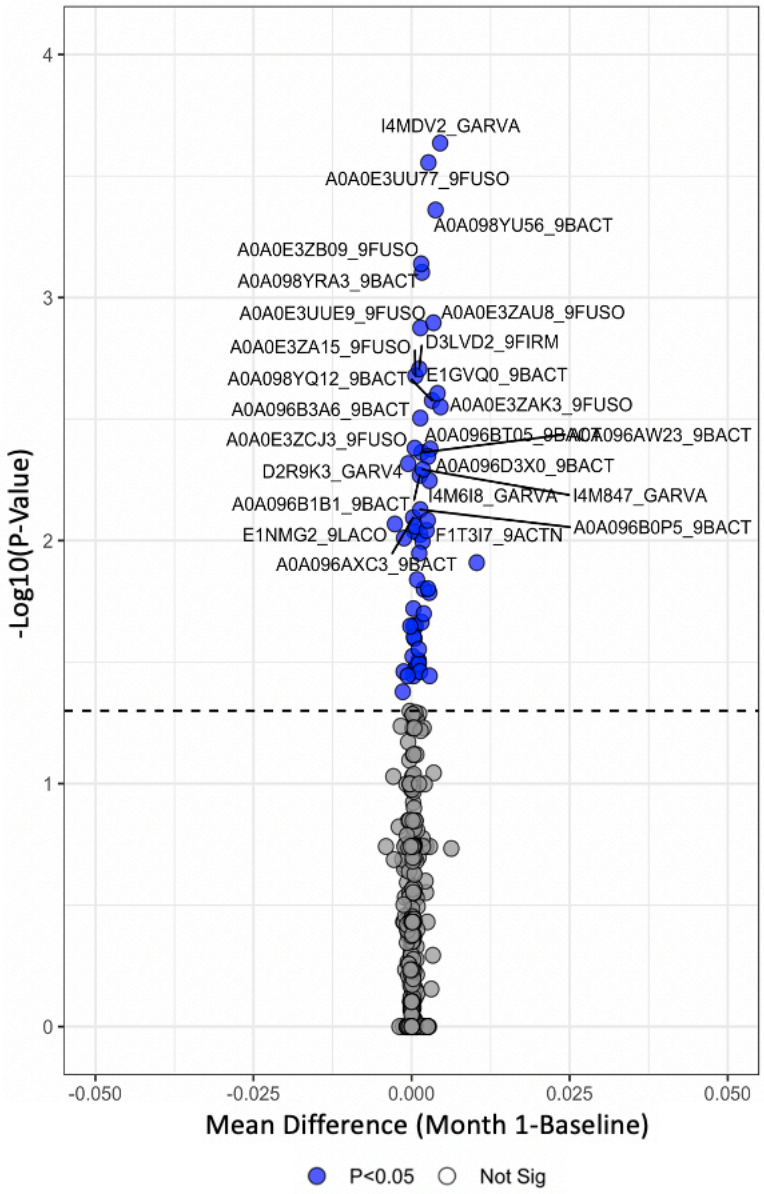

Figure 18. Volcano plot illustrating changes in mean bacterial protein group abundances between month 1 and baseline timepoints with Copper IUD use. Protein proportions that were significant (p-value<0.05) are indicated in blue and above the black dashed line. Positive abundance differences suggest changes that are increasing with Copper IUD use while negative abundance differences suggest a decrease.

Table 15. Top 10 Bacterial protein groups that were observed to be differentially abundant at timepoints month 1 and baseline with Copper IUD use.

Group	Protein[a]	Genus	P-Value*
I4MDV2_GARVA	Elongation factor Tu	*Gardnerella*	0.00023
A0A0E3UU77_9FUSO	Glyceraldehyde-3-phosphate dehydrogenase	*Sneathia*	0.00028
A0A098YU56_9BACT	Phosphoenolpyruvate carboxykinase ATP	*Prevotella*	0.00044
A0A0E3ZB09_9FUSO	50S ribosomal protein L7/L12	*Sneathia*	0.00073
A0A098YRA3_9BACT	Fructose-bisphosphate aldolase	*Prevotella*	0.00079
A0A0E3ZAU8_9FUSO	Fructose-bisphosphate aldolase	*Sneathia*	0.0013
A0A0E3UUE9_9FUSO	Pyruvate kinase	*Sneathia*	0.0013
D3LVD2_9FIRM	Putative glycolate oxidase subunit GlcD	*Megasphaera*	0.0020
A0A0E3ZA15_9FUSO	Inorganic pyrophosphatase	*Sneathia*	0.0021
E1GVQ0_9BACT	Phosphoenolpyruvate carboxykinase ATP	*Prevotella*	0.0025

[a]Proteins identified were significant with at least 2 of the 3 zero replacement methods.
*P-value in table representing that of the "true zero" zero replacement method.

3.6.3 MICROBIOME AND BACTERIAL FUNCTIONAL CHANGES WITH 1-MONTH OF LEVONORGESTREL IMPLANT (LNG IMPLANT) USE

Interestingly, similar to what was observed with DMPA-IM use, LNG Implant use revealed no significant difference in the Shannon-H diversity index (Figure 19B; Wilcoxon rank-sum P=0.75) between baseline and month 1. Nor was a difference in the proportion of LD and nLD classifications observed (McNemar's Chi-square P=0.80). In addition, there was no significant change in the abundance of bacterial species (Table 16; Figure 19A). After analysis of KEGG pathway-level changes no significant changes were observed at the b- and ko-levels. Univariate analysis identified five bacterial protein groups that were differentially abundant (P<0.05; Figure 20), however, none passed multiple comparison correction. Those that were differentially abundant (Table 17) included 30S ribosomal protein S1 from *Gardnerella* (D2RAK2_GARV4), ABC transporter solute-binding protein from *Gardnerella* (D2RCE8_GARV4), acetyl-CoA C-acetyltransferase from *Megasphaera* (D3LU79_9FIRM), chaperone protein DnaK from *Megasphaera* (D3LV85_9FIRM), and flagellin from *Mobiluncus* (E1MH24_9ACTO) all of which increased with 1-month on the LNG Implant except for 30S ribosomal protein S1 and flagellin. Overall, LNG Implant was observed to have no significant effect on the composition of the vaginal microbiome, nor on the functional proteome.

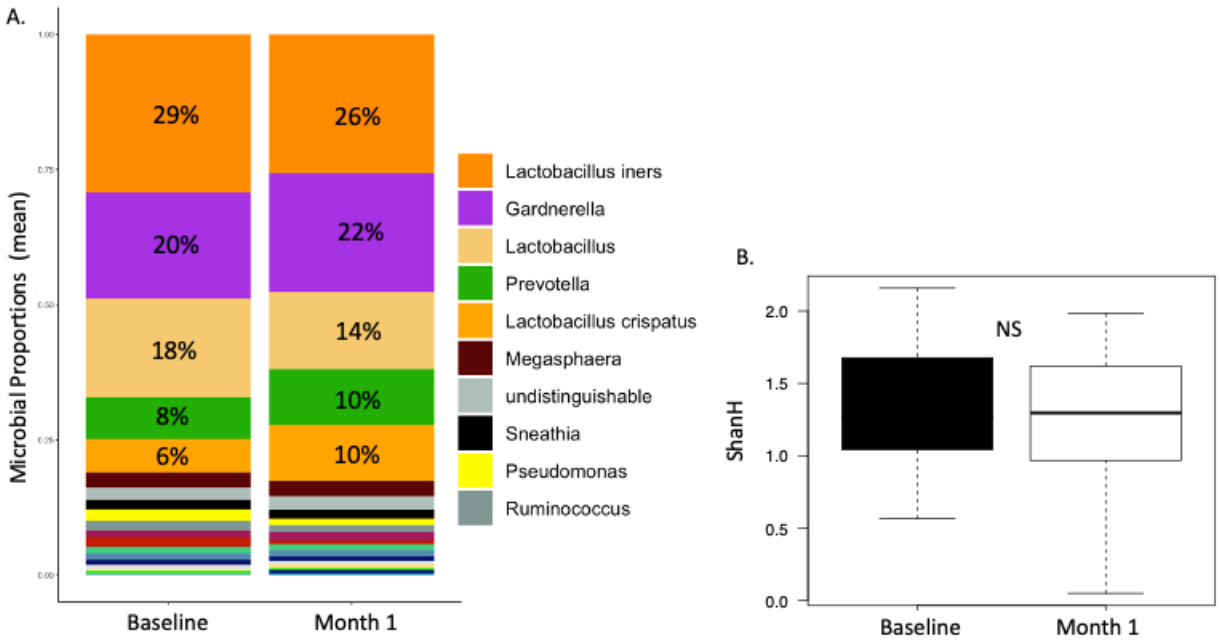

Figure 19. Comparison of mean microbiome changes following 1-month of LNG Implant use. (A) Analysis of average bacterial genus proportion changes between baseline and month 1 with LNG Implant use show no significant changes. (B) Diversity the microbiome at baseline and month 1 were determine with respect to total bacterial genera identified by shanH. No significant difference was observed in diversity of bacterial genus between baseline and month 1 (NS = P-value>0.05).

Table 16. Relative abundance of major vaginal bacterial taxa following LNG Implant initiation use compared to baseline as identified by mass spectrometry.

Bacterial genus*	P-Value	Mean Difference (M1-Baseline)	Benjamini-Hochberg P-Value
Lactobacillus	0.090	-0.27	0.72
Fusobacterium	0.093	0.10	0.72
Porphyromonas	0.10	0.069	0.72
Streptococcus	0.15	0.15	0.72
Lactobacillus crispatus	0.15	0.24	0.72
Lactobacillus iners	0.18	-0.34	0.73
Mobiluncus	0.22	-0.15	0.76
Atopobium	0.29	-0.14	0.76
Prevotella	0.29	0.25	0.76
Peptoniphilus	0.35	-0.041	0.81

*Species level identification was used for *L. crispatus* and *L. iners*

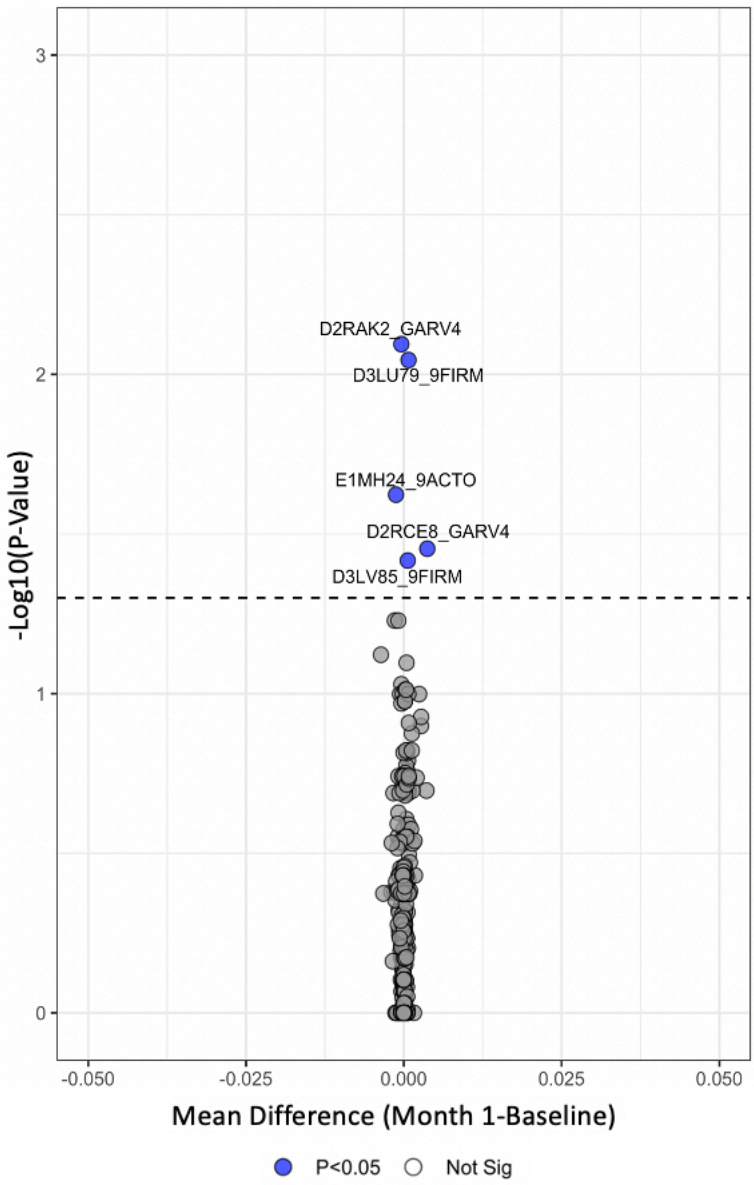

Figure 20. Volcano plot illustrating changes in mean bacterial protein abundances between month 1 and baseline timepoints with LNG Implant use. Protein proportions that were significant (p-value<0.05) are indicated in blue and above the black dashed line. Positive abundance differences suggest changes that are increasing with LNG Implant use while negative abundance differences suggest a decrease.

Table 17. Bacterial protein groups that were observed to be differentially abundant at timepoints month 1 and baseline with LNG Implant use.

Group	Protein[a]	Genus	P-Value*
D2RAK2_GARV4	30S ribosomal protein S1	*Gardnerella*	0.0080
D3LU79_9FIRM	Acetyl-CoA C-acetyltransferase	*Megasphaera*	0.0090
E1MH24_9ACTO	Flagellin	*Mobiluncus*	0.024
D2RCE8_GARV4	ABC transporter solute-binding protein	*Gardnerella*	0.035
D3LV85_9FIRM	Chaperone protein DnaK	*Megasphaera*	0.038

[a]Proteins identified were significant with all 3 zero replacement methods.
*P-value in table representing that of the "true zero" zero replacement method.

3.7 OBJECTIVE 3: PROTEOMIC CHANGES RELATING TO HIV-SEROCONVERSION

This objective aimed to determine proteomic changes relating to HIV seroconversion. Host and bacterial factors that were identified were then compared to the proteomic signatures that significantly changed with 1-month of contraceptive use in objectives 1 (Section 3.5) and 2 (Section 3.6) to identify any overlap. This objective utilizes samples obtained immediately preceding HIV seroconversion for those categorized as cases (PCR positive identifications). To determine whether significant changes to the vaginal mucosal proteome occurred before seroconversion which may suggest susceptibility to HIV infection. This cross-sectional analysis includes a comparison of the proteomic changes of cases compared to that of age-matched controls.

3.7.1 EVALUATION OF PROTEOMIC DATA IN THE HIV CASE-CONTROL STUDY COHORT

During sample processing, one sample lacked sufficient volume to carry out our proteomic sample processing pipeline and was removed from the final sample set. Following our data clean-up and outlier determination pipelines two samples were flagged as outliers, with a resulting final sample set of 124 from which 594 unique proteins were identified. At the bacterial functional level, 49 b-level pathways, 193 ko-level pathways, 546 bacterial proteins, and 1467 bacterial protein groups were identified. Following power curation for inclusion of pathways with 80% power and a coefficient of variance cut-off of 2.38 there were 14 b-level pathways, 26 ko-level pathways, 433 bacterial proteins, and 1158 bacterial protein groups identified from 122 women. The sample-set was further reduced following a focus on samples collected after contraceptive initiation. The final set consisted of 107 women, 20 cases and 87 controls with the contraceptive breakdown being: N=36 DMPA-IM, N=27 Copper IUD, and N=44 LNG Implant, with an even distribution of cases in each contraceptive arm (N=7 cases using DMPA, N=7 cases using Copper IUD, and N=6 cases using LNG Implant). Focusing on pathways identified in samples with which contraception was initiated there were 14 b-level pathways, 26 ko-level pathways, 428 bacterial proteins, and 1147 bacterial protein groups from 105 women that were identified. Further curation (KEGG path type "pathway") reduced our functional dataset to 13 b-level pathways, 25 ko-level pathways, 181 bacterial proteins and 451 bacterial protein groups identified from 100 women. This was our final dataset with which to do bacterial functional analysis.

3.7.2 EVALUATION OF TECHNICAL CONTRIBUTORS TO VARIANCE IN THE PROTEOME DATASET IN SAMPLES FROM THE HIV CASE-CONTROL STUDY COHORT

Sample processing variables of interest for this cohort mirrored those outlined in Objective 1, with influence on proteome variability determined using PVCA. These included: MS batch number, presence of blood in sample seen as visible discoloration, calendar date of BCA assay, number of times a BCA assay was performed on a sample, protein content determined by BCA assay, calendar date of protein digestions, calendar date of LC cleaning of each sample was performed, and calendar date peptide quantifications were performed. Of these 8 variables of interest, 6 were identified to have a weighted percent variance greater than 1% (Table 18). This included the number of times a BCA assay was performed on a sample, the presence of blood in the sample, protein content determined by BCA assay, calendar date of peptide quantifications, calendar date of LC cleaning, and digestion calendar date (Figure 21). Similar to the pre/post-contraception cohort, protein content and presence of blood had a weighted variance >5%, in addition to the number of times a BCA was performed for a sample.

Table 18. Sample processing variables determined by principal variance component analysis to have a percent weighted variance greater than 1% in the case/control secondary cohort.

Sample Processing Variables	Weighted Percent Variance (%)
Residual	66.61
Number of times BCA assay	10.52
Presence of blood in sample	8.53
Protein content	5.54
Calendar date of peptide quant	3.073
Calendar date of LC cleaning	3.053
Digestion calendar date	1.79

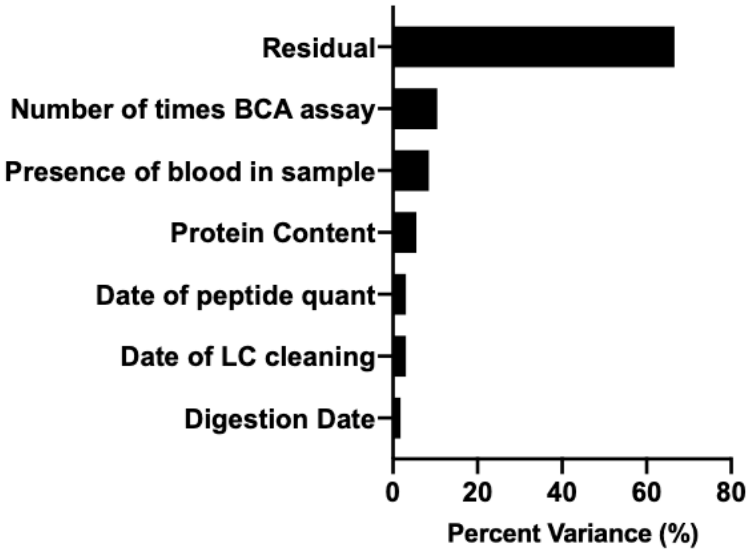

Figure 21. Sample processing variables that contribute to host proteome variability in the case/control cohort as determined by principal variance component analysis. Sample processing variables are those documented during sample processing. From the total sample processing variables tested (N=9) those that are shown here to have a percent weighted variance greater than 1%.

3.7.3 DEMOGRAPHIC INFORMATION ON THE HIV CASE-CONTROL STUDY COHORT

Table 19a and b show baseline demographic and clinical information of the HIV case-control study cohort. Baseline information such as age, marriage category, education category, BMI, clinical site, number of times previously pregnant, and number of living children before contraceptive initiation were considered (Table 19a). Additional clinical variables collected post-contraceptive initiation related to contraceptive side effects including bleeding pattern, duration of bleeding, and vaginal itch, however, 25 women in this cohort did not have documented answers. Information collected during the ECHO trial about behavioural patterns considered in this analysis and included: the HIV status of partner, new sex partners in the last 3-months, whether the primary partner is circumcised, the total number of partners in the last 3-months, condom usage during last vaginal sex act, and the last time each woman practiced vaginal sex act. Similar trends were observed concerning our variables of interest in this cohort and in the pre-and post-contraceptive initiation cohort. As such, there were no significant differences observed between cases and controls, except for bleeding patterns post-contraceptive initiation which was significantly different (Table 19b; Chi-square p-value= 4.74E-02).

Table 19a. Comparison of demographic information collected at enrollment and following contraception initiation between cases and controls.

	Case (N, %)	Control (N, %)	P-ValueΩ
	n=20	n=87	
Location			1.00
Kenya	7 (35.00)	29 (33.33)	
South Africa	13 (65.00)	58 (66.67)	
Contraception			0.43
DMPA-IM	7 (35.00)	29 (33.33)	
Copper IUD	7 (35.00)	20 (22.99)	
LNG Implant	6 (30.00)	38 (43.68)	
Time in days in trial (Mean ± SD)	244.50±117.72	229.31±122.42	0.98
Age (Mean ± SD, range)*	24.15±5.07, 18-35	23.51±3.81, 18-33	1.00
Marriage category			0.35
Married	8 (40.00)	23 (26.44)	
Never married	12 (60.00)	64 (73.56)	
Education (primary school)	18 (90.00)	73 (83.91)	0.73
Previously pregnant (>=1)	17 (85.00)	71 (81.61)	0.97
Number of kids (1 to 2)✤	12 (60.00)	50 (57.47)	0.67
BMI (kg/m2)			0.37
<=30	16 (80.00)	58 (66.67)	
>30	4 (20.00)	29 (33.33)	
Cervical ectopy >1%	0 (0.00)	3 (3.45)	NA

Additional Information

ΩP-value determined by Chi-square test, demographic and behavioural variable with categories containing less than 5 women could only foster an approximate p-value. Chi-square tests for each variable of interest included additional variables not highlighted in the above table. Age comparisons were made between those that were above 25 and below 25. For marriage category women that reported being previously married and currently married were included. For education category women that reported no schooling, only post-secondary, and primary school education were included. For cervical ectopy women were compared to those with 0% ectopy. For Body mass index (BMI) women that had a BMI >30 was included. For the number of children variable comparisons included women that had either no kids and those that had more than or equal to 3 children. For number of times previously pregnant, women that had reported never being pregnant were included.

✤ 19 women did not report their number of living children.

Table 19b. Comparison of behavioural characteristics collected at enrollment and contraceptive effects following contraception initiation between cases and controls. ▼

	Case (N, %)	Control (N, %)	P-valueΩ
	n=20	**n=87**	
Number of partners in last 3 months			0.067
<=1	16 (80.00)	64 (73.56)	
No new sexual partners in last 3 months⊙	15 (75.00)	60 (68.97)	0.052
Condom used with last vaginal sex act	11 (55.00)	30 (34.48)	0.46
Primary partner is HIV negative	15 (75.00)	49 (56.32)	0.81
Partner is circumcised	14 (70.00)	55 (63.22)	0.51
Had practiced vaginal sex > 3days ago	13 (65.00)	35 (40.23)	0.29
Contraceptive effects#			
Bleeding pattern			**0.047**
Regular	11 (55.00)	26 (29.89)	
Spotting only	0 (0.00)	4 (4.60)	
Irregular	5 (25.00)	11 (12.64)	
No bleeding	3 (15.00)	35 (40.23)	
Duration of vaginal bleeding			0.16
Too short	0 (0.00)	5 (5.75)	
About right	15 (75.00)	29 (33.33)	
Too long	1 (5.00)	7 (8.05)	
Vaginal irritation			0.70
Yes	0 (0.00)	4 (4.60)	
No	19 (95.00)	72 (82.76)	

Additional information

Φ P-values were determined using chi-square analysis, for categories consisting of <5 women approximate p-values were determined. Chi-square tests for each variable of interest included additional variables not highlighted in the above table. For number of partners a woman had in the last 3-months women that reported having more than 1 partner were included. For whether the women reported having a new sexual partner in the last 3-months women that reported "yes" were included. For whether condom was used with their last vaginal sex act, women that reported no or reported having a partner, but no sex, were included. For whether the woman's primary partner was on ARV women that reported "yes" were included. For whether their primary partner is circumcised women that reported "no" were included. For when was the last time the women practiced vaginal sex comparisons between >3 days and <=3days were made. Finally, for whether vaginal irritation was experienced following contraception initiation variable comparisons included those that reported irritation.

▼25 women were unchecked for sexual behavioural characteristics. Additionally, 6 women were unchecked for condom usage during last vaginal sex act, 15 were unchecked or did not know the HIV status of their primary partner, and 8 women were unchecked or did not know whether their partner was on ARVs

⊙ One women did not report whether they had any new sexual partners in the last 3 months

#12 were unchecked for bleeding pattern, 50 were unchecked for the duration of vaginal bleeding, and 12 were unchecked for vaginal irritation with contraceptive use

3.7.4 MUCOSAL PROTEOME ANALYSIS OF WOMEN WHO ACQUIRED HIV DURING THE ECHO TRIAL (CASES) COMPARED TO WOMEN WHO REMAINED UNINFECTED (CONTROLS) AND THEIR COMPARISON TO CONTRACEPTIVE USE

Host proteome differences between cases and controls: Proteomic analysis identified 596 unique mucosal host proteins of which 70 were observed to be significantly differentially abundant (P<0.05) between HIV cases and controls (Figure 22). Although, none passed BH multiple comparison corrections (Supplementary Table 7; Figure 22). Following Pearson correlation cluster analysis, samples identified as cases were observed to cluster together amongst some control samples (n=74; Figure 23). Mucosal proteins that associated with this cluster were thus suspected to associate with HIV susceptibility and labelled accordingly as the 'HIV risk cluster' (Figure 23 yellow annotation column). The remaining control samples (N=32) clustered separately (Figure 23 pink annotation column). Functional annotation of proteins within the risk (yellow branch) and control (pink branch) clusters was conducted using DAVID gene ontology (Figure 24). Based on cluster analysis, DAVID functional annotation identified cell-cell adhesion (P=3.12E-06, FDR-BH=0.0012), platelet degranulation (P=0.0019, FDR-BH>0.05), and proteasome-mediated ubiquitin-dependent protein catabolic process (P=0.012, FDR-BH>0.05) as increasing for the HIV risk cluster (Table 20). For the control cluster, B-cell receptor signalling pathway (P=6.07E-05, FDR-BH=0.014), proteolysis (P=0.0051, FDR-BH>0.05), and oxidation-reduction processes (P= 0.0093, FDR-BH>0.05) increased (Table 20). However, it is difficult to make any conclusions from this dataset, since none of the identified significant host factors passed our additional significance threshold (FDR-BH<0.05).

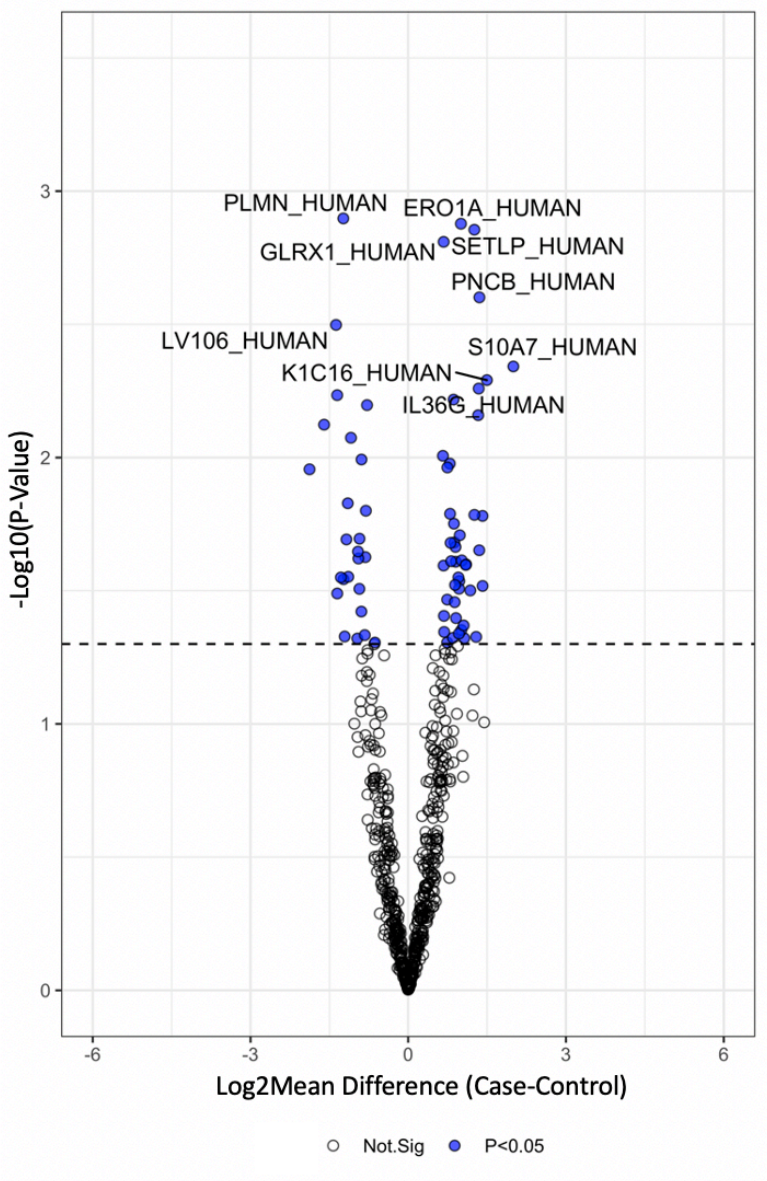

Figure 22. Volcano plot illustrating changes in mean protein abundances between HIV cases and controls. Protein proportions changes that were significant (P-Value<0.05) are indicated in blue and above the dashed black line. No proteins passed BH comparison (FDR-BH<0.05).

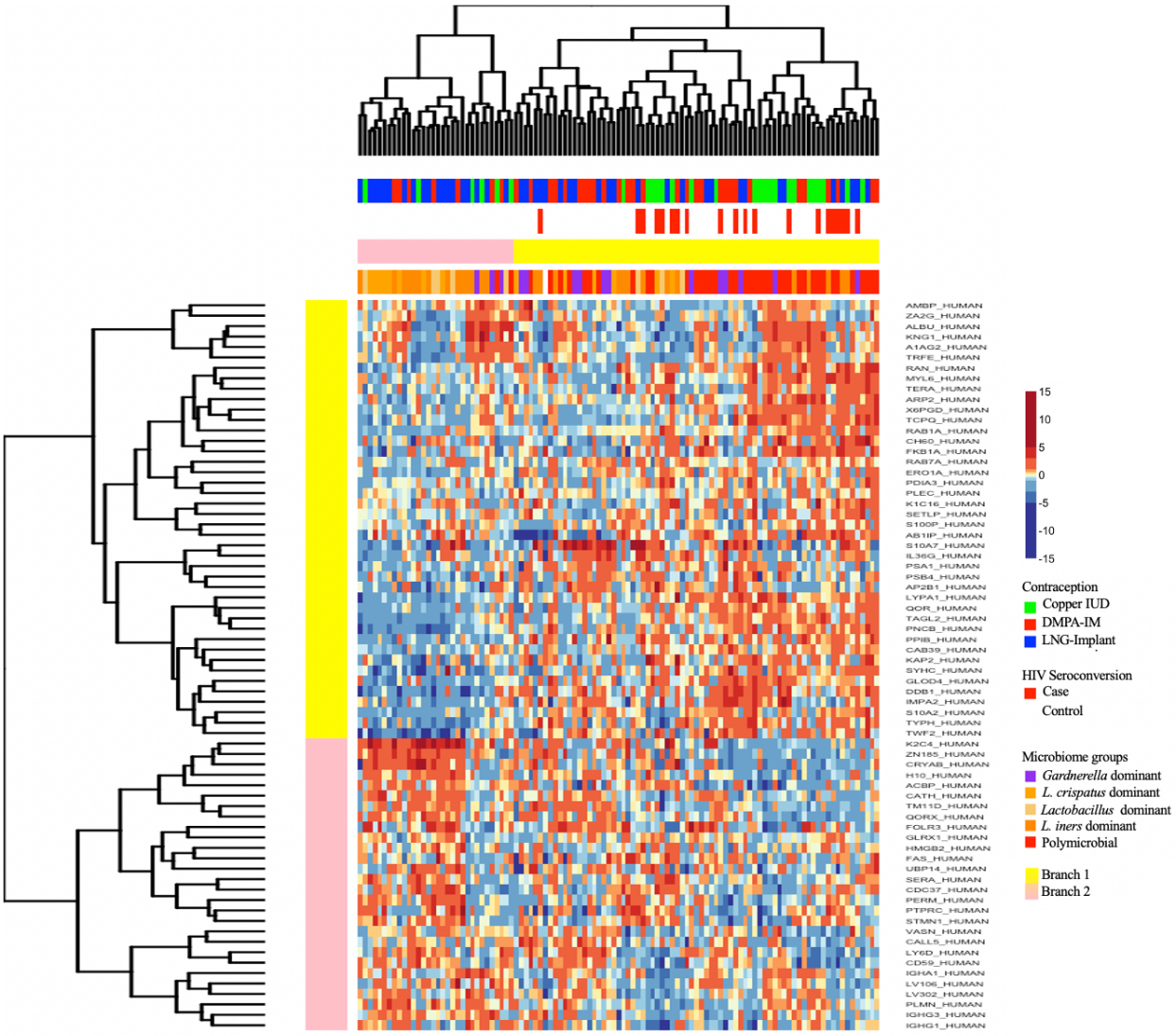

Figure 23. Pearson correlation clustering of differentially abundant host proteins identified between cases and controls. Log2 abundances of the 70 proteins observed to be significantly ($P<0.05$) differentially abundant between cases and controls. Proteins that were observed to increase in abundance in are illustrated in red, while those that decreased are illustrated in blue. Pearson correlation clustering of the differentially abundant proteins identified two branches, one in which the majority of case samples clustered (Branch 1 in yellow) and thus identified as proteins potentially relating to HIV susceptibility ('HIV risk cluster') while the other cluster (Branch 2 in pink) consist only of control samples.

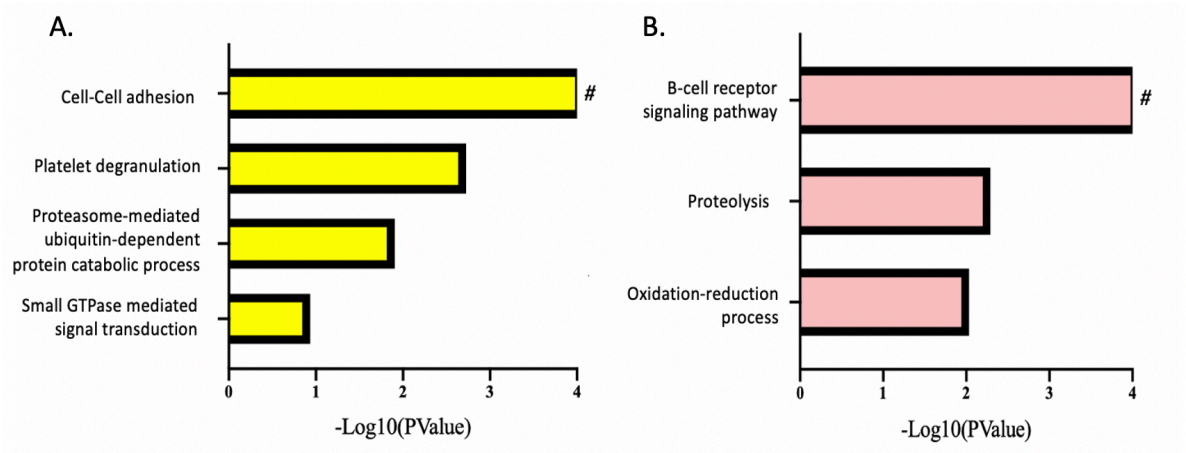

Figure 24. Biological functions identified according to hierarchical cluster analysis. According to cluster analysis in Figure 23 two clusters were identified, one of which consisted of cases while the other controls. Functional analysis using DAVID ontology was conducted based on these identified clusters (branch 1 vs. branch 2). Significant ($P<0.05$) functions specific to host proteins within branch 1 (yellow) are represented in yellow for proteins found in control cluster, while those specific to branch 2 (pink) were those found in the cluster consisting of cases. # Indicates functions that were significant with BH correction.

Table 20. Biological processes identified by DAVID functional annotation from differentially abundant proteins identified after cluster analysis.

DAVID Functional Annotation^	Cluster info	P-Value	Benjamini-Hochberg P-Value	Count
Proteasome-mediated ubiquitin-dependent protein catabolic process	HIV risk	0.012	0.55	4
Platelet degranulation	HIV risk	0.0019	0.31	4
Cell-cell adhesion	HIV risk	3.12E-06	0.0012	8
Oxidation-reduction process	Control	0.0093	0.27	5
Proteolysis	Control	0.0051	0.21	5
B cell receptor signaling pathway	Control	6.07E-05	0.014	4

^DAVID functional pathways with 4 or more host proteins identified were focused on for reported purposes.

Comparison of host proteomic changes observed to have significant associations with contraceptive use and HIV seroconversion: Between the host factors significantly differentially abundant between cases and controls (N=70) and contraceptive use (N=326), 24 were observed to overlap. (Figure 25A) The majority were associated with Copper IUD use (Figure 25B). Due to the level of proteomic changes observed with Copper IUD compared to DMPA-IM and LNG Implant use, this is not surprising. Pathway analysis of the 24 host proteins using DAVID functional annotation identified cell-cell adherens junction pathway to be represented (P=0.0527, FDR-BH= 0.479), which was also observed with Copper IUD use. Additionally, direction of change of these 24 host factors were similar for contraceptive use and between the cases and control comparisons for 14/24 (58.33%) factors (Figure 25B).

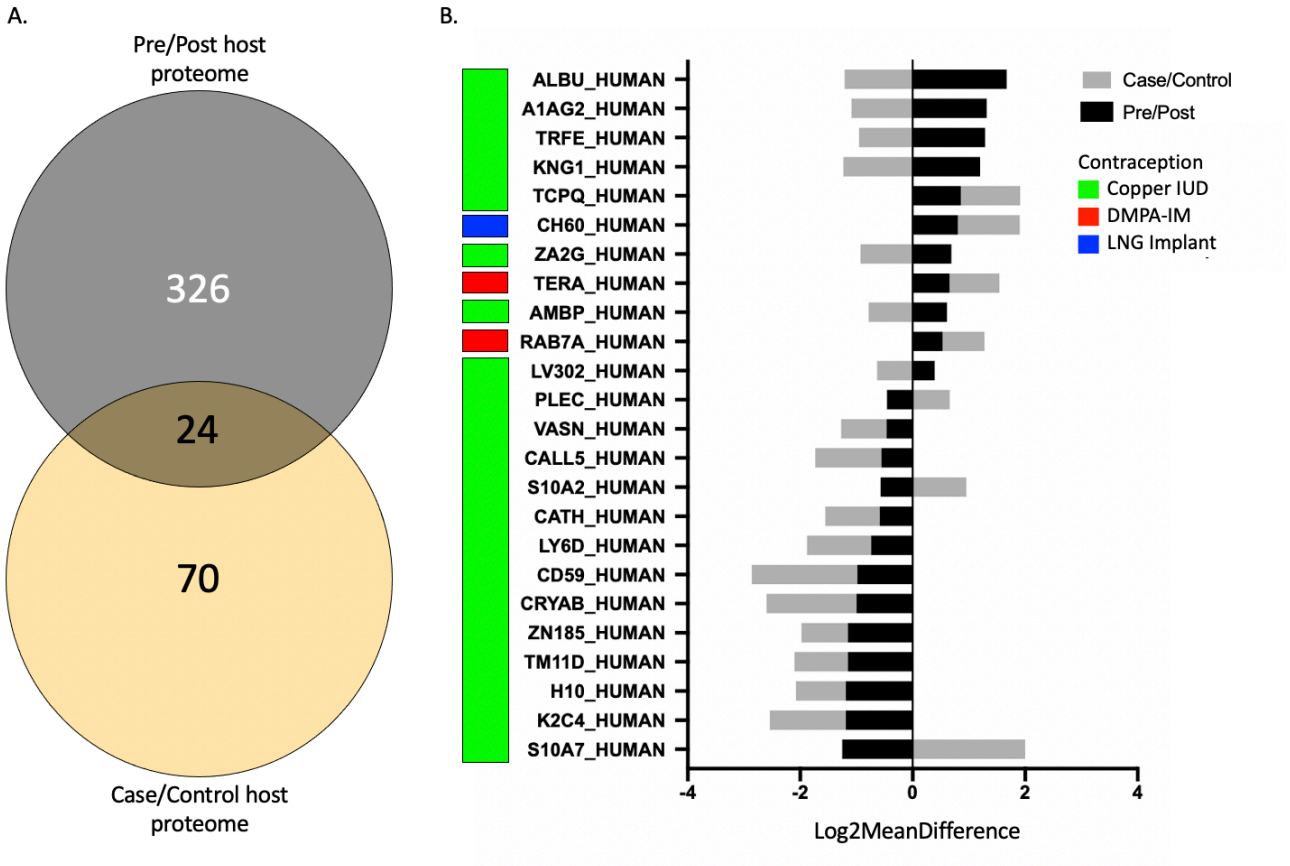

Figure 25. Comparison of host proteins associated with both contraceptive use and HIV seroconversion. (A) Venn diagram of host factors that are overlapping (n=24) between those identified with contraceptive use (n=326) and those identified with HIV seroconversion (n=70). (B) Stacked bar plot illustrating Log2-mean difference (MD) of each overlapping protein, which differed based on dataset used. Grey bars represent Log2MD seen with the case/control dataset, while the black bars represent Log2MD observed in the Pre/Post dataset.

3.7.5 COMPARISON OF MICROBIAL PROTEOME DIFFERENCES BETWEEN HIV CASES AND CONTROLS

Compositional differences in the vaginal microbiome between HIV cases and controls: In the case/control cohort, one woman lacked sufficient microbial proteome data and was removed from downstream analyses. This resulted in a total of 106 women to perform microbial composition analysis. Microbial proteomic analysis identified 22 bacterial genus and 92 unique bacterial species (Figure 26). Euclidean hierarchical clustering identified five community types (CTs): *Lactobacillus iners* dominant (N=28), *Lactobacillus crispatus* dominant (N=14), *L. iners/ L. crispatus* dominant (N=8), *Gardnerella* dominant (N=15) and polymicrobial dominant (N=41) (Figure 26). No association was observed between HIV seroconversion grouping and the identified CT groups (Table 21; Figure 27AC; Chi-square test p-value = 0.936). Based on these defined community types, 30% of women were *L. iners* dominant, 10% were *L. crispatus* dominant, 10% were *Lactobacillus* dominant, 10% were *Gardnerella* dominant, and 40% had a polymicrobial microbiome and seroconverted to HIV positive (N=20), while 26% women were *L. iners* dominant, 14% were *L. crispatus* dominant, 7% were *Lactobacillus* dominant, 15% were *Gardnerella* dominant, and 38% had a polymicrobial microbiome and were HIV negative and classified as controls (N=86) in this cohort. Overall, the diversity of bacterial species between women that seroconverted (cases) and controls, did not significantly differ (P=0.566; Figure 27E). At the genus level, a decrease of *Lactobacillus* species (P=0.053) in cases compared to controls was observed, although this observation did not pass our significance threshold of p-value<0.05 (Table 23). Comparing to observations made with contraceptive use, specifically with the Copper IUD, a decrease in *Lactobacillus* species was also observed. In summary, similar observations were made with contraceptive use. No overall change was observed in the vaginal microbiome in terms of bacterial diversity, which was also observed with both progestin-based contraceptives. At the genus level a decrease of *Lactobacillus* species was seen, although not significant, and was similarly observed with Copper IUD use.

Table 21. Frequency of women within the identified microbial community groups and their relative percentages.

	Case (n, %[a])	Control (n, %[a])	Total	
Polymicrobial	8,20	33,80	41	
L. iners dominant	6,21	22,79	28	
L. crispatus dominant	2,14	12,86	14	P-Value*= 0.94
L. iners and *L. crispatus* dominant	2,25	6,75	8	
Gardnerella dominant	2,13	12,87	15	
Total	20	86	106	

[a]Percent determined relative to total number of women in each CT group
*Chi-square P-value

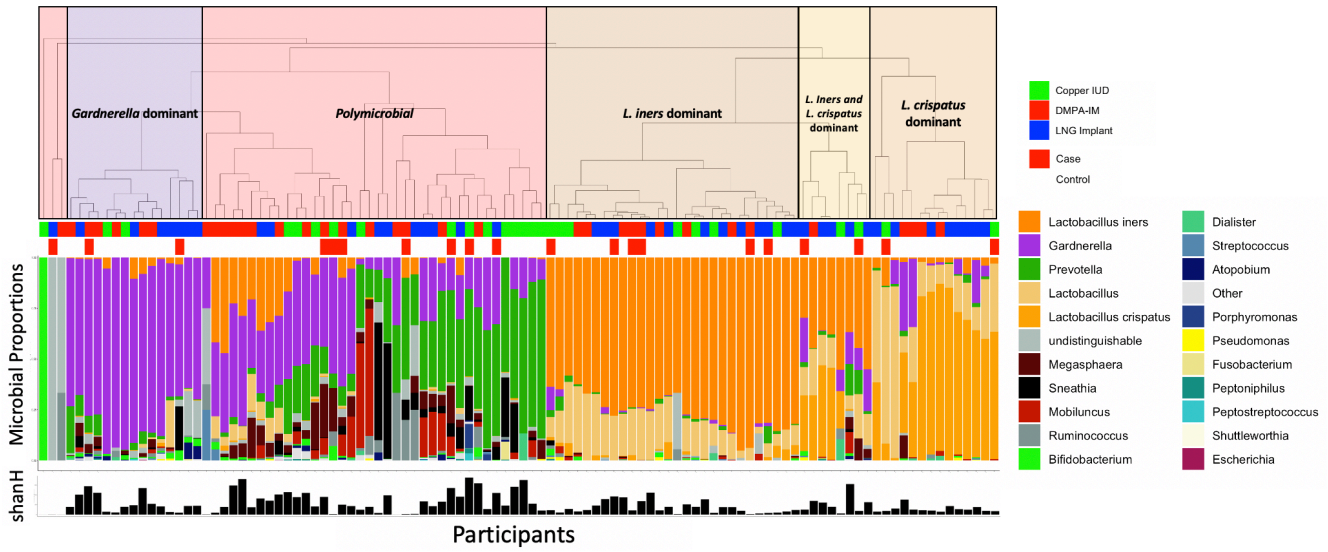

Figure 26. Hierarchical clustering of the vaginal microbiome composition of HIV seroconvertors and controls from the ECHO trial. Each stacked bar plot represents proportions of bacterial genera identified in the microbiome for each woman. Cluster analysis identified 5 community groups which included those that were *Lactobacillus iners* dominant (N=28), *Lactobacillus crispatus* dominant (N=14), *Lactobacillus* dominant (N=8), *Gardnerella* dominant (N=15) and polymicrobial (N=41). Nevertheless, clustering according to HIV seroconversion was not observed as illustrated visually with the case/control annotation column.

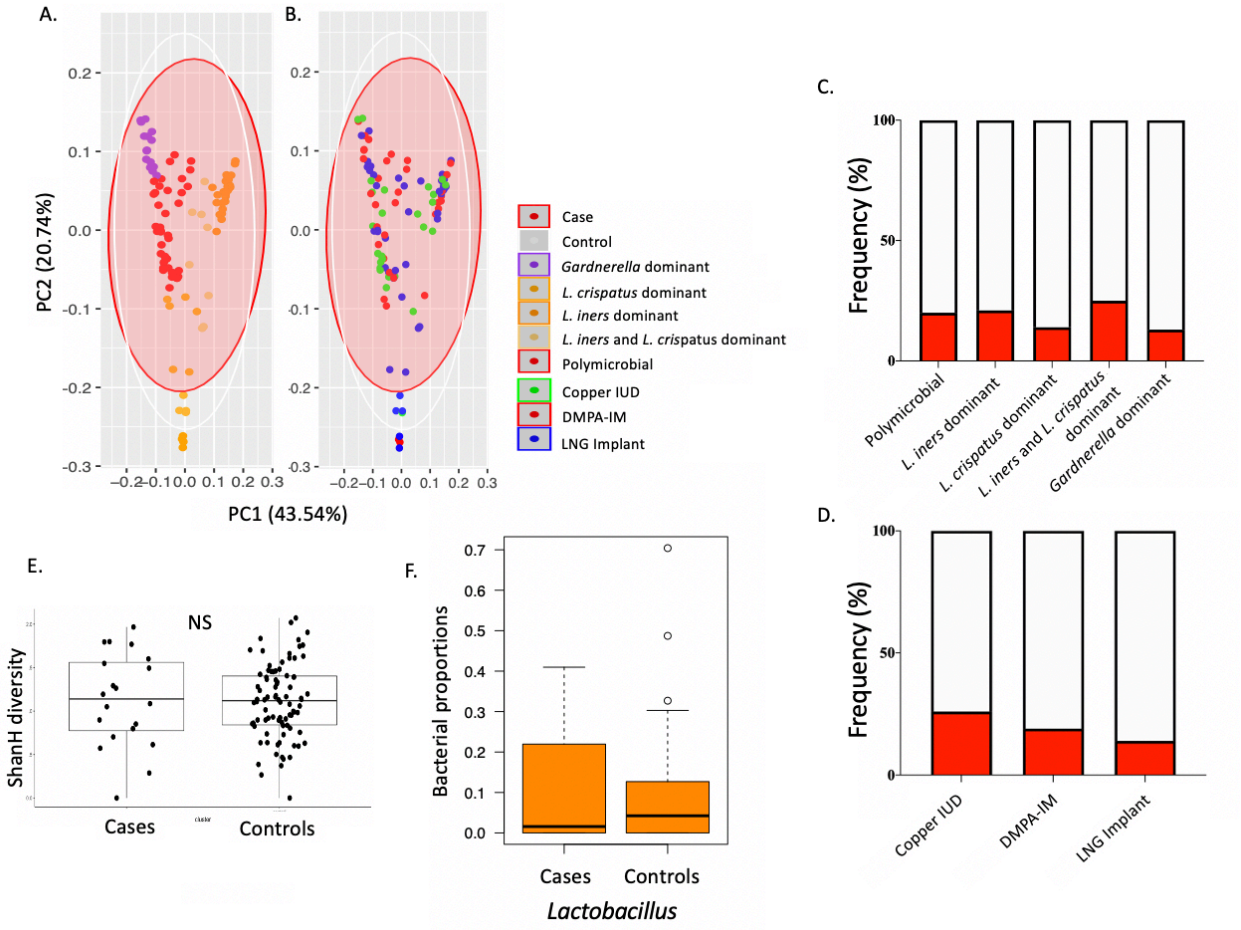

Figure 27. Analysis of vaginal microbiome differences between HIV cases and controls. (A) Principal component analysis (PCA) showing the clustering of the bacterial proteome by (A) CT group and (B) contraception, illustrating no significant clustering differences according to CT group and contraception method amongst cases and controls. (C) Frequency of women in each CT group that were classified as either a case (red) or control (white) corresponding to the PCA plot in B, with the majority having either a *L. iners* or polymicrobial dominant microbiome. (D) Frequency of women in each contraceptive arm with same colour distinctions for cases and controls. (E) Diversity at the species level between cases and controls was determined using Shannon's H diversity index. Comparison of diversity indices using Wilcoxon rank sum test shows no significant differences. Although (F) at the genus level *Lactobacillus* saw a trending decrease in HIV cases compared to controls.

Table 22. Bacterial genus that was observed to be differentially abundant between HIV cases and controls.

Bacterial genus*	P-Value	Mean Difference (Case-Control)	Benjamini-Hochberg P-Value
Lactobacillus	0.053	-0.55	0.55
Peptostreptococcus	0.084	0.054	0.55
Mobiluncus	0.13	0.25	0.55
Lactobacillus crispatus	0.14	-0.45	0.55
Ruminococcus	0.15	0.24	0.55
Porphyromonas	0.18	0.15	0.55
Dialister	0.33	0.053	0.73
Pseudomonas	0.36	0.13	0.73
Shuttleworthia	0.41	0.054	0.73
Lactobacillus iners	0.42	-0.32	0.73

*Species level identification was used for *L. crispatus* and *L. iners*

Bacterial proteome differences between cases and controls: For this analysis, our dataset consisted of 100 women with 13 b-level pathways, 25 ko-level pathways, 181 bacterial proteins and 451 bacterial protein groups identified. Following a Wilcoxon rank-sum test no significant differences were observed for b-level and ko-level pathways between cases and controls. However, at the bacterial protein level protein groups that were significantly different with a p-value <0.05 are listed in Table 24; none passed BH correction (Figure 28). Exploration of whether any overlap could be seen with significant (P<0.05) bacterial protein groups observed between cases vs. controls and those identified with contraceptive use was also done. In terms of bacterial protein groups, 3 (1 observed with DMPA-IM use and 2 observed with Copper-IUD use; Table 25) that belonged to either *Megasphaera* or *Sneathia* bacterial species were observed to increase with contraceptive use compared to their corresponding baseline sample timepoint and between cases and controls. However, the overall analysis of bacterial protein groups did not reach our threshold of statistical significance (FDR-BH<0.05) for the case/control cohort and therefore it was concluded that no significant effects were observed.

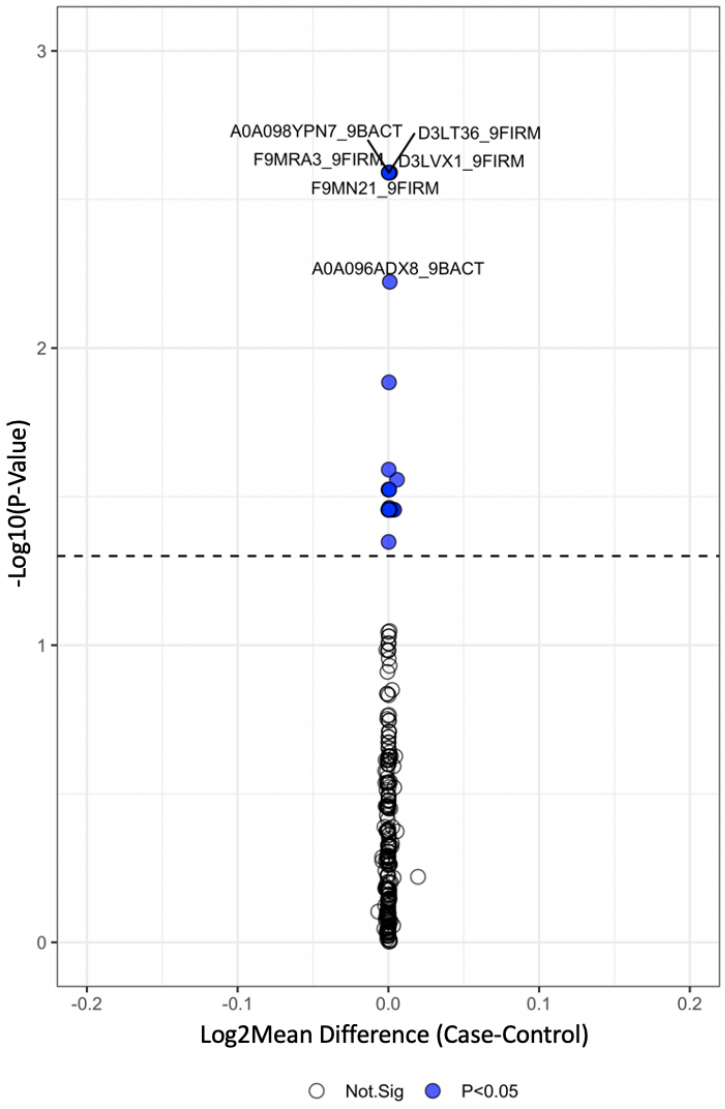

Figure 28. Volcano plot illustrating differences in mean bacterial protein group abundance between HIV cases and controls. Protein proportions that were significant (P-value<0.05) are indicated in blue and above the black dashed line. None of the bacterial protein groups passed BH correction. Positive abundance differences suggest changes that are increased abundance in HIV cases while the latter suggests lower abundance in cases.

Table 23. Top 10 bacterial proteins that were observed to be differentially abundant between HIV cases and controls.

Group	Protein[a]	Genus	P-value*
A0A098YPN7_9BACT	Beta-N-acetylhexosaminidase	*Prevotella*	0.0026
D3LT36_9FIRM	Pyruvate-flavodoxin oxidoreductase	*Megasphaera*	0.0026
D3LVX1_9FIRM	Butyryl-CoA dehydrogenase	*Megasphaera*	0.0026
F9MN21_9FIRM	Aldehyde-alcohol dehydrogenase family protein	*Megasphaera*	0.0026
F9MRA3_9FIRM	Glycerol kinase	*Megasphaera*	0.0026
A0A096ADX8_9BACT	Phosphoglycerate kinase	*Prevotella*	0.0060
A0A0E3ZDE1_9FUSO	Triosephosphate isomerase	*Sneathia*	0.013
D3LUG3_9FIRM	Phosphate acetyltransferase	*Megasphaera*	0.026
A0A0D9NE67_PREIN	Elongation factor Tu	*Prevotella*	0.028
A0A096ACI1_9BACT	30S ribosomal protein S1	*Prevotella*	0.030

[a]Proteins identified were significant with all 3 zero replacement methods.

*P-value in table representing that of the "true zero" zero replacement method.

Table 24. Bacterial proteins significant in comparisons between cases and controls that were similarly observed with contraceptive use.

Group	Protein	Genus	P-value	Contraception
A0A0E3ZDE1_9FUSO	Triosephosphate isomerase	*Sneathia*	0.013	Copper IUD
D3LVK3_9FIRM	5-methyltetrahydropteroyltriglutamate--homocysteine methyltransferase	*Megasphaera*	0.035	DMPA-IM
A0A0E3ZAV1_9FUSO	Adenylate kinase	*Sneathia*	0.045	Copper IUD

CHAPTER 4: DISCUSSION

Progestin-based contraceptives, more specifically DMPA, have been a topic of concern in regions of the world, such as in sub-Saharan Africa, where incidence of HIV infection is high. Several meta-analyses have shown an association between progestin-based contraceptives on susceptibility to HIV infection, which provided the rationale for the ECHO study to better answer this question in a randomized trial. The ECHO trial observed no differences in HIV infection between contraceptive arms; however, the work described by this thesis explores changes to mucosal immunology and microbiology of the female genital tract in participants from this trial (*168*). This work also explores the potential proteome effects that could associate with HIV infection risk. Several major observations were made included that all contraceptives were observed to affect the mucosal proteome with distinct and different magnitudes of change. Women randomized to the Copper IUD were observed to have the greatest magnitude of change to the host mucosal proteome (Figure 7), specifically with respect to inflammatory signatures (Figure 10). The progestin-based contraceptives, DMPA-IM and LNG Implant, saw a lesser magnitude of effect (Figure 3 and 12, respectively). Signatures relating to innate immunity were observed to decrease with DMPA (Figure 5) while the vaginal microbiome, for both progestin-based contraceptives (DMPA-IM and LNG Implant), saw no significant alterations. Copper IUD use was shown to have considerable effects on the mucosal proteome including increased diversity of the vaginal microbiome post-initiation. Decreased abundances of *Lactobacillus* species and increased abundances of *Prevotella* and *Sneathia* species were observed for women using the Copper IUD (Figure 17B). In the secondary cohort of HIV cases and age-matched controls, cases were shown to have significant differences in protein levels relating to cell-cell adhesion (Figure 24AB), while differences to the microbiome were minimal. Although the vaginal microbiome of women that seroconverted to HIV did exhibit a decrease in *Lactobacillus* (not significant) (Figure 27F). Interestingly, host proteome changes related to HIV seroconversion overlapped with early changes associated with contraceptive initiation, especially those identified with Copper IUD use. These findings suggest that both hormonal and non-hormonal contraceptives have a significant impact on the mucosal proteome of the FGT. The observed changes to the host proteome saw some associations with HIV infection risk. In terms of the microbiome, Copper IUD use was the only contraceptive to elicit significant effects both to the microbial diversity and the functional bacterial proteome.

Mucosal host and bacterial proteomic changes associated with contraceptive use.

Progestin-based contraceptives, DMPA-IM and LNG Implant, use showed significant changes to the vaginal mucosal proteome. DMPA-IM use showed a decrease in innate immune response which coincides with its proposed mechanism of interaction with steroid receptors. Progestins interact with several steroid receptors ultimately affecting the expression of certain gene products (*124*). Overall progestins interact with the progesterone receptor with high affinity, as well as the glucocorticoid receptor (GR), androgen mineralocorticoid receptor and several estrogen receptors with varying affinities (*124*). Medroxyprogesterone acetate, specifically, has a high affinity for GR, compared to progesterone and other progestins (i.e., levonorgestrel, and etonogestrel, norethisterone) (*124*). Interaction of ligands with GR has shown an immunosuppressive effect reducing the transcription of several cytokine and chemokine genes such as IL-2, IL-8, IL-6, and RANTES, observed in models of cervical cell lines and PBMCs (*124, 169*). The mechanism by which progestins suppress transcription is through their interaction with activator protein 1 and nuclear factor $\kappa\beta$ which would normally activate their transcription (*124, 169*). GR has also been implicated in activating the secretion of T-helper 2 (Th2) anti-inflammatory cytokines (*124*).

This agrees with our observation of decreased signatures relating to innate immune response suggesting immunosuppression following 1-month of DMPA-IM use. In fact, real-world application of this immunosuppressive effect is shown for the treatment of cancer patients. MPA has often been used as a therapeutic in breast cancer patients for the purpose of suppressing lymphocyte production (*124, 170*). Within the innate immune response pathway, which was identified to significantly decrease with DMPA use, specific protein factors identified included mucins (MUC5A/5B) (Table 4). Mucins make up a significant portion of the mucosal fluid, their structure resembling a filamentous protein contributing to its viscosity (*157*). Pro-inflammatory cytokines have also shown to mediate the expression of mucins, meaning a decrease in inflammatory cytokines could mean a decrease in the concentration of mucins in the vaginal mucus, an essential component of this physical barrier (*157*). In addition, mucins have also been shown to have anti-microbial and anti-viral characteristics. Their anti-viral characteristics have been observed in saliva concentrated for MUC5B and MUC7, where anti-HIV activity have been reported (*158*). Their anti-microbial activity has been reported for microbial pathogens like *Vibrio cholerae* and *Helicobacter pylori (157)*. Secretion of digestive enzymes by *V. cholerae* and *H. pylori* target mucin carbohydrates, reducing their degree of glycosylation ultimately affecting the

viscosity of the vaginal mucus allowing bacterial translocation to the underlying epithelium (*157*). These are just a few examples of how pathogens can target mucins to facilitate their infection, although these specific mechanisms have not been characterized for common vaginal bacterial species. Therefore, the observation of decreased abundance of mucin proteins with DMPA-IM use may have implications on the permeability of the vaginal mucus. Transglutaminase 3 was also observed to decrease with DMPA use which reflects negatively on the cornified envelope of the vaginal epithelium, negatively altering the integrity of the epithelium. In terms of the vaginal epithelium, plenty of studies have explored whether DMPA use negatively alters its integrity in several model systems (i.e., macaque models) with a consensus being that DMPA use negatively alters the epithelial barrier (*110, 127, 138, 140, 149, 151-154, 171, 172*). Another protein signature of interest was Serpin B2, identified following both univariate and multivariate analysis and was shown to increase with DMPA-IM use. This observation my allude to increased anti-coagulation due to Serpin B2 being an anti-coagulation factor (*159, 160*). Other reports have documented multiple other functions of Serpin B2 including those relating to immune response such as regulating T-helper response and inhibition of IL-1β production (*159*). Additionally, an increased abundance of SerpinB2 may indicate the presence of monocytes/macrophages in the vaginal mucosa, which are known to express Serpin B2 during periods of inflammation (*159*). Also, quite interesting is the paralog of Serpin B2, Serpin B1, has been speculated to have protective effects against HIV infection (*173*). Although our pathway analysis identified a pathway which suggests immunosuppression with DMPA use, the observed increase of Serpin B2 could additionally mean the increased presence of certain inflammatory factors in the FGT. A conclusion recently hypothesized in the Hapgood *et al* 2018 review (*124*). In terms of the vaginal microbiome, DMPA use did not associate with significant changes to the diversity or the abundances of bacterial species. An observation that has been observed in multiple studies focusing on the vaginal microbiome with DMPA use (*43, 127, 131, 145, 147*). In terms of the functional capacity of the organisms the b-level pathway amino acid metabolism was shown to significantly increase post-initiation. While at the ko-level, several metabolic pathways were observed to significantly change including galactose, cysteine and methionine, and pyruvate metabolism. Although both the b- and ko-level pathways did not pass our additional significance threshold (FDR-BH<0.05). In addition, ten bacterial protein groups were observed to significantly change although none were significant following application of additional significance thresholds (FDR-BH<0.05). As a result, it was

concluded that no significant changes to the vaginal microbiome nor bacterial proteome due to these observations not passing our additional significance threshold.

LNG Implant, in this cohort, did not have any significant effects on the mucosal proteome. Currently, there are very few reports that have looked at the effects of subdermal LNG Implant, but from those that have their observations vary. Ildgruben *et al* 2003 observed an increased presence of CD45+ and CD4+ cells with LNG Implant use, while Achilles *et al* 2020 observed no significant changes in immune cell populations and soluble factors (*128, 174*). Goldfien *et al* 2015 conducted gene expression analysis on endometrial and cervical transformation zone tissues (*149*). Their observations included an increase in chemotaxis of myeloid cells and binding of phagocytes and lymphocytes, while at the cervical transformation zone they observed a decrease in cell proliferation and blood cell adhesion (*149*). Therefore, there is definitely a need for more studies focusing on use of the LNG subdermal implant as well as the LNG-IUD since there may be differential effects due to their difference in application.

From the three contraceptive arms, Copper IUD use exhibited the greatest host proteomic changes. Nearly 50% of the host proteome changed, majority of which were factors indicating activation and recruitment of immune cells (Figure 10). This would agree with the mechanism of action of Copper IUDs, which is to prevent pregnancy by inducing an inflammatory environment not conducive for sperm viability (*27, 28*). Congruently, a recent study on Copper IUD use published by Achilles *et al* 2020 observed an increase in the presence HIV target cells and inflammatory mediators following 30 days of use (*128*). Sharma *et al* 2018 made similar observations, with increased pro-inflammatory cytokines observed in women who used the Copper IUD in comparison to the LNG intrauterine device (*175*). Observations of increased inflammation with Copper IUD use have similarly been observed in macaques (*176*). Additionally, the results of this thesis showed a decrease in proteomic signatures relating to cell-cell adhesion and keratinocyte differentiation, which suggests an altered epithelial barrier, an observation considerably novel for Copper IUD use. There are very few reports that discuss the effect of the Copper IUD on the vaginal epithelium, although a 1987 review does mention the disruption of the superficial layer of the epithelium in contact with the IUD (*177*). Whether disruption occurs in the FGT besides the area directly in contact with the Copper IUD is still

relatively unknown. Copper IUD use demonstrated a significant increase in bacterial diversity, specifically decreasing *Lactobacillus* species and *L. iners*, and increasing *Sneathia* and *Prevotella* species. *Sneathia* and *Prevotella* species are anaerobic bacteria commonly observed in molecular cases of BV (*81*). Achilles *et al* 2018 observed a longitudinal increase in BV in Copper IUD users, which was not similarly observed in their hormonal contraceptive groups (*121*). Achilles *et al* 2018 explored changes in specific bacterial taxa, particularly those often classified as non-optimal due to their presence in cases of BV including *A. vaginae*, *G. vaginalis*, and *Megasphaera* and those classified as optimal, *Lactobacillus (121)*. Although this thesis did not observe the same changes in bacterial taxa as the Achilles *et al* 2018 study, the overall observations from both studies indicate an increase in BV-associated bacteria. Onderdonk *et al* 2016 published a comprehensive review of the human microbiome project highlighting specific BV-associated bacteria and their implications on vaginal health (*81*). Both Prevotella and Sneathia species were described to produce collagenase and fibrinolysin, implicated in promoting sloughing, reducing the integrity of the vaginal mucosal barrier (*81*). In fact, commonly observed Sneathia species (*S. amnii* and *S. sanguinegens*) have correlated with the upregulation of pro-inflammatory cytokines (*81*). In addition, *S. sanguinegens* was observed by Gottschick *et al* 2017 to act as a biomarker for the presence of biofilm in cases of BV (*178*). Biofilm presence has been implicated in resistance to antibiotic treatment of BV due to the physical protection it provides hindering movement of the antibiotic to the underlying bacterial population (*178*). *Prevotella* species have been observed to produce products that support the growth and survival of other anaerobic bacteria by increasing vaginal pH (*81*). Our observations could imply the use of the Copper IUD has negative implications on the composition of the vaginal microbiome. Negative implications including an increase in bacterial diversity and bacterial taxa commonly observed with BV, while concurrently decreasing beneficial *Lactobacilli*. At the functional level, several pathways relating to the metabolism of carbohydrates, lipids, and energy were observed to significantly increase post-Copper IUD initiation at the b-level, which was further emulated at the ko-level. Ko-level pathways that were observed to significantly change included an increase in amino sugar and nucleotide sugar metabolism, and glyoxylate and dicarboxylate metabolism, to name a few of those that passed BH-multiple comparison correction.

For this objective this thesis observed an immunosuppressive effect of DMPA with no significant effect on the vaginal microbiome. This could suggest a favourable environment for establishment of the viral founder population during the initial stages of HIV infection at the FGT (*124, 179*). LNG Implant was observed to have no effect on both the host and bacterial proteome and vaginal microbiome. This observation is not surprising due to the differential affinities levonorgestrel has for GR compared to MPA, where MPA has a higher affinity for GR and levonorgestrel has very little to no affinity. Rather surprising was our observations within the Copper IUD arm. Copper IUD use associated with vaginal inflammation and negatively altered the vaginal epithelial barrier with significant changes to the diversity of the vaginal microbiome and optimal *Lactobacillus* and non-optimal BV-associated bacteria. Increased inflammation that was observed within this arm does coincide with the pregnancy prevention mechanism of Copper IUD. Although our altered epithelial barrier and vaginal microbiome observations are rather novel and further support a non-optimal vaginal mucosal environment following Copper IUD use. Thus, drawing into question its use as a control arm in the ECHO trial.

Mucosal proteomic changes associated with HIV seroconversion and its relationship with contraceptive use.

For objective 3 samples prior to HIV seroconversion were used to compare against matched controls who remained HIV-negative in this study. The purpose was to determine whether specific biological mechanisms could be captured that would suggest increased HIV susceptibility. Women that were classified as cases in this subset clustered together, with cluster driven pathway analysis showing a decrease in B cell receptor signaling pathway and an increase in cell-cell adhesion compared to the cluster containing only controls. B cells, and their regulation, have been commonly observed to be altered with HIV infection suggesting B cell dysfunction (*180*). Although dysfunction was correlated with HIV viremia (*180*). Our observation of reduced B cell receptor signaling included host factors like tyrosine-protein phosphatase C (PTPRC) which regulates B cell receptor signaling and several immunoglobulin factors (IGHA1, IGHG1, IGHG3) produced by B cells. This does not coincide with current observations regarding B lymphocytes and HIV infection as mentioned above; however, this could be a result of an increased focus of studies on an association after HIV seroconversion. Cases were also observed to associate with an increase in signatures relating to cell-cell adhesion

(Figure 24). In a 1995 study, HIV was observed to acquire cell adhesion factors from its host for use in the establishment of infection (*181*). The observation of an increase in cell adhesion factors may suggest an increased likelihood of establishing HIV infection in our case cluster. An interesting direction to take with this analysis is to explore if a specific contraceptive were causing this increase. However, this secondary cohort was not designed to study this question as we were not powered (number of cases in each contraceptive arm: N= 7 Copper IUD, N=7 DMPA-IM, N=6 LNG Implant) to explore this relationship. From the significant host factors that were observed in this subset, several were additionally observed with contraceptive use, specifically with Copper IUD. Pathway analysis revealed cell adhesion to be the dominating pathway represented by these factors, although analysis of these proteins and their functions also highlighted immune-related signatures. In terms of microbiome changes between cases and controls, obvious clustering of seroconversion status with the identified community types nor with the contraceptive method was not observed. However, analysis of significance at the genus level identified *Lactobacillus* to decrease in cases compared to controls (Figure 27F). Despite host and bacterial proteomic and microbial changes observed in this objective not passing the additional threshold of significance (FDR-BH<0.05), the observations suggest some differences between cases and controls. Something to consider with this objective is the lack of information regarding time to seroconversion. The vaginal samples that were provided for this objective were those collected immediately preceding the clinical visit when seroconversion status was determined. As such, the samples we received ranged from 1-month post-contraception initiation to over 1 year. This brings up concerns regarding the comparison of samples of long-term contraceptive users (>1year) to short-term.

4.1 STUDY LIMITATIONS: This study was designed to have >80% power to detect 3.0-fold changes in microbiome taxa, 1.35-fold changes in the host proteome, and 1.4-fold changes in microbial functional pathways. Principal component variance analysis (PVCA) and Chi-square tests identified several sample processing (less so clinical) variables as potential confounding factors contributing to mucosal proteome variability in the pre-and post-contraception use cohort. These included protein content, presence of blood in the sample, number of times a sample underwent the digestion protocol, and calendar date of LC cleaning. Of the clinical variables collected, excluding method of contraception randomized to, bleeding pattern following contraceptive initiation was found to be significantly different between contraceptive arms. Otherwise, no significant difference between the contraceptive arms was observed for our clinical variables of interest. In our secondary cohort looking at cases vs. controls, sample processing variables contributing to mucosal host proteome variability included the number of times a BCA assay was performed on each sample, presence of blood in the sample, protein content, calendar date of peptide quantifications, calendar date of LC cleaning, and digestion calendar date. Our clinical variables of interest similar to the pre-/post-contraceptive cohort, showed bleeding pattern as significantly different (Table 3B and 19B). The data presented in the results section of this thesis did not control for these potential confounding variables and thus presents as a limitation of this study. In addition, the vaginal microbiome was not controlled for in our mucosal host proteome analysis objective. Our lab has previously shown the impact the microbiome has on mucosal host pathways, therefore, further validation of our findings with contraception use controlling for the microbiome would be required. Additional limitations include our sample access. For this study access to 1-month and a few 3-month post-contraception timepoints were provided making it difficult to discern whether the effects observed are transient or long-term. An additional study following contraception use past 1-month would be necessary to make this distinction. In addition, our secondary cohort lacked the power to detect differences between women classified as a case compared to matched controls within each contraceptive arm due to the small sample size of cases.

4.2 FUTURE DIRECTIONS:

Our findings provide insight into the transient effects of each contraceptive from the ECHO trial. What is not capture is whether the effects observed persist beyond 1-month. However, significant changes to the mucosal proteome that has been associated with increased risk of HIV susceptibility were observed. MPA (medroxyprogesterone acetate) concentrations immediately preceding DMPA injection have been shown to peak in serum within 20 days with a gradual decline thereafter (*21*). As a result, this study may potentially be capturing a period of susceptibility with the 1-month post-contraception timepoints. However, this is difficult to determine without comparisons to more post-initiation timepoints. Further illustrating the need to conduct this study specifically focusing on long-term use of these contraceptives.

Future analyses include exploring associations of proteomic changes observed with DMPA-IM use with changes in immune cell types in the same subset of women. Our collaborators from the University of Cape Town (Drs. Rubina Bunjun and Jo-Ann Passmore) have provided data specifically on Th17 cells which Laura Noël-Romas in the Burgener lab has begun comparing to proteomic results generated from this study. It would also be interesting to expand this analysis to include more immune cell subsets and potentially cytokines. Hopefully, this will help further elucidate our observations of decreased innate immune response signatures post-DMPA initiation and whether this is similarly observed with immune factors. It would also be interesting to explore how proteome variability with contraceptive use relates to the vaginal microbiome. Our lab has taken this approach with data gathered from the CAPRISA-004 trial and made interesting insights. Noël-Romas *et al* 2020 observed proteome variability, relative to MPA concentration, to be more significant for women with *Lactobacillus*-dominant microbiomes compared to those that were non-*Lactobacillus* dominant (*182*). I will be conducting this analysis with the hypothesis being, grouping according to *Lactobacillus* dominance would capture our initial observations at a greater scale. This would also be an enlightening avenue to take in our second cohort to determine whether our initial proteomic observations amongst cases would be more pronounced within women that were *Lactobacillus* dominant compared to non-*Lactobacillus* dominant. Additionally, I will also be confirming the MS-based microbiome classifications with 16S rRNA data conducted by Bryan Brown apart of Dr. Heather Jaspan's lab, for the purpose of validating this project's microbiome findings, further strengthening our

methods of identification. Those are just a few of many avenues of future analysis that could be taken for this project.

CHAPTER 5: SUPPLEMENTARY TABLES

Supplementary Table 5. Human proteins that were observed to be differentially abundant at timepoints month 1 and baseline with DMPA-IM use.

UniProt ID	Protein Name	Gene Name	Mean difference (Month 1 - Baseline)	Student t-test p-value	Benjamini-Hochberg p-value
PAI2_HUMAN	Plasminogen activator inhibitor 2	SERPINB2	0.65	2.69E-06	0.0017
PRDX3_HUMAN	Thioredoxin-dependent peroxide reductase, mitochondrial	PRDX3	0.68	3.16E-05	0.0090
GSTO1_HUMAN	Glutathione S-transferase omega-1	GSTO1	0.59	4.25E-05	0.0090
PADI1_HUMAN	Protein-arginine deiminase type-1	PADI1	0.61	0.00013	0.017
TGM3_HUMAN	Protein-glutamine gamma-glutamyltransferase E	TGM3	-0.92	0.00016	0.017
ECI1_HUMAN	Enoyl-CoA delta isomerase 1, mitochondrial	ECI1	0.75	0.00019	0.017
MUC5A_HUMAN	Mucin-5AC	MUC5AC	-0.73	0.00022	0.017
CH10_HUMAN	10 kDa heat shock protein, mitochondrial	HSPE1	0.76	0.00022	0.017
AL1A3_HUMAN	Aldehyde dehydrogenase family 1 member A3	ALDH1A3	1.15	0.00050	0.030
CBPM_HUMAN	Carboxypeptidase M	CPM	-0.67	0.00056	0.030
BPIB1_HUMAN	BPI fold-containing family B member 1	BPIFB1	-0.64	0.00057	0.030
RAB7A_HUMAN	Ras-related protein Rab-7a	RAB7A	0.53	0.00061	0.030
ODO2_HUMAN	Dihydrolipoyllysine-residue succinyl transferase component of 2-oxoglutarate dehydrogenase complex, mitochondrial	DLST	0.71	0.00066	0.030
PIGR_HUMAN	Polymeric immunoglobulin receptor	PIGR	-0.57	0.00067	0.030
MUC5B_HUMAN	Mucin-5B	MUC5B	-0.92	0.00085	0.036
TERA_HUMAN	Transitional endoplasmic reticulum ATPase	VCP	0.65	0.0010	0.037
FOLR1_HUMAN	Folate receptor alpha	FOLR1	-0.92	0.0010	0.037
FBLN1_HUMAN	Fibulin-1	FBLN1	-0.91	0.0011	0.037
CLUS_HUMAN	Clusterin	CLU	-0.72	0.0014	0.048

Supplementary Table 6. Human proteins that were observed to be differentially abundant at timepoints month 1 and baseline with Copper IUD use.

Uniprot ID	Protein name	Gene name	Mean difference (Month 1 - Baseline)	Student t-test p-value	Benjamini-Hochberg p-value
CFAB_HUMAN	Complement factor B	CFB	1.46	1.39E-09	5.15E-07
ZO1_HUMAN	Tight junction protein ZO-1	TJP1	-1.12	2.18E-09	5.15E-07
ANXA2_HUMAN	Annexin A2	ANXA2	-2.06	2.90E-09	5.15E-07
SPB3_HUMAN	Serpin B3	SERPINB3	-1.68	3.25E-09	5.15E-07
MANF_HUMAN	Mesencephalic astrocyte-derived neurotrophic factor	MANF	-1.12	4.18E-09	5.24E-07
CNBP_HUMAN	Cellular nucleic acid-binding protein	CNBP	-1.27	6.13E-09	5.24E-07
CO3_HUMAN	Complement C3	C3	1.65	6.60E-09	5.24E-07
FIBG_HUMAN	Fibrinogen gamma chain	FGG	1.96	6.61E-09	5.24E-07
SPR1A_HUMAN	Cornifin-A	SPRR1A	-2.16	8.98E-09	5.47E-07
ECM1_HUMAN	Extracellular matrix protein 1	ECM1	-1.36	9.13E-09	5.47E-07
EDF1_HUMAN	Endothelial differentiation-related factor 1	EDF1	-1.27	9.49E-09	5.47E-07
THIO_HUMAN	Thioredoxin	TXN	-1.26	1.16E-08	6.11E-07
PEPL_HUMAN	Periplakin	PPL	-1.42	1.32E-08	6.35E-07
A2MG_HUMAN	Alpha-2-macroglobulin	A2M	1.19	1.40E-08	6.35E-07
BAG3_HUMAN	BAG family molecular chaperone regulator 3	BAG3	-1.38	1.61E-08	6.79E-07
TACD2_HUMAN	Tumor-associated calcium signal transducer 2	TACSTD2	-1.42	1.92E-08	7.59E-07
HSPB1_HUMAN	Heat shock protein beta-1	HSPB1	-1.17	2.23E-08	8.28E-07
SPRR3_HUMAN	Small proline-rich protein 3	SPRR3	-2.31	2.35E-08	8.28E-07
FIBB_HUMAN	Fibrinogen beta chain [Cleaved into: Fibrinopeptide B; Fibrinogen beta chain]	FGB	1.77	2.51E-08	8.39E-07
ISK5_HUMAN	Serine protease inhibitor Kazal-type 5	SPINK5	-1.26	3.76E-08	1.15E-06

MARCS_HUMAN	Myristoylated alanine-rich C-kinase substrate	MARCKS	-1.24	3.81E-08	1.15E-06
STX7_HUMAN	Syntaxin-7	STX7	-1.76	4.14E-08	1.19E-06
CYTA_HUMAN	Cystatin-A	CSTA	-1.48	4.87E-08	1.34E-06
HPT_HUMAN	Haptoglobin	HP	1.49	5.40E-08	1.43E-06
ITIH3_HUMAN	Inter-alpha-trypsin inhibitor heavy chain H3	ITIH3	1.82	6.36E-08	1.53E-06
CO4B_HUMAN	Complement C4-B	C4B	1.38	6.40E-08	1.53E-06
SPR1B_HUMAN	Cornifin-B	SPRR1B	-2.03	6.52E-08	1.53E-06
ANXA1_HUMAN	Annexin A1	ANXA1	-1.63	7.56E-08	1.70E-06
TM11E_HUMAN	Transmembrane protease serine 11E	TMPRSS 11E	-1.30	7.77E-08	1.70E-06
A1BG_HUMAN	Alpha-1B-glycoprotein	A1BG	1.68	8.65E-08	1.83E-06
KLK13_HUMAN	Kallikrein-13	KLK13	-1.21	8.99E-08	1.84E-06
GGCT_HUMAN	Gamma-glutamylcyclotransferase	GGCT	-0.81	1.19E-07	2.36E-06
SAP3_HUMAN	Ganglioside GM2 activator	GM2A	-1.08	1.25E-07	2.39E-06
INVO_HUMAN	Involucrin	IVL	-1.75	1.71E-07	3.18E-06
FETUA_HUMAN	Alpha-2-HS-glycoprotein	AHSG	2.00	1.80E-07	3.26E-06
TM11D_HUMAN	Transmembrane protease serine 11D	TMPRSS 11D	-1.15	2.01E-07	3.44E-06
FIBA_HUMAN	Fibrinogen alpha chain [Cleaved into: Fibrinopeptide A; Fibrinogen alpha chain]	FGA	1.71	2.05E-07	3.44E-06
CD59_HUMAN	CD59 glycoprotein	CD59	-0.98	2.06E-07	3.44E-06
HRG_HUMAN	Histidine-rich glycoprotein	HRG	1.68	2.16E-07	3.51E-06
EWS_HUMAN	RNA-binding protein EWS	EWSR1	-1.21	2.52E-07	3.98E-06
CBPA4_HUMAN	Carboxypeptidase A4	CPA4	-0.91	2.57E-07	3.98E-06
TETN_HUMAN	Tetranectin	CLEC3B	1.14	2.85E-07	4.30E-06
HEMO_HUMAN	Hemopexin	HPX	1.49	3.11E-07	4.58E-06
ALBU_HUMAN	Albumin	ALB	1.67	3.84E-07	5.42E-06
LAD1_HUMAN	Ladinin-1	LAD1	-2.25	3.85E-07	5.42E-06
RET4_HUMAN	Retinol-binding protein 4	RBP4	1.46	4.00E-07	5.43E-06
RL6_HUMAN	60S ribosomal protein L6	RPL6	-1.50	4.02E-07	5.43E-06
AFAM_HUMAN	Afamin	AFM	1.36	4.59E-07	6.06E-06

A2ML1_HUMAN	Alpha-2-macroglobulin-like protein 1	A2ML1	-0.94	6.03E-07	7.81E-06
LYPD3_HUMAN	Ly6/PLAUR domain-containing protein 3	LYPD3	-1.13	6.58E-07	8.22E-06
NSF1C_HUMAN	NSFL1 cofactor p47	NSFL1C	-0.92	6.61E-07	8.22E-06
KNG1_HUMAN	Kininogen-1	KNG1	1.20	7.42E-07	8.79E-06
SLPI_HUMAN	Antileukoproteinase	SLPI	-1.39	7.44E-07	8.79E-06
VTDB_HUMAN	Vitamin D-binding protein	GC	1.50	7.48E-07	8.79E-06
VTNC_HUMAN	Vitronectin	VTN	0.97	8.16E-07	9.40E-06
CRNN_HUMAN	Cornulin	CRNN	-1.44	8.66E-07	9.81E-06
FABP5_HUMAN	Fatty acid-binding protein 5	FABP5	-1.74	1.01E-06	1.12E-05
APOA1_HUMAN	Apolipoprotein A-I	APOA1	2.25	1.21E-06	1.33E-05
PROS_HUMAN	Vitamin K-dependent protein S	PROS1	1.10	1.26E-06	1.35E-05
TRFE_HUMAN	Serotransferrin	TF	1.29	1.33E-06	1.41E-05
CERU_HUMAN	Ceruloplasmin	CP	1.32	1.45E-06	1.51E-05
CBG_HUMAN	Corticosteroid-binding globulin	SERPINA6	1.60	1.89E-06	1.93E-05
APOB_HUMAN	Apolipoprotein B-100	APOB	1.38	1.93E-06	1.93E-05
SPB13_HUMAN	Serpin B13	SERPINB13	-0.78	1.95E-06	1.93E-05
IPYR_HUMAN	Inorganic pyrophosphatase	PPA1	-0.86	2.13E-06	2.08E-05
CFAH_HUMAN	Complement factor H	CFH	0.83	2.50E-06	2.40E-05
RL13_HUMAN	60S ribosomal protein L13	RPL13	-2.15	3.20E-06	3.03E-05
PEDF_HUMAN	Pigment epithelium-derived factor	SERPINF1	1.30	3.63E-06	3.39E-05
SPIT1_HUMAN	Kunitz-type protease inhibitor 1	SPINT1	-0.76	3.80E-06	3.49E-05
FUBP2_HUMAN	Far upstream element-binding protein 2	KHSRP	-1.29	3.91E-06	3.54E-05
THBG_HUMAN	Thyroxine-binding globulin	SERPINA7	1.57	4.00E-06	3.55E-05
IGHM_HUMAN	Immunoglobulin heavy constant mu	IGHM	1.26	4.03E-06	3.55E-05
ECI1_HUMAN	Enoyl-CoA delta isomerase 1, mitochondrial	ECI1	-0.81	4.32E-06	3.76E-05
CLIC1_HUMAN	Chloride intracellular channel protein 1	CLIC1	1.04	4.42E-06	3.79E-05
QSOX1_HUMAN	Sulfhydryl oxidase 1	QSOX1	-0.85	4.51E-06	3.81E-05

TKT_HUMAN	Transketolase	TKT	1.20	4.65E-06	3.88E-05
NPC2_HUMAN	NPC intracellular cholesterol transporter 2	NPC2	-0.82	5.19E-06	4.27E-05
CO8A_HUMAN	Complement component C8 alpha chain	C8A	0.75	5.26E-06	4.27E-05
ITIH4_HUMAN	Inter-alpha-trypsin inhibitor heavy chain H4	ITIH4	1.32	5.47E-06	4.34E-05
AHNK_HUMAN	Neuroblast differentiation-associated protein AHNAK	AHNAK	-1.18	5.48E-06	4.34E-05
CYTM_HUMAN	Cystatin-M	CST6	-0.82	5.64E-06	4.39E-05
SCEL_HUMAN	Sciellin	SCEL	-0.92	5.68E-06	4.39E-05
ITIH2_HUMAN	Inter-alpha-trypsin inhibitor heavy chain H2	ITIH2	1.16	6.44E-06	4.89E-05
S10AE_HUMAN	Protein S100-A14	S100A14	-0.82	6.48E-06	4.89E-05
S10AG_HUMAN	Protein S100-A16	S100A16	-0.74	6.74E-06	5.02E-05
SBSN_HUMAN	Suprabasin	SBSN	-1.48	7.16E-06	5.23E-05
S10AD_HUMAN	Protein S100-A13	S100A13	-0.87	7.17E-06	5.23E-05
A1AG2_HUMAN	Alpha-1-acid glycoprotein 2	ORM2	1.31	7.27E-06	5.23E-05
AHNK2_HUMAN	Protein AHNAK2	AHNAK2	-0.81	8.34E-06	5.94E-05
FUBP1_HUMAN	Far upstream element-binding protein 1	FUBP1	-1.05	8.49E-06	5.98E-05
APOA2_HUMAN	Apolipoprotein A-II	APOA2	1.73	8.59E-06	5.99E-05
ZN185_HUMAN	Zinc finger protein 185	ZNF185	-1.15	9.26E-06	6.31E-05
MMP9_HUMAN	Matrix metalloproteinase-9	MMP9	0.90	9.35E-06	6.31E-05
CATB_HUMAN	Cathepsin B	CTSB	-0.61	9.35E-06	6.31E-05
SIAE_HUMAN	Sialate O-acetyl esterase	SIAE	-1.02	9.54E-06	6.37E-05
RPTN_HUMAN	Repetin	RPTN	-1.50	1.04E-05	6.85E-05
EVPL_HUMAN	Envoplakin	EVPL	-0.89	1.11E-05	7.26E-05
IC1_HUMAN	Plasma protease C1 inhibitor	SERPING1	0.94	1.20E-05	7.77E-05
KLK8_HUMAN	Kallikrein-8	KLK8	-1.06	1.22E-05	7.80E-05
CLIP1_HUMAN	CAP-Gly domain-containing linker protein 1	CLIP1	-1.08	1.23E-05	7.80E-05
TACC2_HUMAN	Transforming acidic coiled-coil-containing protein 2	TACC2	-1.21	1.25E-05	7.86E-05

ILEU_HUMAN	Leukocyte elastase inhibitor	SERPINB1	-0.64	1.44E-05	8.92E-05
ILF3_HUMAN	Interleukin enhancer-binding factor 3	ILF3	-0.74	1.48E-05	9.14E-05
PAIRB_HUMAN	Plasminogen activator inhibitor 1 RNA-binding protein	SERBP1	-1.17	1.54E-05	9.37E-05
GELS_HUMAN	Gelsolin	GSN	0.90	1.61E-05	9.73E-05
CAP1_HUMAN	Adenylyl cyclase-associated protein 1	CAP1	0.97	1.73E-05	0.00010
KLK7_HUMAN	Kallikrein-7	KLK7	-1.25	1.79E-05	0.00011
PLIN3_HUMAN	Perilipin-3	PLIN3	-0.82	1.86E-05	0.00011
IGHD_HUMAN	Immunoglobulin heavy constant delta	IGHD	1.49	1.88E-05	0.00011
SRC8_HUMAN	Src substrate cortactin	CTTN	-1.04	2.01E-05	0.00012
PSMD2_HUMAN	26S proteasome non-ATPase regulatory subunit 2	PSMD2	-2.00	2.07E-05	0.00012
IMPA1_HUMAN	Inositol monophosphatase 1	IMPA1	-0.77	2.30E-05	0.00013
KLK6_HUMAN	Kallikrein-6	KLK6	-0.76	2.37E-05	0.00013
ANT3_HUMAN	Antithrombin-III	SERPINC1	1.44	2.41E-05	0.00013
MAP4_HUMAN	Microtubule-associated protein 4	MAP4	-0.82	2.56E-05	0.00014
HBA_HUMAN	Hemoglobin subunit alpha	HBA1	2.06	2.94E-05	0.00016
CO5_HUMAN	Complement C5	C5	1.44	3.28E-05	0.00018
BPIB1_HUMAN	BPI fold-containing family B member 1	BPIFB1	0.72	3.32E-05	0.00018
PDLI5_HUMAN	PDZ and LIM domain protein 5	PDLIM5	-1.04	3.41E-05	0.00018
GRN_HUMAN	Progranulin	GRN	-0.90	3.59E-05	0.00019
CD5L_HUMAN	CD5 antigen-like	CD5L	0.85	3.81E-05	0.00020
CO8G_HUMAN	Complement component C8 gamma chain	C8G	1.50	3.86E-05	0.00020
PHS_HUMAN	Pterin-4-alpha-carbinolamine dehydratase	PCBD1	-1.06	4.29E-05	0.00022
PRS27_HUMAN	Serine protease 27	PRSS27	-0.70	4.47E-05	0.00023
PLBL1_HUMAN	Phospholipase B-like 1	PLBD1	-0.86	4.51E-05	0.00023
HBD_HUMAN	Hemoglobin subunit delta	HBD	1.76	4.56E-05	0.00023

EEA1_HUMAN	Early endosome antigen 1	EEA1	-0.89	5.13E-05	0.00026
TGM1_HUMAN	Protein-glutamine gamma-glutamyltransferase K	TGM1	-0.78	5.50E-05	0.00027
H10_HUMAN	Histone H1.0	H1-0	-1.19	5.54E-05	0.00027
CO9_HUMAN	Complement component C9 [Cleaved into: Complement component C9a; Complement component C9b]	C9	1.20	5.96E-05	0.00029
APOC1_HUMAN	Apolipoprotein C-I	APOC1	1.40	6.29E-05	0.00030
K2C6A_HUMAN	Keratin, type II cytoskeletal 6A	KRT6A	-1.24	6.43E-05	0.00031
ICAL_HUMAN	Calpastatin	CAST	-0.76	6.54E-05	0.00031
S10AB_HUMAN	Protein S100-A11	S100A11	-1.06	6.86E-05	0.00032
UGDH_HUMAN	UDP-glucose 6-dehydrogenase	UGDH	-0.79	7.35E-05	0.00034
SPR2F_HUMAN	Small proline-rich protein 2F	SPRR2F	-1.20	7.44E-05	0.00035
NGAL_HUMAN	Neutrophil gelatinase-associated lipocalin	LCN2	-1.17	7.75E-05	0.00036
ANGT_HUMAN	Angiotensinogen	AGT	1.53	8.24E-05	0.00038
ANX11_HUMAN	Annexin A11	ANXA11	-0.68	8.39E-05	0.00038
HN1L_HUMAN	Jupiter microtubule associated homolog 2	JPT2	-0.99	8.45E-05	0.00038
PEBP1_HUMAN	Phosphatidylethanolamine-binding protein 1	PEBP1	-0.77	8.58E-05	0.00039
A1AT_HUMAN	Alpha-1-antitrypsin	SERPINA1	1.46	9.49E-05	0.00042
ODO2_HUMAN	Dihydrolipoyllysine-residue succinyl transferase component of 2-oxoglutarate dehydrogenase complex, mitochondrial	DLST	-0.83	0.00010	0.00046
RAB2A_HUMAN	Ras-related protein Rab-2A	RAB2A	-0.72	0.00012	0.00053
HEP2_HUMAN	Heparin cofactor 2	SERPIND1	1.13	0.00012	0.00053
CRIS3_HUMAN	Cysteine-rich secretory protein 3	CRISP3	-0.76	0.00012	0.00054
ELAF_HUMAN	Elafin	PI3	-1.09	0.00012	0.00054
K2C4_HUMAN	Keratin, type II cytoskeletal 4	KRT4	-1.19	0.00013	0.00055

HNRPK_HUMAN	Heterogeneous nuclear ribonucleoprotein K	HNRNPK	-0.81	0.00013	0.00055
PRDX6_HUMAN	Peroxiredoxin-6	PRDX6	0.90	0.00013	0.00056
K2C6B_HUMAN	Keratin, type II cytoskeletal 6B	KRT6B	-0.87	0.00014	0.00058
A1AG1_HUMAN	Alpha-1-acid glycoprotein 1	ORM1	1.54	0.00016	0.00067
ERBB2_HUMAN	Receptor tyrosine-protein kinase erbB-2	ERBB2	-1.56	0.00017	0.00070
GGH_HUMAN	Gamma-glutamyl hydrolase	GGH	-0.54	0.00018	0.00073
TTC9A_HUMAN	Tetratricopeptide repeat protein 9A	TTC9	-1.28	0.00018	0.00074
TGM3_HUMAN	Protein-glutamine gamma-glutamyltransferase E	TGM3	-0.79	0.00018	0.00074
CO8B_HUMAN	Complement component C8 beta chain	C8B	1.29	0.00018	0.00075
APOD_HUMAN	Apolipoprotein D	APOD	1.21	0.00019	0.00075
VINC_HUMAN	Vinculin	VCL	-0.64	0.00019	0.00075
CF132_HUMAN	Uncharacterized protein C6orf132	C6orf132	-1.36	0.00019	0.00076
TTHY_HUMAN	Transthyretin	TTR	1.30	0.00022	0.00087
SERB_HUMAN	Phosphoserine phosphatase	PSPH	-0.69	0.00025	0.00097
RL7A_HUMAN	60S ribosomal protein L7a	RPL7A	-1.57	0.00026	0.0010
CPNS2_HUMAN	Calpain small subunit 2	CAPNS2	-0.61	0.00029	0.0011
COR1A_HUMAN	Coronin-1A	CORO1A	0.70	0.00030	0.0012
A2GL_HUMAN	Leucine-rich alpha-2-glycoprotein	LRG1	0.58	0.00030	0.0012
ENSA_HUMAN	Alpha-endosulfine	ENSA	-0.97	0.00030	0.0012
CRYAB_HUMAN	Alpha-crystallin B chain	CRYAB	-1.00	0.00034	0.0013
TIMP2_HUMAN	Metalloproteinase inhibitor 2	TIMP2	-0.45	0.00037	0.0014
FINC_HUMAN	Fibronectin	FN1	0.66	0.00042	0.0016
TPD52_HUMAN	Tumor protein D52	TPD52	-0.71	0.00046	0.0017
LY6D_HUMAN	Lymphocyte antigen 6D	LY6D	-0.74	0.00047	0.0017
ITIH1_HUMAN	Inter-alpha-trypsin inhibitor heavy chain H1	ITIH1	1.07	0.00049	0.0018
ECH1_HUMAN	Delta	ECH1	-0.69	0.00051	0.0019
COF1_HUMAN	Cofilin-1	CFL1	0.82	0.00052	0.0019
PZP_HUMAN	Pregnancy zone protein	PZP	0.97	0.00056	0.0020

TCPQ_HUMAN	T-complex protein 1 subunit theta	CCT8	0.86	0.00058	0.0021
TENA_HUMAN	Tenascin	TNC	0.76	0.00059	0.0021
IF4B_HUMAN	Eukaryotic translation initiation factor 4B	EIF4B	-0.83	0.00060	0.0021
PSMD9_HUMAN	26S proteasome non-ATPase regulatory subunit 9	PSMD9	-0.87	0.00062	0.0022
BCAS1_HUMAN	Breast carcinoma-amplified sequence 1	BCAS1	-0.94	0.00064	0.0022
PPAP_HUMAN	Prostatic acid phosphatase	ACP3	-0.64	0.00064	0.0022
VS10L_HUMAN	V-set and immunoglobulin domain-containing protein 10-like	VSIG10L	-0.74	0.00066	0.0023
HEM2_HUMAN	Delta-aminolevulinic acid dehydratase	ALAD	-1.09	0.00070	0.0024
K1C19_HUMAN	Keratin, type I cytoskeletal 19	KRT19	-0.51	0.00070	0.0024
HPTR_HUMAN	Haptoglobin-related protein	HPR	1.31	0.00071	0.0024
LMNA_HUMAN	Prelamin-A/C [Cleaved into: Lamin-A/C	LMNA	-0.57	0.00072	0.0024
LMO7_HUMAN	LIM domain only protein 7	LMO7	-0.76	0.00078	0.0026
SPTB2_HUMAN	Spectrin beta chain, non-erythrocytic 1	SPTBN1	-0.80	0.00082	0.0028
FOLR1_HUMAN	Folate receptor alpha	FOLR1	-0.96	0.00083	0.0028
PKP1_HUMAN	Plakophilin-1	PKP1	-0.58	0.00084	0.0028
S10A7_HUMAN	Protein S100-A7	S100A7	-1.25	0.00086	0.0028
ANXA3_HUMAN	Annexin A3	ANXA3	-0.70	0.00086	0.0028
RD23B_HUMAN	UV excision repair protein RAD23 homolog B	RAD23B	-0.55	0.00090	0.0029
PAEP_HUMAN	Glycodelin	PAEP	1.20	0.00095	0.0031
DAF_HUMAN	Complement decay-accelerating factor	CD55	-0.51	0.00095	0.0031
VIME_HUMAN	Vimentin	VIM	0.65	0.00097	0.0031
KLK10_HUMAN	Kallikrein-10	KLK10	-0.67	0.00098	0.0031
TPM4_HUMAN	Tropomyosin alpha-4 chain	TPM4	-0.62	0.00098	0.0031
CEAM5_HUMAN	Carcinoembryonic antigen-related cell adhesion molecule 5	CEACAM5	-0.76	0.0010	0.0032

LEG7_HUMAN	Galectin-7	LGALS7	-0.88	0.0010	0.0032
ARPC2_HUMAN	Actin-related protein 2/3 complex subunit 2	ARPC2	0.85	0.0010	0.0032
RETN_HUMAN	Resistin	RETN	0.62	0.0011	0.0033
DIAC_HUMAN	Di-N-acetylchitobiase	CTBS	-0.55	0.0011	0.0033
CO6_HUMAN	Complement component C6	C6	0.72	0.0011	0.0033
LYAG_HUMAN	Lysosomal alpha-glucosidase	GAA	-0.98	0.0011	0.0034
AIM1_HUMAN	Beta/gamma crystallin domain-containing protein 1	AIM1	-0.97	0.0012	0.0035
K1C13_HUMAN	Keratin, type I cytoskeletal 13	KRT13	-0.84	0.0012	0.0037
HBB_HUMAN	Hemoglobin subunit beta	HBB	1.61	0.0012	0.0037
AATC_HUMAN	Aspartate aminotransferase, cytoplasmic	GOT1	-0.55	0.0013	0.0040
NUDT5_HUMAN	ADP-sugar pyrophosphatase	NUDT5	-0.61	0.0013	0.0040
CAH1_HUMAN	Carbonic anhydrase 1	CA1	0.89	0.0014	0.0042
DBNL_HUMAN	Drebrin-like protein	DBNL	-0.71	0.0015	0.0044
PLXB2_HUMAN	Plexin-B2	PLXNB2	-0.82	0.0015	0.0045
S10A4_HUMAN	Protein S100-A4	S100A4	0.62	0.0015	0.0045
S10A8_HUMAN	Protein S100-A8	S100A8	-0.95	0.0016	0.0047
PGM2_HUMAN	Phosphoglucomutase-2	PGM2	0.78	0.0018	0.0052
SODC_HUMAN	Superoxide dismutase [Cu-Zn]	SOD1	-0.64	0.0018	0.0052
RL10A_HUMAN	60S ribosomal protein L10a	RPL10A	-1.05	0.0019	0.0056
KLK11_HUMAN	Kallikrein-11	KLK11	-0.72	0.0020	0.0059
KINH_HUMAN	Kinesin-1 heavy chain	KIF5B	0.83	0.0021	0.0059
K1C10_HUMAN	Keratin, type I cytoskeletal 10	KRT10	-0.66	0.0021	0.0060
ZA2G_HUMAN	Zinc-alpha-2-glycoprotein	AZGP1	0.69	0.0021	0.0060
FLNB_HUMAN	Filamin-B	FLNB	-0.72	0.0021	0.0060
PSCA_HUMAN	Prostate stem cell antigen	PSCA	-1.17	0.0021	0.0060
S10A2_HUMAN	Protein S100-A2	S100A2	-0.57	0.0022	0.0063
CAZA1_HUMAN	F-actin-capping protein subunit alpha-1	CAPZA1	0.72	0.0024	0.0066
KLK14_HUMAN	Kallikrein-14	KLK14	-0.84	0.0026	0.0072

F16P1_HUMAN	Fructose-1,6-bisphosphatase 1	FBP1	-0.69	0.0028	0.0078
H15_HUMAN	Histone H1.5	H1-5	-0.69	0.0030	0.0083
CATH_HUMAN	Pro-cathepsin H [Cleaved into: Cathepsin H mini chain; Cathepsin H	CTSH	-0.58	0.0034	0.0092
SARG_HUMAN	Specifically, androgen-regulated gene protein	SARG	-0.75	0.0035	0.0095
FCGBP_HUMAN	IgGFc-binding protein	FCGBP	-0.55	0.0037	0.010
APOE_HUMAN	Apolipoprotein E	APOE	0.90	0.0037	0.010
K2C1_HUMAN	Keratin, type II cytoskeletal 1	KRT1	-0.66	0.0037	0.010
CATL2_HUMAN	Cathepsin L2	CTSV	-0.59	0.0040	0.011
LDHA_HUMAN	L-lactate dehydrogenase A chain	LDHA	0.75	0.0043	0.011
S10A9_HUMAN	Protein S100-A9	S100A9	-0.84	0.0043	0.012
HV306_HUMAN	Immunoglobulin heavy variable 3-53	IGHV3-53	0.33	0.0045	0.012
C1R_HUMAN	Complement C1r subcomponent	C1R	0.65	0.0047	0.012
FILA_HUMAN	Filaggrin	FLG	-0.91	0.0048	0.013
LV302_HUMAN	Immunoglobulin heavy variable 3-21	IGLV3-21	0.39	0.0052	0.014
CPNS1_HUMAN	Calpain small subunit 1	CAPNS1	-0.46	0.0052	0.014
LKHA4_HUMAN	Leukotriene A-4 hydrolase	LTA4H	0.48	0.0053	0.014
ARP3_HUMAN	Actin-related protein 3	ACTR3	0.56	0.0055	0.014
PYGL_HUMAN	Glycogen phosphorylase, liver form	PYGL	0.63	0.0056	0.014
AMBP_HUMAN	Protein AMBP [Cleaved into: Alpha-1-microglobulin	AMBP	0.61	0.0058	0.015
VAT1_HUMAN	Synaptic vesicle membrane protein VAT-1 homolog	VAT1	-0.55	0.0059	0.015
RL23A_HUMAN	60S ribosomal protein L23a	RPL23A	-0.59	0.0062	0.016
CAN1_HUMAN	Calpain-1 catalytic subunit	CAPN1	-0.51	0.0062	0.016
PSA_HUMAN	Puromycin-sensitive aminopeptidase	NPEPPS	0.69	0.0065	0.016
MDHC_HUMAN	Malate dehydrogenase, cytoplasmic	MDH1	0.54	0.0065	0.016

CASPE_HUMAN	Caspase-14	CASP14	-0.51	0.0065	0.016
LUM_HUMAN	Lumican	LUM	0.62	0.0066	0.016
CK054_HUMAN	Ester hydrolase C11orf54	C11orf54	-0.77	0.0066	0.016
PSME1_HUMAN	Proteasome activator complex subunit 1	PSME1	0.79	0.0067	0.017
K22O_HUMAN	Keratin, type II cytoskeletal 2 oral	KRT76	-0.89	0.0068	0.017
ENDOU_HUMAN	Poly	ENDOU	-0.55	0.0068	0.017
DPP3_HUMAN	Dipeptidyl peptidase 3	DPP3	0.97	0.0070	0.017
VASN_HUMAN	Vasorin	VASN	-0.47	0.0070	0.017
GRP78_HUMAN	Endoplasmic reticulum chaperone BiP	HSPA5	-0.47	0.0070	0.017
GDIR2_HUMAN	Rho GDP-dissociation inhibitor 2	ARHGDIB	0.68	0.0071	0.017
IGHA2_HUMAN	Immunoglobulin heavy constant alpha 2	IGHA2	-0.73	0.0072	0.017
NUCL_HUMAN	Nucleolin	NCL	0.61	0.0080	0.019
GLTP_HUMAN	Glycolipid transfer protein	GLTP	0.53	0.0085	0.020
RRBP1_HUMAN	Ribosome-binding protein 1	RRBP1	-0.54	0.0085	0.020
TR150_HUMAN	Thyroid hormone receptor-associated protein 3	THRAP3	-1.09	0.0086	0.020
LRC20_HUMAN	Leucine-rich repeat-containing protein 20	LRRC20	-0.59	0.0087	0.020
ARGI1_HUMAN	Arginase-1	ARG1	0.76	0.0087	0.020
CTNA1_HUMAN	Catenin alpha-1	CTNNA1	-0.49	0.0088	0.021
TBCA_HUMAN	Tubulin-specific chaperone A	TBCA	-0.31	0.0090	0.021
MMP8_HUMAN	Neutrophil collagenase	MMP8	0.43	0.0092	0.021
WFDC2_HUMAN	WAP four-disulfide core domain protein 2	WFDC2	-0.59	0.0094	0.022
K2C8_HUMAN	Keratin, type II cytoskeletal 8	KRT8	-0.67	0.0098	0.023
COTL1_HUMAN	Coactosin-like protein	COTL1	0.53	0.010	0.023
CAPG_HUMAN	Macrophage-capping protein	CAPG	-0.55	0.011	0.026
FLNA_HUMAN	Filamin-A	FLNA	-0.42	0.011	0.026
CH10_HUMAN	10 kDa heat shock protein, mitochondrial	HSPE1	-0.51	0.011	0.026

G3P_HUMAN	Glyceraldehyde-3-phosphate dehydrogenase	GAPDH	-0.51	0.012	0.028
CATD_HUMAN	Cathepsin D	CTSD	-0.58	0.013	0.030
POF1B_HUMAN	Protein POF1B	POF1B	-0.93	0.013	0.030
CAMP_HUMAN	Cathelicidin antimicrobial peptide	CAMP	0.42	0.013	0.030
CDD_HUMAN	Cytidine deaminase	CDA	-0.75	0.014	0.031
PLEC_HUMAN	Plectin	PLEC	-0.46	0.014	0.032
KLKB1_HUMAN	Plasma kallikrein	KLKB1	0.57	0.014	0.032
GSLG1_HUMAN	Golgi apparatus protein 1	GLG1	-0.59	0.015	0.033
NDRG1_HUMAN	Protein NDRG1	NDRG1	-0.63	0.015	0.034
G6PI_HUMAN	Glucose-6-phosphate isomerase	GPI	0.42	0.016	0.034
C4BPA_HUMAN	C4b-binding protein alpha chain	C4BPA	0.75	0.016	0.034
CFAI_HUMAN	Complement factor I	CFI	0.50	0.016	0.034
PKP3_HUMAN	Plakophilin-3	PKP3	-0.68	0.016	0.034
HV322_HUMAN	Immunoglobulin heavy variable 3-7	NA	0.39	0.016	0.035
CALL5_HUMAN	Calmodulin-like protein 5	CALML5	-0.56	0.017	0.036
GSTP1_HUMAN	Glutathione S-transferase P	GSTP1	0.61	0.017	0.037
DPP4_HUMAN	Dipeptidyl peptidase 4	DPP4	-0.56	0.018	0.038
SPB4_HUMAN	Serpin B4	SERPINB4	-0.55	0.018	0.038
ACTN1_HUMAN	Alpha-actinin-1	ACTN1	0.44	0.018	0.038
APOH_HUMAN	Beta-2-glycoprotein 1	APOH	0.57	0.018	0.038
BPI_HUMAN	Bactericidal permeability-increasing protein	BPI	-0.55	0.018	0.039
SNAA_HUMAN	Alpha-soluble NSF attachment protein	NAPA	0.87	0.018	0.039
CPPED_HUMAN	Serine/threonine-protein phosphatase CPPED1	CPPED1	0.94	0.019	0.039
PDIA4_HUMAN	Protein disulfide-isomerase A4	PDIA4	-0.46	0.019	0.039
PDIA1_HUMAN	Protein disulfide-isomerase	P4HB	0.49	0.019	0.039
HV320_HUMAN	Immunoglobulin heavy variable 3-20	IGHV3-20	0.34	0.019	0.040
FCN3_HUMAN	Ficolin-3	FCN3	0.83	0.020	0.041

G6PD_HUMAN	Glucose-6-phosphate 1-dehydrogenase	G6PD	0.53	0.020	0.041
LEG3_HUMAN	Galectin-3	LGALS3	0.61	0.020	0.041
TPD54_HUMAN	Tumor protein D54	TPD52L2	-0.46	0.020	0.041
ES8L1_HUMAN	Epidermal growth factor receptor kinase substrate 8-like protein 1	EPS8L1	-0.55	0.022	0.044
CALR_HUMAN	Calreticulin	CALR	0.47	0.022	0.045
C1QC_HUMAN	Complement C1q subcomponent subunit C	C1QC	0.92	0.022	0.046
SYWC_HUMAN	Tryptophan--tRNA ligase, cytoplasmic	WARS1	0.46	0.025	0.050

Supplementary Table 7. Human proteins that were observed to be differentially abundant between those that were identified as cases and controls.

Uniprot ID	Protein name	Gene name	Mean difference (Case-Control)	Student t-test p-value	Benjamini-Hochberg p-value
PLMN_HUMAN	Plasminogen	PLG	-1.23	0.0013	0.23
ERO1A_HUMAN	ERO1-like protein alpha	ERO1A	1.00	0.0013	0.23
SETLP_HUMAN	Protein SETSIP	SETSIP	1.26	0.0014	0.23
GLRX1_HUMAN	Glutaredoxin-1	GLRX	0.67	0.0016	0.23
PNCB_HUMAN	Nicotinate phosphoribosyl transferase	NAPRT	1.35	0.0025	0.30
LV106_HUMAN	Ig lambda chain V-I region WAH	LV106	-1.37	0.0032	0.32
S10A7_HUMAN	Protein S100-A7	S100A7	2.00	0.0046	0.32
K1C16_HUMAN	Keratin, type I cytoskeletal 16	KRT16	1.50	0.0051	0.32
IL36G_HUMAN	Interleukin-36 gamma	IL36G	1.34	0.0055	0.32
K2C4_HUMAN	Keratin, type II cytoskeletal 4	KRT4	-1.35	0.0058	0.32
PDIA3_HUMAN	Protein disulfide-isomerase A3	PDIA3	0.86	0.0061	0.32
AMBP_HUMAN	Protein AMBP [Cleaved into: Alpha-1-microglobulin	AMBP	-0.78	0.0064	0.32
DDB1_HUMAN	DNA damage-binding protein 1	DDB1	1.33	0.0069	0.32
CRYAB_HUMAN	Alpha-crystallin B chain	CRYAB	-1.60	0.0075	0.32
A1AG2_HUMAN	Alpha-1-acid glycoprotein 2	ORM2	-1.09	0.0084	0.33
PLEC_HUMAN	Plectin	PLEC	0.66	0.0099	0.33
H10_HUMAN	Histone H1.0	H1-0	-0.89	0.010	0.33
6PGD_HUMAN	6-phosphogluconate	PGD	0.79	0.011	0.33

	dehydrogenase, decarboxylating				
RAB7A_HUMAN	Ras-related protein Rab-7a	RAB7A	0.75	0.011	0.33
CD59_HUMAN	CD59 glycoprotein	CD59	-1.88	0.011	0.33
FOLR3_HUMAN	Folate receptor gamma	FOLR3	-1.15	0.015	0.36
VASN_HUMAN	Vasorin	VASN	-0.81	0.016	0.36
TAGL2_HUMAN	Transgelin-2	TAGLN2	0.80	0.016	0.36
FKB1A_HUMAN	Peptidyl-prolyl cis-trans isomerase FKBP1A	FKBP1A	1.26	0.016	0.36
AB1IP_HUMAN	Amyloid beta A4 precursor protein-binding family B member 1-interacting protein	APBB1IP	1.41	0.017	0.36
RAB1A_HUMAN	Ras-related protein Rab-1A	RAB1A	0.87	0.018	0.36
PPIB_HUMAN	Peptidyl-prolyl cis-trans isomerase B	PPIB	0.98	0.020	0.36
IGHA1_HUMAN	Immunoglobulin heavy constant alpha 1	IGHA1	-0.93	0.020	0.36
CALL5_HUMAN	Calmodulin-like protein 5	CALML5	-1.18	0.020	0.36
HMGB2_HUMAN	High mobility group protein B2	HMGB2	0.88	0.021	0.36
SERA_HUMAN	D-3-phosphoglycerate dehydrogenase	PHGDH	0.81	0.021	0.36
QOR_HUMAN	Quinone oxidoreductase	CRYZ	0.90	0.022	0.36
TYPH_HUMAN	Thymidine phosphorylase	TYMP	1.35	0.022	0.36
TRFE_HUMAN	Serotransferrin	TF	-0.96	0.023	0.36

QORX_HUMAN	Quinone oxidoreductase PIG3	TP53I3	-0.82	0.024	0.36
TM11D_HUMAN	Transmembrane protease serine 11D	TMPRSS11D	-0.95	0.024	0.36
STMN1_HUMAN	Stathmin	STMN1	1.02	0.024	0.36
GLOD4_HUMAN	Glyoxalase domain-containing protein 4	GLOD4	0.82	0.024	0.36
ARP2_HUMAN	Actin-related protein 2	ACTR2	0.90	0.025	0.36
CH60_HUMAN	60 kDa heat shock protein, mitochondrial	HSPD1	1.10	0.025	0.36
SYHC_HUMAN	Syncoilin	SYNC	1.09	0.025	0.36
CAB39_HUMAN	Calcium-binding protein 39	CAB39	0.67	0.025	0.36
LY6D_HUMAN	Lymphocyte antigen 6D	LY6D	-1.14	0.028	0.36
UBP14_HUMAN	Ubiquitin carboxyl-terminal hydrolase 14	USP14	-1.28	0.028	0.36
S10A2_HUMAN	Protein S100-A2	S100A2	0.95	0.028	0.36
KNG1_HUMAN	Kininogen-1	KNG1	-1.23	0.029	0.36
LYPA1_HUMAN	Acyl-protein thioesterase 1	LYPLA1	0.97	0.029	0.36
TERA_HUMAN	Transitional endoplasmic reticulum ATPase	VCP	0.89	0.030	0.36
TWF2_HUMAN	Twinfilin-2	TWF2	1.42	0.030	0.36
MYL6_HUMAN	Myosin light polypeptide 6	MYL6	0.97	0.031	0.36
ZA2G_HUMAN	Zinc-alpha-2-glycoprotein	AZGP1	-0.93	0.031	0.36
KAP2_HUMAN	cAMP-dependent protein kinase type II-alpha	PRKAR2A	1.18	0.032	0.36

	regulatory subunit				
IGHG1_HUMAN	Immunoglobulin heavy constant gamma 1	IGHG1	-1.35	0.032	0.36
PSA1_HUMAN	Proteasome subunit alpha type-1	PSMA1	0.74	0.034	0.38
PSB4_HUMAN	Proteasome subunit beta type-4	PSMB4	0.88	0.035	0.38
IGHG3_HUMAN	Immunoglobulin heavy constant gamma 3	IGHG3	-0.89	0.038	0.40
S100P_HUMAN	Protein S100-P	S100P	0.68	0.039	0.41
CDC37_HUMAN	Hsp90 co-chaperone Cdc37	CDC37	0.91	0.040	0.41
TCPQ_HUMAN	T-complex protein 1 subunit theta	CCT8	1.05	0.043	0.42
PTPRC_HUMAN	Receptor-type tyrosine-protein phosphatase C	PTPRC	1.01	0.044	0.42
PERM_HUMAN	Myeloperoxidase	MPO	0.68	0.045	0.42
RAN_HUMAN	GTP-binding nuclear protein Ran	RAN	0.96	0.046	0.42
ZN185_HUMAN	Zinc finger protein 185	ZNF185	-0.83	0.046	0.42
ALBU_HUMAN	Albumin	ALB	-1.21	0.047	0.42
IMPA2_HUMAN	Inositol monophosphatase 2	IMPA2	1.29	0.047	0.42
FAS_HUMAN	Fatty acid synthase	FASN	0.85	0.048	0.42
AP2B1_HUMAN	AP-2 complex subunit beta	AP2B1	1.07	0.048	0.42
CATH_HUMAN	Pro-cathepsin H [Cleaved into: Cathepsin	CTSH	-0.97	0.048	0.42

	H mini chain; Cathepsin H				
ACBP_HUMAN	Acyl-CoA-binding protein	DBI	0.74	0.049	0.42
LV302_HUMAN	Immunoglobulin heavy variable 3-21	IGLV3-21	-0.63	0.049	0.42

Chapter 6: References

1. L. B. Finer, M. R. Zolna, Unintended Pregnancy In The United States: Incidence And Disparities, 2006. *Contraception* **84**, 478-485 (2011).
2. A. Y. Black *Et Al.*, The Cost Of Unintended Pregnancies In Canada: Estimating Direct Cost, Role Of Imperfect Adherence, And The Potential Impact Of Increased Use Of Long-Acting Reversible Contraceptives. *J Obstet Gynaecol Can* **37**, 1086-1097 (2015).
3. L. B. Finer, M. R. Zolna, Shifts In Intended And Unintended Pregnancies In The United States, 2001-2008. *Am J Public Health* **104 Suppl 1**, S43-48 (2014).
4. A. Sonfield, K. Kost, R. B. Gold, L. B. Finer, The Public Costs Of Births Resulting From Unintended Pregnancies: National And State-Level Estimates. *Perspect Sex Reprod Health* **43**, 94-102 (2011).
5. E. Crist, C. Mora, R. Engelman, The Interaction Of Human Population, Food Production, And Biodiversity Protection. *Science* **356**, 260-264 (2017).
6. D. J. Anderson, Population And The Environment - Time For Another Contraception Revolution. *N Engl J Med* **381**, 397-399 (2019).
7. National Research Council US Committee On Population, Contraception And Reproduction: Health Consequences For Women And Children In The Developing World. (1989).
8. M. Dott, S. A. Rasmussen, C. J. Hogue, J. Reefhuis, S. National Birth Defects Prevention, Association Between Pregnancy Intention And Reproductive-Health Related Behaviors Before And After Pregnancy Recognition, National Birth Defects Prevention Study, 1997-2002. *Matern Child Health J* **14**, 373-381 (2010).
9. S. Ahmed *Et Al.*, Trends In Contraceptive Prevalence Rates In Sub-Saharan Africa Since The 2012 London Summit On Family Planning: Results From Repeated Cross-Sectional Surveys. *Lancet Glob Health* **7**, E904-E911 (2019).
10. UN, Transforming Our World: The 2030 Agenda For Sustainable Development. (2015).
11. F. L. Cavallaro, L. Benova, O. O. Owolabi, M. Ali, A Systematic Review Of The Effectiveness Of Counselling Strategies For Modern Contraceptive Methods: What Works And What Doesn't? *BMJ Sex Reprod Health*, (2019).
12. UN, Contraceptive Use By Method Data Booklet 2019. (2019).
13. K. Pazol, L. B. Zapata, S. J. Tregear, N. Mautone-Smith, L. E. Gavin, Impact Of Contraceptive Education On Contraceptive Knowledge And Decision Making: A Systematic Review. *Am J Prev Med* **49**, S46-56 (2015).
14. M. M. Baron, B. Potter, S. Schrager, A Review Of Long-Acting Reversible Contraception Methods And Barriers To Their Use. *WMJ* **117**, 156-159 (2018).
15. Centers For Disease Control And Prevention, Effectiveness Of Family Planning Methods. (2011).
16. C. Paul, D. C. Skegg, S. Williams, Depot Medroxyprogesterone Acetate. Patterns Of Use And Reasons For Discontinuation. *Contraception* **56**, 209-214 (1997).
17. A. M. Kaunitz, Long-Acting Injectable Contraception With Depot Medroxyprogesterone Acetate. *Am J Obstet Gynecol* **170**, 1543-1549 (1994).
18. R. Jacobstein, C. B. Polis, Progestin-Only Contraception: Injectables And Implants. *Best Pract Res Clin Obstet Gynaecol* **28**, 795-806 (2014).
19. J. Trussell, Contraceptive Failure In The United States. *Contraception* **83**, 397-404 (2011).

20. A. P. Kourtis *Et Al.*, A Randomized Clinical Trial On The Effects Of Progestin Contraception In The Genital Tract Of HIV-Infected And Uninfected Women In Lilongwe, Malawi: Addressing Evolving Research Priorities. *Contemp Clin Trials* **52**, 27-34 (2017).
21. D. R. Mishell, Jr., Pharmacokinetics Of Depot Medroxyprogesterone Acetate Contraception. *J Reprod Med* **41**, 381-390 (1996).
22. R. Schickler *Et Al.*, The Potential For Intramuscular Depot Medroxyprogesterone Acetate As A Self-Bridging Emergency Contraceptive. *Contracept X* **3**, 100050 (2021).
23. WHO Department Of Reproductive Health Research, John Hopkins Bloomberg School Of Public Health Center For Communication Programs Knowledge For Health Project, Family Planning: A Global Handbook For Providers (2018 Update). *Baltimore And Geneva: CCP And WHO*, (2018).
24. A. S. Critchfield *Et Al.*, Cervical Mucus Properties Stratify Risk For Preterm Birth. *Plos One* **8**, E69528 (2013).
25. Committee Opionion No. 602, Depot Medroxyprogesterone Acetate And Bone Effects. *American College Of Obstetricians And Gynecologists*, 1398-1402 (2014).
26. B. L. Riggs, The Mechanisms Of Estrogen Regulation Of Bone Resorption. *J Clin Invest* **106**, 1203-1204 (2000).
27. B. Kaneshiro, T. Aeby, Long-Term Safety, Efficacy, And Patient Acceptability Of The Intrauterine Copper T-380A Contraceptive Device. *Int J Womens Health* **2**, 211-220 (2010).
28. M. E. Ortiz, H. B. Croxatto, Copper-T Intrauterine Device And Levonorgestrel Intrauterine System: Biological Bases Of Their Mechanism Of Action. *Contraception* **75**, S16-30 (2007).
29. W. Zhao *Et Al.*, Levonorgestrel Decreases Cilia Beat Frequency Of Human Fallopian Tubes And Rat Oviducts Without Changing Morphological Structure. *Clin Exp Pharmacol Physiol* **42**, 171-178 (2015).
30. N. L. Stanwood, J. M. Garrett, T. R. Konrad, Obstetrician-Gynecologists And The Intrauterine Device: A Survey Of Attitudes And Practice. *Obstet Gynecol* **99**, 275-280 (2002).
31. M. A. Biggs, C. C. Harper, J. Malvin, C. D. Brindis, Factors Influencing The Provision Of Long-Acting Reversible Contraception In California. *Obstet Gynecol* **123**, 593-602 (2014).
32. M. L. Kavanaugh, L. Frohwirth, J. Jerman, R. Popkin, K. Ethier, Long-Acting Reversible Contraception For Adolescents And Young Adults: Patient And Provider Perspectives. *J Pediatr Adolesc Gynecol* **26**, 86-95 (2013).
33. M. L. Kavanaugh, J. Jerman, K. Ethier, S. Moskosky, Meeting The Contraceptive Needs Of Teens And Young Adults: Youth-Friendly And Long-Acting Reversible Contraceptive Services In U.S. Family Planning Facilities. *J Adolesc Health* **52**, 284-292 (2013).
34. J. M. Yu, J. T. Henderson, C. C. Harper, G. F. Sawaya, Obstetrician-Gynecologists' Beliefs On The Importance Of Pelvic Examinations In Assessing Hormonal Contraception Eligibility. *Contraception* **90**, 612-614 (2014).
35. K. L. Fleming, A. Sokoloff, T. R. Raine, Attitudes And Beliefs About The Intrauterine Device Among Teenagers And Young Women. *Contraception* **82**, 178-182 (2010).

36. E. L. Spies, N. M. Askelson, E. Gelman, M. Losch, Young Women's Knowledge, Attitudes, And Behaviors Related To Long-Acting Reversible Contraceptives. *Womens Health Issues* **20**, 394-399 (2010).
37. N. L. Stanwood, K. A. Bradley, Young Pregnant Women's Knowledge Of Modern Intrauterine Devices. *Obstet Gynecol* **108**, 1417-1422 (2006).
38. A. K. Whitaker *Et Al.*, Adolescent And Young Adult Women's Knowledge Of And Attitudes Toward The Intrauterine Device. *Contraception* **78**, 211-217 (2008).
39. B. Burns, K. Grindlay, A. Dennis, Women's Awareness Of, Interest In, And Experiences With Long-Acting Reversible And Permanent Contraception. *Womens Health Issues* **25**, 224-231 (2015).
40. J. Deese, S. Pradhan, H. Goetz, C. Morrison, Contraceptive Use And The Risk Of Sexually Transmitted Infection: Systematic Review And Current Perspectives. *Open Access J Contracept* **9**, 91-112 (2018).
41. L. Masese *Et Al.*, Incidence And Correlates Of Chlamydia Trachomatis Infection In A High-Risk Cohort Of Kenyan Women. *Sex Transm Dis* **40**, 221-225 (2013).
42. S. Kapiga *Et Al.*, Risk Factors For Incidence Of Sexually Transmitted Infections Among Women In South Africa, Tanzania, And Zambia: Results From HPTN 055 Study. *Sex Transm Dis* **36**, 199-206 (2009).
43. H. Borgdorff *Et Al.*, The Impact Of Hormonal Contraception And Pregnancy On Sexually Transmitted Infections And On Cervicovaginal Microbiota In African Sex Workers. *Sex Transm Dis* **42**, 143-152 (2015).
44. A. Pettifor *Et Al.*, Use Of Injectable Progestin Contraception And Risk Of STI Among South African Women. *Contraception* **80**, 555-560 (2009).
45. A. N. Russell *Et Al.*, Analysis Of Factors Driving Incident And Ascending Infection And The Role Of Serum Antibody In Chlamydia Trachomatis Genital Tract Infection. *J Infect Dis* **213**, 523-531 (2016).
46. A. Romer *Et Al.*, Depot Medroxyprogesterone Acetate Use Is Not Associated With Risk Of Incident Sexually Transmitted Infections Among Adolescent Women. *J Adolesc Health* **52**, 83-88 (2013).
47. J. M. Baeten *Et Al.*, Hormonal Contraception And Risk Of Sexually Transmitted Disease Acquisition: Results From A Prospective Study. *Am J Obstet Gynecol* **185**, 380-385 (2001).
48. C. S. Morrison *Et Al.*, Hormonal Contraceptive Use, Cervical Ectopy, And The Acquisition Of Cervical Infections. *Sex Transm Dis* **31**, 561-567 (2004).
49. L. Lavreys *Et Al.*, Hormonal Contraception And Risk Of Cervical Infections Among HIV-1-Seropositive Kenyan Women. *AIDS* **18**, 2179-2184 (2004).
50. E. T. Overton, E. Shacham, E. Singhatiraj, D. Nurutdinova, Incidence Of Sexually Transmitted Infections Among HIV-Infected Women Using Depot Medroxyprogesterone Acetate Contraception. *Contraception* **78**, 125-130 (2008).
51. M. E. Socias *Et Al.*, Use Of Injectable Hormonal Contraception And HSV-2 Acquisition In A Cohort Of Female Sex Workers In Vancouver, Canada. *Sex Transm Infect* **93**, 284-289 (2017).
52. M. K. Grabowski *Et Al.*, Use Of Injectable Hormonal Contraception And Women's Risk Of Herpes Simplex Virus Type 2 Acquisition: A Prospective Study Of Couples In Rakai, Uganda. *Lancet Glob Health* **3**, E478-E486 (2015).

53. C. S. Morrison, A. N. Turner, L. B. Jones, Highly Effective Contraception And Acquisition Of HIV And Other Sexually Transmitted Infections. *Best Pract Res Clin Obstet Gynaecol* **23**, 263-284 (2009).
54. A. O. Tsui, W. Brown, Q. Li, Contraceptive Practice In Sub-Saharan Africa. *Popul Dev Rev* **43**, 166-191 (2017).
55. C. S. Morrison *Et Al.*, Hormonal Contraception And The Risk Of HIV Acquisition: An Individual Participant Data Meta-Analysis. *Plos Med* **12**, E1001778 (2015).
56. J. M. Baeten *Et Al.*, Hormonal Contraceptive Use, Herpes Simplex Virus Infection, And Risk Of HIV-1 Acquisition Among Kenyan Women. *AIDS* **21**, 1771-1777 (2007).
57. K. Ungchusak *Et Al.*, Determinants Of HIV Infection Among Female Commercial Sex Workers In Northeastern Thailand: Results From A Longitudinal Study. *J Acquir Immune Defic Syndr Hum Retrovirol* **12**, 500-507 (1996).
58. J. J. Kumwenda *Et Al.*, Natural History And Risk Factors Associated With Early And Established HIV Type 1 Infection Among Reproductive-Age Women In Malawi. *Clin Infect Dis* **46**, 1913-1920 (2008).
59. C. S. Morrison *Et Al.*, Hormonal Contraception And The Risk Of HIV Acquisition Among Women In South Africa. *AIDS* **26**, 497-504 (2012).
60. H. Wand, G. Ramjee, The Effects Of Injectable Hormonal Contraceptives On HIV Seroconversion And On Sexually Transmitted Infections. *AIDS* **26**, 375-380 (2012).
61. M. Bulterys *Et Al.*, Incident HIV-1 Infection In A Cohort Of Young Women In Butare, Rwanda. *AIDS* **8**, 1585-1591 (1994).
62. S. E. Reid *Et Al.*, Pregnancy, Contraceptive Use, And HIV Acquisition In HPTN 039: Relevance For HIV Prevention Trials Among African Women. *J Acquir Immune Defic Syndr* **53**, 606-613 (2010).
63. S. H. Kapiga, E. F. Lyamuya, G. K. Lwihula, D. J. Hunter, The Incidence Of HIV Infection Among Women Using Family Planning Methods In Dar Es Salaam, Tanzania. *AIDS* **12**, 75-84 (1998).
64. I. Kleinschmidt *Et Al.*, Injectable Progestin Contraceptive Use And Risk Of HIV Infection In A South African Family Planning Cohort. *Contraception* **75**, 461-467 (2007).
65. R. Heffron *Et Al.*, Use Of Hormonal Contraceptives And Risk Of HIV-1 Transmission: A Prospective Cohort Study. *Lancet Infect Dis* **12**, 19-26 (2012).
66. J. M. Mcnicholl, T. C. Henning, S. A. Vishwanathan, E. N. Kersh, Non-Human Primate Models Of Hormonal Contraception And HIV. *Am J Reprod Immunol* **71**, 513-522 (2014).
67. P. A. Marx *Et Al.*, Progesterone Implants Enhance SIV Vaginal Transmission And Early Virus Load. *Nat Med* **2**, 1084-1089 (1996).
68. J. M. Smith *Et Al.*, Tenofovir Disoproxil Fumarate Intravaginal Ring Protects High-Dose Depot Medroxyprogesterone Acetate-Treated Macaques From Multiple SHIV Exposures. *J Acquir Immune Defic Syndr* **68**, 1-5 (2015).
69. B. Conway, D. W. Cameron, F. A. Plummer, A. R. Ronald, Heterosexual Transmission Of Human Immunodeficiency Virus Infection - Strategies For Prevention. *Can J Infect Dis* **2**, 30-36 (1991).
70. S. Gregson *Et Al.*, Sexual Mixing Patterns And Sex-Differentials In Teenage Exposure To HIV Infection In Rural Zimbabwe. *Lancet* **359**, 1896-1903 (2002).
71. T. E. Taha *Et Al.*, Bacterial Vaginosis And Disturbances Of Vaginal Flora: Association With Increased Acquisition Of HIV. *AIDS* **12**, 1699-1706 (1998).

72. R. S. Mcclelland *Et Al.*, Vaginal Washing And Increased Risk Of HIV-1 Acquisition Among African Women: A 10-Year Prospective Study. *AIDS* **20**, 269-273 (2006).
73. J. M. Wessels, A. M. Felker, H. A. Dupont, C. Kaushic, The Relationship Between Sex Hormones, The Vaginal Microbiome And Immunity In HIV-1 Susceptibility In Women. *Dis Model Mech* **11**, 1-15 (2018).
74. M. Aldunate *Et Al.*, Antimicrobial And Immune Modulatory Effects Of Lactic Acid And Short Chain Fatty Acids Produced By Vaginal Microbiota Associated With Eubiosis And Bacterial Vaginosis. *Front Physiol* **6**, 164 (2015).
75. M. Ghosh *Et Al.*, Pathogen Recognition In The Human Female Reproductive Tract: Expression Of Intracellular Cytosolic Sensors NOD1, NOD2, RIG-1, And MDA5 And Response To HIV-1 And Neisseria Gonorrhea. *Am J Reprod Immunol* **69**, 41-51 (2013).
76. E. Amabebe, D. O. C. Anumba, The Vaginal Microenvironment: The Physiologic Role Of Lactobacilli. *Front Med (Lausanne)* **5**, 181 (2018).
77. S. K. Lee, C. J. Kim, D. J. Kim, J. H. Kang, Immune Cells In The Female Reproductive Tract. *Immune Netw* **15**, 16-26 (2015).
78. S. A. Shukair *Et Al.*, Human Cervicovaginal Mucus Contains An Activity That Hinders HIV-1 Movement. *Mucosal Immunol* **6**, 427-434 (2013).
79. R. B. Brown, M. A. Hollingsworth, In *Encyclopedia Of Biological Chemistry*. (2013), Pp. 200-204.
80. M. N. Anahtar *Et Al.*, Cervicovaginal Bacteria Are A Major Modulator Of Host Inflammatory Responses In The Female Genital Tract. *Immunity* **42**, 965-976 (2015).
81. A. B. Onderdonk, M. L. Delaney, R. N. Fichorova, The Human Microbiome During Bacterial Vaginosis. *Clin Microbiol Rev* **29**, 223-238 (2016).
82. J. P. Brooks *Et Al.*, Effects Of Combined Oral Contraceptives, Depot Medroxyprogesterone Acetate And The Levonorgestrel-Releasing Intrauterine System On The Vaginal Microbiome. *Contraception* **95**, 405-413 (2017).
83. J. E. Allsworth, J. F. Peipert, Severity Of Bacterial Vaginosis And The Risk Of Sexually Transmitted Infection. *Am J Obstet Gynecol* **205**, 113 E111-116 (2011).
84. R. Amsel *Et Al.*, Nonspecific Vaginitis. Diagnostic Criteria And Microbial And Epidemiologic Associations. *Am J Med* **74**, 14-22 (1983).
85. R. P. Nugent, M. A. Krohn, S. L. Hillier, Reliability Of Diagnosing Bacterial Vaginosis Is Improved By A Standardized Method Of Gram Stain Interpretation. *J Clin Microbiol* **29**, 297-301 (1991).
86. L. R. Mckinnon *Et Al.*, The Evolving Facets Of Bacterial Vaginosis: Implications For HIV Transmission. *AIDS Res Hum Retroviruses* **35**, 219-228 (2019).
87. R. H. Gray *Et Al.*, Probability Of HIV-1 Transmission Per Coital Act In Monogamous, Heterosexual, HIV-1-Discordant Couples In Rakai, Uganda. *Lancet* **357**, 1149-1153 (2001).
88. J. M. Baeten *Et Al.*, Female-To-Male Infectivity Of HIV-1 Among Circumcised And Uncircumcised Kenyan Men. *J Infect Dis* **191**, 546-553 (2005).
89. N. Haddad *Et Al.*, HIV In Canada-Surveillance Report, 2018. *Can Commun Dis Rep* **45**, 304-312 (2019).
90. T. J. Yi, B. Shannon, J. Prodger, L. Mckinnon, R. Kaul, Genital Immunology And HIV Susceptibility In Young Women. *Am J Reprod Immunol* **69 Suppl 1**, 74-79 (2013).
91. A. T. Haase, Targeting Early Infection To Prevent HIV-1 Mucosal Transmission. *Nature* **464**, 217-223 (2010).

92. J. L. Prodger *Et Al.*, Foreskin T-Cell Subsets Differ Substantially From Blood With Respect To HIV Co-Receptor Expression, Inflammatory Profile, And Memory Status. *Mucosal Immunol* **5**, 121-128 (2012).
93. L. R. Mckinnon *Et Al.*, Characterization Of A Human Cervical CD4+ T Cell Subset Coexpressing Multiple Markers Of HIV Susceptibility. *J Immunol* **187**, 6032-6042 (2011).
94. K. K. Venkatesh, S. Cu-Uvin, Assessing The Relationship Between Cervical Ectopy And HIV Susceptibility: Implications For HIV Prevention In Women. *Am J Reprod Immunol* **69 Suppl 1**, 68-73 (2013).
95. P. D. Kell, S. E. Barton, D. K. Edmonds, F. C. Boag, HIV Infection In A Patient With Meyer-Rokitansky-Kuster-Hauser Syndrome. *J R Soc Med* **85**, 706-707 (1992).
96. N. S. Padian *Et Al.*, Diaphragm And Lubricant Gel For Prevention Of HIV Acquisition In Southern African Women: A Randomised Controlled Trial. *Lancet* **370**, 251-261 (2007).
97. F. Hladik, T. J. Hope, HIV Infection Of The Genital Mucosa In Women. *Curr HIV/AIDS Rep* **6**, 20-28 (2009).
98. P. B. Pendergrass, M. W. Belovicz, C. A. Reeves, Surface Area Of The Human Vagina As Measured From Vinyl Polysiloxane Casts. *Gynecol Obstet Invest* **55**, 110-113 (2003).
99. A. M. Carias *Et Al.*, Defining The Interaction Of HIV-1 With The Mucosal Barriers Of The Female Reproductive Tract. *J Virol* **87**, 11388-11400 (2013).
100. M. Stanley, Early Age Of Sexual Debut: A Risky Experience. *J Fam Plann Reprod Health Care* **35**, 118-120 (2009).
101. I. J. Pandya, J. Cohen, The Leukocytic Reaction Of The Human Uterine Cervix To Spermatozoa. *Fertil Steril* **43**, 417-421 (1985).
102. L. A. Thompson, C. L. Barratt, A. E. Bolton, I. D. Cooke, The Leukocytic Reaction Of The Human Uterine Cervix. *Am J Reprod Immunol* **28**, 85-89 (1992).
103. N. A. Nakra *Et Al.*, Loss Of Innate Host Defense Following Unprotected Vaginal Sex. *J Infect Dis* **213**, 840-847 (2016).
104. S. Ayehunie *Et Al.*, Characterization Of A Hormone-Responsive Organotypic Human Vaginal Tissue Model: Morphologic And Immunologic Effects. *Reprod Sci* **22**, 980-990 (2015).
105. S. Titen, S. Sankaran-Walters, E. Waetjen, Hormonal Effects On The Vaginal Mucosa, An In Vitro Model [5A]. *Obstetrics & Gynecology* **127**, 13S (2016).
106. C. R. Wira, M. Rodriguez-Garcia, M. V. Patel, The Role Of Sex Hormones In Immune Protection Of The Female Reproductive Tract. *Nat Rev Immunol* **15**, 217-230 (2015).
107. C. R. Wira, J. V. Fahey, A New Strategy To Understand How HIV Infects Women: Identification Of A Window Of Vulnerability During The Menstrual Cycle. *AIDS* **22**, 1909-1917 (2008).
108. S. A. Vishwanathan *Et Al.*, High Susceptibility To Repeated, Low-Dose, Vaginal SHIV Exposure Late In The Luteal Phase Of The Menstrual Cycle Of Pigtail Macaques. *J Acquir Immune Defic Syndr* **57**, 261-264 (2011).
109. E. N. Kersh *Et Al.*, SHIV Susceptibility Changes During The Menstrual Cycle Of Pigtail Macaques. *J Med Primatol* **43**, 310-316 (2014).
110. A. M. Carias *Et Al.*, Increases In Endogenous Or Exogenous Progestins Promote Virus-Target Cell Interactions Within The Non-Human Primate Female Reproductive Tract. *Plos Pathog* **12**, E1005885 (2016).

111. E. Saba *Et Al.*, Productive HIV-1 Infection Of Human Cervical Tissue Ex Vivo Is Associated With The Secretory Phase Of The Menstrual Cycle. *Mucosal Immunol* **6**, 1081-1090 (2013).
112. K. Birse *Et Al.*, Molecular Signatures Of Immune Activation And Epithelial Barrier Remodeling Are Enhanced During The Luteal Phase Of The Menstrual Cycle: Implications For HIV Susceptibility. *J Virol* **89**, 8793-8805 (2015).
113. S. Mukhopadhyay *Et Al.*, Comparative Transcriptome Analysis Of The Human Endocervix And Ectocervix During The Proliferative And Secretory Phases Of The Menstrual Cycle. *Sci Rep* **9**, 13494 (2019).
114. K. E. Mckinnon, S. Getsios, T. K. Woodruff, Distinct Follicular And Luteal Transcriptional Profiles In Engineered Human Ectocervical Tissue Dependent On Menstrual Cycle Phase. *Biol Reprod* **103**, 487-496 (2020).
115. A. R. Thurman *Et Al.*, Comparison Of Follicular And Luteal Phase Mucosal Markers Of HIV Susceptibility In Healthy Women. *AIDS Res Hum Retroviruses* **32**, 547-560 (2016).
116. L. A. Vodstrcil *Et Al.*, Hormonal Contraception Is Associated With A Reduced Risk Of Bacterial Vaginosis: A Systematic Review And Meta-Analysis. *Plos One* **8**, E73055 (2013).
117. J. H. Van De Wijgert, M. C. Verwijs, A. N. Turner, C. S. Morrison, Hormonal Contraception Decreases Bacterial Vaginosis But Oral Contraception May Increase Candidiasis: Implications For HIV Transmission. *AIDS* **27**, 2141-2153 (2013).
118. S. B. Rifkin, M. R. Smith, R. M. Brotman, R. M. Gindi, E. J. Erbelding, Hormonal Contraception And Risk Of Bacterial Vaginosis Diagnosis In An Observational Study Of Women Attending STD Clinics In Baltimore, MD. *Contraception* **80**, 63-67 (2009).
119. S. C. Francis *Et Al.*, Bacterial Vaginosis Among Women At High Risk For HIV In Uganda: High Rate Of Recurrent Diagnosis Despite Treatment. *Sex Transm Infect* **92**, 142-148 (2016).
120. R. S. Mcclelland *Et Al.*, A Prospective Study Of Risk Factors For Bacterial Vaginosis In HIV-1-Seronegative African Women. *Sex Transm Dis* **35**, 617-623 (2008).
121. S. L. Achilles *Et Al.*, Impact Of Contraceptive Initiation On Vaginal Microbiota. *Am J Obstet Gynecol* **218**, 622 E621-622 E610 (2018).
122. E. St John, D. Mares, G. T. Spear, Bacterial Vaginosis And Host Immunity. *Curr HIV/AIDS Rep* **4**, 22-28 (2007).
123. D. Mares, J. A. Simoes, R. M. Novak, G. T. Spear, TLR2-Mediated Cell Stimulation In Bacterial Vaginosis. *J Reprod Immunol* **77**, 91-99 (2008).
124. J. P. Hapgood, C. Kaushic, Z. Hel, Hormonal Contraception And HIV-1 Acquisition: Biological Mechanisms. *Endocr Rev* **39**, 36-78 (2018).
125. A. Thurman *Et Al.*, The Effect Of Hormonal Contraception On Cervicovaginal Mucosal End Points Associated With HIV Acquisition. *AIDS Res Hum Retroviruses* **35**, 853-864 (2019).
126. K. G. Michel, R. P. Huijbregts, J. L. Gleason, H. E. Richter, Z. Hel, Effect Of Hormonal Contraception On The Function Of Plasmacytoid Dendritic Cells And Distribution Of Immune Cell Populations In The Female Reproductive Tract. *J Acquir Immune Defic Syndr* **68**, 511-518 (2015).
127. K. D. Birse *Et Al.*, Genital Injury Signatures And Microbiome Alterations Associated With Depot Medroxyprogesterone Acetate Usage And Intravaginal Drying Practices. *J Infect Dis* **215**, 590-598 (2017).

128. S. L. Achilles *Et Al.*, Zim CHIC: A Cohort Study Of Immune Changes In The Female Genital Tract Associated With Initiation And Use Of Contraceptives. *Am J Reprod Immunol* **84**, E13287 (2020).
129. G. Edfeldt *Et Al.*, Regular Use Of Depot Medroxyprogesterone Acetate Causes Thinning Of The Superficial Lining And Apical Distribution Of HIV Target Cells In The Human Ectocervix. *J Infect Dis*, 1-11 (2020).
130. K. K. Smith-Mccune *Et Al.*, Effects Of Depot-Medroxyprogesterone Acetate On The Immune Microenvironment Of The Human Cervix And Endometrium: Implications For HIV Susceptibility. *Mucosal Immunol* **10**, 1270-1278 (2017).
131. E. H. Byrne *Et Al.*, Association Between Injectable Progestin-Only Contraceptives And HIV Acquisition And HIV Target Cell Frequency In The Female Genital Tract In South African Women: A Prospective Cohort Study. *Lancet Infect Dis* **16**, 441-448 (2016).
132. C. Tasker *Et Al.*, Depot Medroxyprogesterone Acetate Administration Increases Cervical CCR5+CD4+ T Cells And Induces Immunosuppressive Milieu At The Cervicovaginal Mucosa. *AIDS* **34**, 729-735 (2020).
133. J. Lajoie *Et Al.*, Increased Cervical CD4(+)CCR5(+) T Cells Among Kenyan Sex Working Women Using Depot Medroxyprogesterone Acetate. *AIDS Res Hum Retroviruses* **35**, 236-246 (2019).
134. S. Dabee *Et Al.*, Defining Characteristics Of Genital Health In South African Adolescent Girls And Young Women At High Risk For HIV Infection. *Plos One* **14**, E0213975 (2019).
135. N. E. Quispe Calla, M. G. Ghonime, T. L. Cherpes, R. D. Vicetti Miguel, Medroxyprogesterone Acetate Impairs Human Dendritic Cell Activation And Function. *Hum Reprod* **30**, 1169-1177 (2015).
136. B. O'Sullivan, R. Thomas, CD40 And Dendritic Cell Function. *Crit Rev Immunol* **23**, 83-107 (2003).
137. R. M. Ray *Et Al.*, The Contraceptive Medroxyprogesterone Acetate, Unlike Norethisterone, Directly Increases R5 HIV-1 Infection In Human Cervical Explant Tissue At Physiologically Relevant Concentrations. *Sci Rep* **9**, 4334 (2019).
138. N. E. Quispe Calla *Et Al.*, Medroxyprogesterone Acetate And Levonorgestrel Increase Genital Mucosal Permeability And Enhance Susceptibility To Genital Herpes Simplex Virus Type 2 Infection. *Mucosal Immunol* **9**, 1571-1583 (2016).
139. S. E. Bosinger *Et Al.*, Progestin-Based Contraception Regimens Modulate Expression Of Putative HIV Risk Factors In The Vaginal Epithelium Of Pig-Tailed Macaques. *Am J Reprod Immunol* **80**, E13029 (2018).
140. K. Butler *Et Al.*, Analysis Of Putative Mucosal SHIV Susceptibility Factors During Repeated DMPA Treatments In Pigtail Macaques. *J Med Primatol* **44**, 286-295 (2015).
141. V. Jespers *Et Al.*, A Longitudinal Analysis Of The Vaginal Microbiota And Vaginal Immune Mediators In Women From Sub-Saharan Africa. *Sci Rep* **7**, 11974 (2017).
142. J. M. Wessels *Et Al.*, Medroxyprogesterone Acetate Alters The Vaginal Microbiota And Microenvironment In Women And Increases Susceptibility To HIV-1 In Humanized Mice. *Dis Model Mech* **12**, (2019).
143. C. S. Morrison *Et Al.*, A Longitudinal Assessment Of Cervical Inflammation And Immunity Associated With HIV-1 Infection, Hormonal Contraception, And Pregnancy. *AIDS Res Hum Retroviruses* **34**, 889-899 (2018).

144. L. B. Haddad *Et Al.*, Hormonal Contraception And Vaginal Infections Among Couples Who Are Human Immunodeficiency Virus Serodiscordant In Lusaka, Zambia. *Obstet Gynecol* **134**, 573-580 (2019).
145. C. Gosmann *Et Al.*, Lactobacillus-Deficient Cervicovaginal Bacterial Communities Are Associated With Increased HIV Acquisition In Young South African Women. *Immunity* **46**, 29-37 (2017).
146. B. M. Whitney *Et Al.*, Changes In Key Vaginal Bacteria Among Postpartum African Women Initiating Intramuscular Depot-Medroxyprogesterone Acetate. *Plos One* **15**, E0229586 (2020).
147. L. Yang *Et Al.*, Differential Effects Of Depot Medroxyprogesterone Acetate Administration On Vaginal Microbiome In Hispanic White And Black Women. *Emerg Microbes Infect* **8**, 197-210 (2019).
148. A. C. Roxby *Et Al.*, Changes In Vaginal Microbiota And Immune Mediators In HIV-1-Seronegative Kenyan Women Initiating Depot Medroxyprogesterone Acetate. *J Acquir Immune Defic Syndr* **71**, 359-366 (2016).
149. G. A. Goldfien *Et Al.*, Progestin-Containing Contraceptives Alter Expression Of Host Defense-Related Genes Of The Endometrium And Cervix. *Reprod Sci* **22**, 814-828 (2015).
150. D. J. Anderson, J. Marathe, J. Pudney, The Structure Of The Human Vaginal Stratum Corneum And Its Role In Immune Defense. *Am J Reprod Immunol* **71**, 618-623 (2014).
151. I. A. Zalenskaya *Et Al.*, Use Of Contraceptive Depot Medroxyprogesterone Acetate Is Associated With Impaired Cervicovaginal Mucosal Integrity. *J Clin Invest* **128**, 4622-4638 (2018).
152. M. Simbar, F. R. Tehrani, Z. Hashemi, H. Zham, I. S. Fraser, A Comparative Study Of Cyclofem And Depot Medroxyprogesterone Acetate (DMPA) Effects On Endometrial Vasculature. *J Fam Plann Reprod Health Care* **33**, 271-276 (2007).
153. N. E. Quispe Calla *Et Al.*, Exogenous Sex Steroids Regulate Genital Epithelial Barrier Function In Female Rhesus Macaques. *Biol Reprod* **103**, 310-317 (2020).
154. N. E. Quispe Calla *Et Al.*, Exogenous Oestrogen Inhibits Genital Transmission Of Cell-Associated HIV-1 In DMPA-Treated Humanized Mice. *J Int AIDS Soc* **21**, (2018).
155. J. R. Wisniewski, A. Zougman, N. Nagaraj, M. Mann, Universal Sample Preparation Method For Proteome Analysis. *Nat Methods* **6**, 359-362 (2009).
156. N. R. Klatt *Et Al.*, Vaginal Bacteria Modify HIV Tenofovir Microbicide Efficacy In African Women. *Science* **356**, 938-945 (2017).
157. S. K. Linden, P. Sutton, N. G. Karlsson, V. Korolik, M. A. Mcguckin, Mucins In The Mucosal Barrier To Infection. *Mucosal Immunol* **1**, 183-197 (2008).
158. A. S. Mall, H. Habte, Y. Mthembu, J. Peacocke, C. De Beer, Mucus And Mucins: Do They Have A Role In The Inhibition Of The Human Immunodeficiency Virus? *Virol J* **14**, 192 (2017).
159. W. A. Schroder *Et Al.*, Serpinb2 Inhibits Migration And Promotes A Resolution Phase Signature In Large Peritoneal Macrophages. *Sci Rep* **9**, 12421 (2019).
160. J. Hoover-Plow, Does Plasmin Have Anticoagulant Activity? *Vasc Health Risk Manag* **6**, 199-205 (2010).
161. A. Pole, M. Dimri, G. P. Dimri, Oxidative Stress, Cellular Senescence And Ageing. *AIMS Molecular Science* **3**, 300-324 (2016).

162. R. Herwig, C. Hardt, M. Lienhard, A. Kamburov, Analyzing And Interpreting Genome Data At The Network Level With Consensuspathdb. *Nat Protoc* **11**, 1889-1907 (2016).
163. J. P. D. Boer *Et Al.*, Alpha-2-Macroglobulin Functions As An Inhibitor Of Fibrinolytic, Clotting, And Neutrophilic Proteinases In Sepsis: Studies Using A Baboon Model. *Infection And Immunity* **61**, 5035-5043 (1993).
164. D. C. Berry, S. M. O'Byrne, A. C. Vreeland, W. S. Blaner, N. Noy, Cross Talk Between Signaling And Vitamin A Transport By The Retinol-Binding Protein Receptor STRA6. *Mol Cell Biol* **32**, 3164-3175 (2012).
165. M. Cassandri *Et Al.*, Zinc-Finger Proteins In Health And Disease. *Cell Death Discov* **3**, 17071 (2017).
166. P. Petrova *Et Al.*, MANF: A New Mesencephalic, Astrocyte-Derived Neurotrophic Factor With Selectivity For Dopaminergic Neurons. *J Mol Neurosci* **20**, 173-188 (2003).
167. J. Ravel *Et Al.*, Vaginal Microbiome Of Reproductive-Age Women. *Proc Natl Acad Sci U S A* **108 Suppl 1**, 4680-4687 (2011).
168. O. Evidence For Contraceptive, H. I. V. O. T. Consortium, HIV Incidence Among Women Using Intramuscular Depot Medroxyprogesterone Acetate, A Copper Intrauterine Device, Or A Levonorgestrel Implant For Contraception: A Randomised, Multicentre, Open-Label Trial. *Lancet* **394**, 303-313 (2019).
169. C. M. Bamberger, H. M. Schulte, Molecular Mechanisms Of Dissociative Glucocorticoid Activity. *Eur J Clin Invest* **30 Suppl 3**, 6-9 (2000).
170. P. Mallmann, K. Dietrich, D. Krebs, Effect Of Tamoxifen And High-Dose Medroxyprogesterone Acetate (MPA) On Cell-Mediated Immune Functions In Breast Cancer Patients. *Methods Find Exp Clin Pharmacol* **12**, 699-706 (1990).
171. L. Miller *Et Al.*, Depomedroxyprogesterone-Induced Hypoestrogenism And Changes In Vaginal Flora And Epithelium. *Obstet Gynecol* **96**, 431-439 (2000).
172. C. K. Mauck *Et Al.*, The Effect Of One Injection Of Depo-Provera On The Human Vaginal Epithelium And Cervical Ectopy. *Contraception* **60**, 15-24 (1999).
173. A. Burgener *Et Al.*, Comprehensive Proteomic Study Identifies Serpin And Cystatin Antiproteases As Novel Correlates Of HIV-1 Resistance In The Cervicovaginal Mucosa Of Female Sex Workers. *J Proteome Res* **10**, 5139-5149 (2011).
174. A. K. Ildgruben, I. M. Sjoberg, M. L. Hammarstrom, Influence Of Hormonal Contraceptives On The Immune Cells And Thickness Of Human Vaginal Epithelium. *Obstet Gynecol* **102**, 571-582 (2003).
175. P. Sharma *Et Al.*, Cervico-Vaginal Inflammatory Cytokine Alterations After Intrauterine Contraceptive Device Insertion: A Pilot Study. *Plos One* **13**, E0207266 (2018).
176. R. M. Engel *Et Al.*, Evaluation Of Pigtail Macaques As A Model For The Effects Of Copper Intrauterine Devices On HIV Infection. *J Med Primatol* **43**, 349-359 (2014).
177. B. L. Sheppard, Endometrial Morphological Changes In IUD Users: A Review. *Contraception* **36**, 1-10 (1987).
178. C. Gottschick *Et Al.*, Treatment Of Biofilms In Bacterial Vaginosis By An Amphoteric Tenside Pessary-Clinical Study And Microbiota Analysis. *Microbiome* **5**, 119 (2017).
179. R. P. Huijbregts, K. G. Michel, Z. Hel, Effect Of Progestins On Immunity: Medroxyprogesterone But Not Norethisterone Or Levonorgestrel Suppresses The Function Of T Cells And Pdcs. *Contraception* **90**, 123-129 (2014).
180. S. Amu, N. Ruffin, B. Rethi, F. Chiodi, Impairment Of B-Cell Functions During HIV-1 Infection. *AIDS* **27**, 2323-2334 (2013).

181. M. M. Guo, J. E. Hildreth, HIV Acquires Functional Adhesion Receptors From Host Cells. *AIDS Res Hum Retroviruses* **11**, 1007-1013 (1995).
182. L. Noel-Romas *Et Al.*, Vaginal Microbiome-Hormonal Contraceptive Interactions Associate With The Mucosal Proteome And HIV Acquisition. *Plos Pathog* **16**, E1009097 (2020).